Chapter 5

Chlorophyll *a* Fluorescence in Cyanobacteria: Relation to Photosynthesis☆

Alexandrina Stirbet*, Dušan Lazár†, George C. Papageorgiou‡, Govindjee§

**Newport News, VA, United States, †Department of Biophysics, Centre of the Region Haná for Biotechnological and Agricultural Research, Faculty of Science, Palacký University, Olomouc, Czech Republic, ‡Institute of Biosciences and Applications, National Centre for Scientific Research Demokritos, Attikis, Greece, §Departments of Biochemistry and Plant Biology, and Centre of Biophysics and Quantitative Biology, University of Illinois at Urbana-Champaign, Urbana, IL, United States*

1. INTRODUCTION

Cyanobacteria, earlier known as blue-green algae, are oxygenic photosynthesizers. They are prokaryotes that live in different ecological niches (including extreme environments). Although mainly free living in aquatic environments, they are also found in symbiotic associations [for a background on molecular biology of cyanobacteria, see Bryant, 1994]. They have various morphologies (e.g., rod shaped, spherical, or filamentous) and manifest a diversity of metabolic pathways. Cyanobacteria are important globally since >25% of the global net primary photosynthetic productivity is due to these organisms (Flombaum et al., 2013); moreover, some of them also participate in the nitrogen cycle (Zehr, 2011). Furthermore, cyanobacteria have high technological potential, as engineered cyanobacteria can convert CO_2 and light into many products of interest, such as renewable fuels, various chemicals, and nutritional products (see reviews by, e.g., Al-Haj et al., 2016; Gao et al., 2016; Kitchener and Grunden, 2018; Lai and Lan, 2015; Vermaas, 2007): these include hydrogen (H_2) (Khanna and Lindblad, 2015), ethylene (Veetil et al., 2017), poly-β-hydroxybutyrate (Carpine et al., 2018), erythritol (van der Woude et al., 2016), and acetone (Zhou et al., 2012). In addition, McGrath and Long (2014) have provided a new hope, through a theoretical analysis, for increasing crop yields by suggesting that we bioengineer a cyanobacterial carbon-concentrating mechanism (partially or totally) into C3 plants, which is expected to decrease photorespiration and, thus, increase their yield by 36% to 60%.

1.1 Photosynthetic Apparatus and Oxygenic Photosynthesis in Cyanobacteria Compared to Plants and Algae

Cyanobacteria are considered to be the ancestors of chloroplasts (see, e.g., Douglas, 1994; Shih and Matzke, 2013). There is no doubt that plastids (chloroplasts) are derived from once free-living cyanobacteria that were acquired by eukaryote host cells through intracellular (or endosymbiotic) gene transfer; moreover, it is very possible that plastid evolution involved primary, secondary, and even tertiary endosymbiosis, as suggested by phylogenetic and phylogenomic analyses (see McFadden, 2001). This explains the close similarity of many components of the cyanobacterial photosynthetic apparatus with those in eukaryotes (algae and higher plants): for example, photosystem (PS) I, PSII, plastoquinone (PQ), cytochrome (Cyt) b_6f complex, plastocyanin (Pc), ferredoxin (Fd), nicotinamide adenine dinucleotide phosphate ($NADP^+$, oxidized form), Fd-$NADP^+$ oxidoreductase (FNR), and ATP synthase. However, the PSI/PSII ratio, instead of being close to 1, as in plants and green algae, is much higher in cyanobacteria, ranging from 2 to 10 (under different environmental conditions) (see, e.g., Fraser et al., 2013; Sonoike et al., 2001). Changes in PS stoichiometry in cyanobacteria are mainly due to variations in PSI abundance (Fujita et al., 1994). Moreover, the thylakoid membranes (TMs) in cyanobacteria have topologies different from those in higher plants, as they do not have grana stacks, but often form pairs of sheets that follow the

☆ In memory of Ram Nagina Singh (1915–77)—one of the greatest biologists of our time and a dear friend to one of us (Govindjee); see R.N. Singh and S.P. Singh (1978) Advances in Cyanophyte Research: Professor R.N. Singh memorial volume, published by Algal Research Laboratory, Banaras Hindu University, Varanasi, India.

Note: See Glossary on page: 110

Cyanobacteria. https://doi.org/10.1016/B978-0-12-814667-5.00005-2

periphery of the cell, as, for example, in *Synechocystis* sp. PCC 6803 (van de Meene et al., 2006). Further, Nevo et al. (2007) have shown that there are membrane bridges that connect multiple TM layers, suggesting that the TM forms a single continuous surface with a single interconnected lumen.

Unlike algae and plants, TMs of cyanobacteria contain protein complexes for both respiratory and photosynthetic electron transport (ET), which share several components such as PQ, Cyt b_6f complexes, and even Pc (see Fig. 1, and reviews by Ermakova et al., 2016; Lea-Smith et al., 2016; Liu, 2016; Mullineaux, 2014; Vermaas, 2001); however, some of the respiratory ET components are also located in the plasma membrane. In the TM, the respiratory electron flow involves a bacterial NAD(P)H:quinone oxidoreductase (NDH-1) and succinate dehydrogenase (SDH) as the main respiratory electron donor complexes (Battchikova et al., 2011; Cooley and Vermaas, 2001) that transfer electrons from certain organic molecules (e.g., glucose) into the PQ pool and supply electrons to cyclic electron flow (CEF) around PSI, in addition to the Fd-mediated PQ reduction pathway (see discussion below). The thylakoidal respiratory electron flow also includes the participation of terminal oxidases: Cyt *bd* quinol oxidase (Cyd) and Cyt *c* oxidase (Cox) (see Fig. 1), with Cox being mostly responsible for dark respiration, but also competing with P700 for electrons under high light (Ermakova et al., 2016). Therefore, the thylakoidal ET in cyanobacteria is even more complex than in plants and algae (see, e.g., Ogawa and Sonoike, 2015; Schuurmans et al., 2015).

The first phase of oxygenic photosynthesis takes place in the TM and involves several major processes (see, e.g., Adams and Terashima 2018; Mimuro et al., 2008; Shevela et al., 2013): (1) absorption of light by different light-harvesting pigment-protein complexes and excitation energy transfer (EET) to the reaction centers (RCs) of PSII and PSI (i.e., P680 and P700); (2) photochemical conversion of the trapped excitation energy (EE) through charge separation, at the RC; and (3) ET between the different redox components. Various routes of electron flow exist. The electron flow from water to $NADP^+$ includes both PSII and PSI and is a linear electron flow (LEF): $H_2O \rightarrow$ PSII $\rightarrow$ PQ pool $\rightarrow$ Cyt $b_6f \rightarrow$ Pc (or Cyt c_6) $\rightarrow$ PSI $\rightarrow$ Fd (or flavodoxin) $\rightarrow$ FNR $\rightarrow NADP^+$ (Govindjee et al., 2017; Nelson and Yocum, 2006). Coupled to LEF, a proton motive force (*pmf*) across the TM is generated (see Fig. 1) which is then used for ATP synthesis (Armbruster et al., 2017; Lyu and Lazár, 2017; Mitchell, 1966; Murata and Nishiyama, 2018); the *pmf* has two components, the membrane electric potential $\Delta\Psi$ and the transmembrane proton difference ΔpH, and is calculated as $pmf = \Delta\Psi + (2.3RT/F)\,\Delta$pH, where F is the Faraday constant, R is the gas constant, and T is the absolute temperature. The final products of this phase, NADPH and ATP, are then used for carbon assimilation and other metabolic processes in cytosol/stroma. Like plants and algae, cyanobacteria perform CEF around PSI involving the Cyt b_6f, but also a pseudo-CEF mediated by soluble flavodiiron proteins (i.e., Flv1/Flv3 heterodimer) functioning in a "Mehler-like" reaction (Allahverdiyeva et al., 2013, 2015; Ilík et al., 2017), without concomitant formation of reactive oxygen species (ROSs, see Fig. 1). Both CEF and pseudo-CEF contribute to the regulation of photosynthesis by preventing over-reduction of electron carriers under oscillating (fluctuating) light (see, e.g., Shikanai and Yamamoto, 2017) and to the adjustment of the ATP/NADPH ratio according to the metabolic demands. For example, Allahverdiyeva et al. (2011) estimated that up to 20% of electrons might pass from PSI to O_2 via the Flv1/Flv3 heterodimer; this suggests that the "Mehler-like" reaction in cyanobacteria may play an important role in photoprotection (Allahverdiyeva et al., 2015).

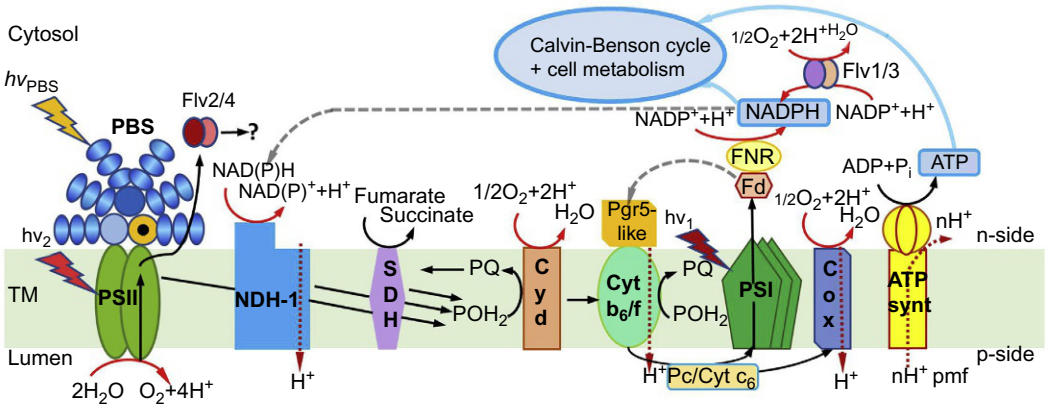

FIG. 1 Schematic diagram of photosynthetic and respiratory electron transport (ET) in the thylakoid membrane (TM) of *Synechocystis* sp. PCC 6803. *Black arrows* indicate photosynthetic and respiratory ET, *red arrows* indicate proton translocation, and *gray dashed arrows* show cyclic electron transport (CEF) around PSI. The PQ redox reactions involve the uptake of two protons from the cytosol. *Abbreviations*: *ATP synth*, ATP synthase; *Cox*, cytochrome *c* oxidase; *Cyd*, cytochrome bd quinol oxidase; *Cyt*, cytochrome; *Fd*, ferredoxin; *Flv1/3 and Flv2/4*, flavodiiron proteins 1/3 and 2/4; *FNR*, ferredoxin-$NADP^+$ oxidoreductase; *NADPH*, nicotinamide-adenine dinucleotide phosphate (reduced form); *NDH-1*, NAD (P)H dehydrogenase-like complex type 1; *PBS*, phycobilisome; *Pc*, plastocyanin; *Pgr5 (proton gradient regulation 5)*, a thylakoidal protein involved in ET from Fd to PQ; *pmf* [$=\Delta\Psi + (2.3RT/F)\Delta$pH], the proton motive force necessary for ATP synthesis; *PQ*, plastoquinone; *PSI and PSII*, photosystems I and II; *SDH*, succinate dehydrogenase. *(Modified from Ermakova, M., Huokko, T., Richaud, P., Bersanini, L., Howe, C.J., Lea-Smith, D.J., Peltier, G., Allahverdiyeva, Y., 2016. Distinguishing the roles of thylakoid respiratory terminal oxidases in the cyanobacterium* Synechocystis *sp. PCC 6803. Plant Physiol. 171, 1307–1319.)*

While the PSs in cyanobacteria have similar intrinsic antenna to those in eukaryotes [96 Chls and 22 carotenoids (Car) in PSI, and 35 Chls and 11 all trans-β-Car in PSII; Jordan et al., 2001; Umena et al., 2011], they lack transmembrane peripheral antenna containing chlorophyll (Chl) *a/b* (i.e., light-harvesting complexes, Lhcb in PSII and Lhca in PSI), and thus, do not contain Chl *b*; on the other hand, the carotenoids present in cyanobacterial PSII, compared to those in PSI, do not effectively transfer energy to Chl *a*, being mainly involved in photoprotection and in ^{3}Chl* quenching (de Weerd et al., 2003a,b; Stamatakis et al., 2014). While LHC proteins are missing in cyanobacteria, they still possess a family of single-helix proteins with a typical LHC-like Chl-binding motif, labeled as high-light-inducible proteins (HliPs) (Dolganov et al., 1995; Komenda and Sobotka, 2016), which are considered to be the ancestors of LHCs (Engelken et al., 2012).

The HliPs are not involved in light harvesting, but play an important role in Chl synthesis, PSII assembly, and photoprotection, particularly under stress conditions (Komenda and Sobotka, 2016; Staleva et al., 2015). Instead of LHCs, cyanobacteria, as well as red algae and glaucophytes, have very large (3–7 MDa) brightly colored protein complexes called phycobilisomes (PBSs), which attach to the cytosolic side of the TM and harvest light in a wide spectral range, especially in the 500–670 nm region (Gantt, 1981). The PBSs, megacomplexes with dimensions of 80 × 50 × 12 nm, cover the stromal surface of the TM (see a review by Harris et al., 2018). They contain hundreds of phycobiliproteins (PBPs) that covalently bind phycobilins (PBs) (linear tetrapyrrole chromophores), as well as few colorless polypeptides (called linkers, L), which are involved in the assembly of the PBPs into the PBS. The PBSs transfer EE very efficiently, especially to PSII (Acuña et al., 2018a; Wang et al., 1977), but also to PSI in certain circumstances (see, e.g., Joshua and Mullineaux, 2004; Liu et al., 2013; Kondo et al., 2009; Watanabe et al., 2014).

As in plants and algae, the localization of different protein complexes in the TM of cyanobacteria is heterogeneous. For example, by using hyperspectral confocal fluorescence imaging of *Synechocystis* sp. 6803, Vermaas et al. (2008) observed that PBS and PSII were much more prevalent along the outer thylakoids, while PSIs were localized on the inner membrane thylakoids, as the latter disappeared in mutants lacking PSI. On the other hand, PSI of *Synechoccoccus* sp. 7942 was found to be preferentially located in the thylakoids close to the cytoplasmic membrane (Sherman et al., 1994). By means of cryogenic confocal microscopy, Steinbach et al. (2015) observed three types of areas in the TMs of the native cyanobacterial cells of *Anabaena* sp. 7120 that preferentially contained: (1) PSI; (2) PBS with PSII; and (3) PBS with both PSII and PSI. Such domains have also been observed by using atomic force microscopy on several cyanobacteria (MacGregor-Chatwin et al., 2017; Casella et al., 2017). The third mixed zone most probably contains PBS-PSII-PSI supercomplexes, which have been isolated and characterized by Liu et al. (2013). On the other hand, PSIs also exist in separate domains; these must remain functional because of long-distance diffusion of electron carriers. Further, these may be considered as early evolutionary indicators of PSI that ended up, in plants, in their stromal lamellae.

1.2 Photosynthetic Regulatory Processes in Cyanobacteria

Based on results from the fluorescence recovery after photobleaching method (see, e.g., Papáček et al., 2015), Mullineaux et al. (1997) concluded that PBSs are capable of moving on the surface of the TM during illumination (see also Yang et al., 2007; Kaňa, 2013). Since PSI and PSII complexes have been found to be much less mobile in the TM (Mullineaux et al., 1997), Joshua and Mullineaux (2004) proposed a theory regarding state transitions in cyanobacteria based on PBS mobility. State transitions are short-term light-adaptive processes that regulate the distribution of EE between PSII and PSI that are induced by changes in the redox state of the PQ pool (see reviews by Allen and Mullineaux, 2004; Papageorgiou and Govindjee, 2011, 2014). During a State 1-to-State 2 transition, the EE received by PSII decreases and that by PSI increases, whereas the reverse happens during a State 2-to-State 1 transition. State transitions also take place in plants and algae with both primary (E1) and secondary plastids (E2; see, e.g., McFadden, 2001), but are more important in cyanobacteria and involve different mechanisms. However, the interactions of PBS with PSI and PSII during state transitions in cyanobacteria are not yet clear, and different mechanisms that do not involve PBS mobility have also been proposed (Chukhutsina et al., 2015; Liu et al., 2013).

Cyanobacteria have also developed special photoprotective mechanisms against excess EE, in which part of the energy captured is not transferred to the RCs, but dissipated as heat and manifested as nonphotochemical quenching (NPQ) of Chl excited state. The main NPQ mechanism in cyanobacteria involves the orange carotenoid protein (OCP), a soluble protein binding a ketocarotenoid (Wilson et al., 2006). After being activated by high-intensity white or blue light, the OCP interacts with the PBS, dissipating the EE harvested by PBPs, and reducing drastically the energy received by the RCs of PSII and PSI (see reviews by, e.g., Bao et al., 2017; Kirilovsky et al., 2014). The interaction of PBS with OCP, at the molecular level, as well as some other aspects of this NPQ mechanism, is still under study. For a quite different system, the cyanobacterial lichen, see discussion in Demmig-Adams et al. (1990a,b).

PBSs are optimized to allow maximum absorption of light available, and their structural organization varies not only among different species (see reviews by Adir, 2005; Glazer, 1984; Harris et al., 2018; Watanabe and Ikeuchi, 2013), but also

in the same organism when the environmental conditions change (Akimoto et al., 2013; Montgomery, 2017). In some cyanobacteria, the relationship between the amounts of different PBPs or the ratio between PBPs and Chl *a* can vary, depending on the color of the light under which they are grown, the process being called chromatic acclimation, or adaptation (Kehoe, 2010; Montgomery, 2017). For example, studies on the cyanobacterium *Anacystis nidulans* (*Synechococcus* PCC 7942) showed that the ratio of phycocyanin (a PB) to Chl *a* is higher under strong orange light and is lower under strong red light (Ghosh and Govindjee, 1966). We note that there indeed exist cyanobacteria that contain Chl *b* in addition to Chl *a* (e.g., prochlorophytes; Govindjee and Satoh, 1986; Matthijs et al., 1994), or in which Chl *d* is dominant (~97%) (i.e., *Acaryochloris*-like organisms; Miyashita et al., 1996; Larkum and Kuhl, 2005); since Chl *d* absorbs at a longer wavelength (by 40 nm) than Chl *a*, the "red limit" (i.e., the minimum energy required for oxygenic photosynthesis) is extended beyond 700 nm in *Acaryachloris*. Furthermore, the first reported Chl *f*-containing organism was *Halomicronema hongdechloris*, a filamentous cyanobacterium isolated from stromatolites in Australia. This cyanobacterium contains four main carotenoids, as well as Chl *a* and Chl *f* in a ratio of 1:8 when grown under red light, and an undetectable level of Chl *f* under white-light conditions (Chen et al., 2012). Chl *f* has a chemical structure relatively similar to that of Chl *b*, and is the most red-shifted type of Chl, having an absorption peak at 706 nm and a fluorescence maximum at 722 nm at room temperature in methanol (Chen et al., 2012). Moreover, it was recently shown that, when grown under far-red light of 750 nm, the extremophile cyanobacterium *Chroococcidiopsis thermalis* contained ~90% Chl *a*, ~10% Chl *f*, and <1% Chl *d* and the wavelength dependence of PSI and PSII activity (action spectra) was red shifted with new peaks at 745 nm for PSI and 715 nm for PSII (Nürnberg et al., 2018). Spectroscopic measurements showed that these long-wavelength Chls participate not only in light harvesting, but also as primary electron donors in photochemical reactions of PSI (i.e., Chl *f* at 745 nm in vivo) and PSII [i.e., Chl *f* (or *d*) at 727 nm] (Nürnberg et al., 2018).

1.3 The Importance of Chlorophyll *a* Fluorescence Measurements in the Study of the Photosynthetic Processes

Chl *a* fluorescence (ChlF) emitted by plants, algae, and cyanobacteria can provide both qualitative and quantitative information on a large variety of photosynthetic events, due to its intricate connection with the processes taking place during the conversion of light energy into stable chemical products via initial charge separation at the RCs of PSI and PSII (see reviews by Falkowski and Raven, 2007; Kalaji et al., 2012; Kolber et al., 1998; Lazár, 1999; Papageorgiou, 1975, 1996; Ogawa et al., 2017; Stirbet et al., 2014; and chapters in Govindjee et al., 1986; Papageorgiou and Govindjee, 2004).

Steady-state emission and excitation spectra of Chl *a*, as well as results obtained with various time-resolved fluorescence spectroscopy, have provided information on different chromophore-protein components and the EET among them (see reviews by Clegg et al., 2010; Fleming, 2018; Govindjee, 1999, 2004; Govindjee and Shevela, 2011; Mamedov et al. 2015; Mirkovic et al., 2017). In addition, the kinetics of ChlF decay after light flashes (Cao et al., 1991; Eaton-Rye and Govindjee, 1988; Robinson and Crofts, 1983), or changes in ChlF during dark-light transitions [i.e., Chl *a* fluorescence induction (ChlFI); Kautsky and Hirsch, 1931] measured under continuous or modulated light, have been used to study the kinetics of various intermediates on the electron acceptor side of PSII as well as the NPQ kinetics and to assess responses to various types of stress (Campbell et al., 1998; Govindjee, 1995, 2004; Govindjee and Papageorgiou, 1971; Kalaji et al., 2016; Lazár, 2006, 2015; Mishra et al., 2016; Ogawa et al., 2017; Papageorgiou and Govindjee, 2011; Papageorgiou et al., 2007; Stirbet and Govindjee, 2011; Stirbet et al., 2018; Strasser et al., 2004; Suggett et al., 2010).

In this chapter, we present basic structural data on PBS, PSII, and PSI in cyanobacteria, and up-to-date information obtained mainly by means of ChlF on topics related to different photosynthetic processes, such as: (1) EET from PBS to both PSI and PSII; (2) EET from antenna to the RC(s), primary charge separation, and ET reactions in PSII and PSI; (3) quantum yield of PSII, as inferred from the ratio of variable to maximum ChlF, and its relation to overall photosynthesis; (4) analysis of ChlFI measured under continuous and modulated light; (5) regulation of EE distribution to PSs by state transitions; and (6) by OCP-induced NPQ or other NPQ mechanisms. We will end this chapter by discussing challenges we face in using ChlF to monitor some of the photosynthetic processes in cyanobacteria discussed here.

2. PHOTOSYNTHETIC SYSTEMS AND ANTENNA: EXCITATION ENERGY TRANSFER, TRAPPING, AND ELECTRON TRANSPORT

2.1 Phycobilisomes

2.1.1 Composition and Spectral Properties of Phycobiliproteins

As mentioned above, the PBPs are the main components of the PBSs. A PBP is composed of two polypeptide subunits α and β (of approximately 17 and 18 kDa) that covalently bind few PBs (the water-soluble open-chain tetrapyrrole chromophores).

Further, the (αβ) monomers are assembled into trimers $(\alpha\beta)_3$ that stack face to face to form a ring-shaped hexamer $(\alpha\beta)_6$. Several linkers, mostly colorless polypeptides, are responsible for the assembly of PBPs into the PBS (see a review by Liu et al., 2005); they also optimize the absorption and energy transfer characteristics of the PBs (Chang et al., 2015; Harris et al., 2018).

The PBPs are classified into four main groups, depending on their chromophore composition and spectral properties (Mimuro, 2004; Nobel, 2009; Yamanaka et al., 1982): allophycocyanin (APC) and phycocyanin (PC) are found in all cyanobacteria, and bind the blue-colored chromophore, the phycocyanobilin (PCB), while phycoerythrin (PE) and phycoerythrocyanin (PEC) bind the red-colored chromophore phycoerythrobilin (PEB), present in only some cyanobacterial species. Furthermore, a yellow-colored PB, phycourobilin (PUB), is found, for example, in the PBS rods of *Synechococcus* WH7803 (Ong and Glazer, 1991; Six et al., 2007).

Just as is the case for the chlorophylls, PBs are tetrapyrrolic pigments, but the four pyrroles in the PBs occur in an open chain (see Fig. 2 for chemical structures of PCB, PEB, and PUB). They are present in much higher concentrations than Chl *a* in most cyanobacteria, and besides a small Soret band in the UV, they have absorption bands from 520 to 650 nm (see, e.g., Mimuro, 2004; Ong and Glazer, 1991; Nobel, 2009). PBs in solution are highly fluorescent, but when connected to the PSs through the PBS, their fluorescence is very low, since they transfer energy efficiently to Chl *a* (see Duysens, 1952; Ghosh and Govindjee, 1966).

The spectroscopic characteristics of PBs in solution depend greatly not only on the bilin prosthetic group, but also on pH, ionic strength, as well as on temperature (Fork and Mohanty, 1986). In vivo, these chromophores are strongly influenced by their interactions with the environment within their native PBP, which explains the diversity of the spectra of different PBPs (Glazer, 1989). APCs have a major absorption peak at ~650 nm, and their emission peak is at ~660 nm, while PCs absorb between 610 and 635 nm and have fluorescence maxima between 635 and 648 nm; further, allophycocyanin-B (AP-B) has its absorption maximum at ~650 nm with a shoulder at 675 nm, and has emission bands at 660 nm, and at ~680 nm (see reviews by Bryant, 1982; Mimuro, 2004; Nobel, 2009; Yamanaka et al., 1982). Furthermore, there are different types of PEs, with at least one main absorption band between 530 and 570 nm and the fluorescence maximum at ~576 nm, while the PECs have their absorption maximum between 560 and 600 nm and a fluorescence maximum at ~635 nm (Mimuro, 2004). For a list of the main absorption maxima and the corresponding fluorescence maxima of the PBPs from cyanobacteria, see Table 1.

2.1.2 *Architecture of Phycobilisomes and the Excitation Energy Transfer Between Different Phycobiliproteins*

We summarize below basic information on the structure of hemi-discoidal PBSs, the most common PBS type in cyanobacteria (see, e.g., Adir, 2005; Arteni et al., 2009; Chang et al., 2015; Glazer, 1984; Six et al., 2007; Watanabe and Ikeuchi, 2013). A hemi-discoidal PBS has two main domains, a "core" and a few "peripheral rods." The core consists of two (e.g., in *Synechococcus* sp. PCC 6301), three (e.g., in *Synechococcus* sp. PCC7002, *Synechocystis* sp. PCC6701 and PCC6803), or five (e.g., in *Mastigocladus laminosus* and *Anabaena* sp. PCC7120) cylindrical substructures, which contain stacked trimeric $(\alpha\beta)_3$ discs of APC660 and APC680 emitting at 660 and 680 nm (Table 1); the APC680 discs collect and transfer

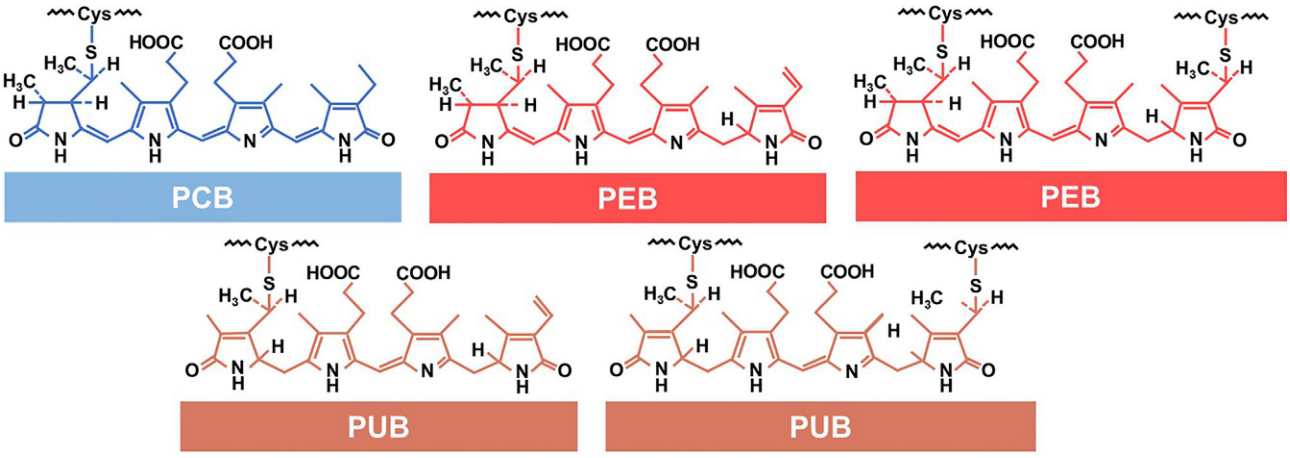

FIG. 2 Molecular structures (with the phycobilin-peptide linkages) of the phycocyanobilin (PCB), phycoerythrobilins (PEB), and phycourobilins (PUB). *(Modified from Glazer, A.N., 1989. Light guides. Directional energy transfer in a photosynthetic antenna. J. Biol. Chem. 264, 1–4.)*

TABLE 1 Absorption and Fluorescence Band Maxima of Phycobilin-Containing Protein Complexes in Cyanobacteria at Room Temperature

Phycobiliprotein		A_{max} (nm)	F_{max} (nm)
Phycoerythrocyanin	$(PEC)_6L_R$	575	635
Phycoerythrin	$(PE)_6L_R$	560	576
Phycocyanin	$(PC)_6L_R$	620	640, 650
Allophycocyanin	$(APC)_3L_C$	650	660
Allophycocyanin-B	$(AP\text{-}B)L_C$, $(AP\text{-}B)L_{CM}$	650, 675[a]	680

Abbreviations: *LR*, rod linker; *LC and LCM*, core linkers.
[a]*Minor bands.*

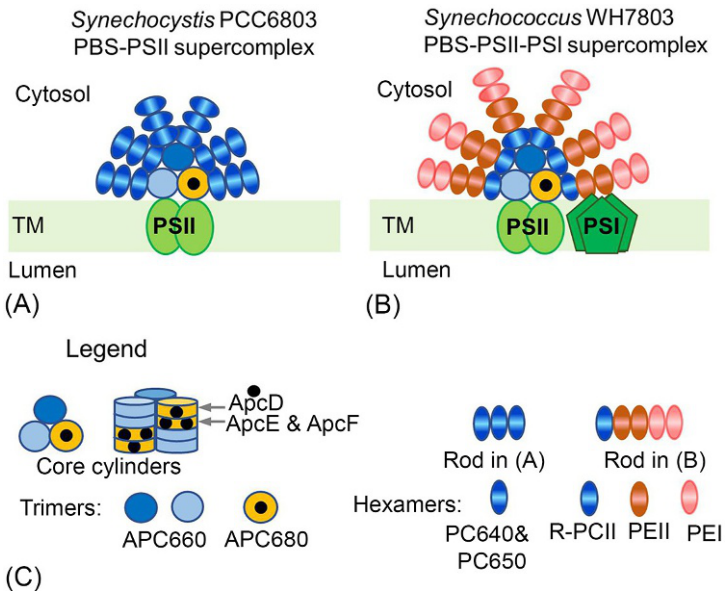

FIG. 3 Diagram of (A) PBS-PSII supercomplex (from *Synechocystis* sp. PCC 6803) and (B) PBS-PSII-PSI supercomplex (from *Synechococcus* sp. WH 7803). Embedded in the thylakoid membrane (TM) are: the photosystem (PS) II dimer *(light green)* and the PSI trimer *(dark green)*. The structure of core cylinders, peripheral rods of both the phycobilisomes (PBSs), as well as their pigment composition, are shown schematically in (C), as a legend. One of the core cylinders contains allophycocyanin (APC) trimers emitting at 660 nm (APC660), *colored blue*, and the other two contain both APC660 and APC680 trimers; the APC680 trimers are shown in *orange* and include the three terminal energy emitters ApcD, ApcE, and ApcF (see *black dots*). In *Synechocystis* sp. PCC 6803, a rod has three hexamers containing phycocyanin (PC640 and PC650). In *Synechococcus* sp. WH 7803, a rod has five hexamers: one containing PC (shown as R-PCII), two containing phycoerythrin (PE) and phycourobilin (PUB) (marked as PEII), and two containing only PE (PEI). *(Modified from Acuña, A.M., van Alphen, P., van Grondelle, R., van Stokkum, I.H.M., 2018a. The phycobilisome terminal emitter transfers its energy with a rate of (20 ps)−1 to photosystem II. Photosynthetica 56, 265–274; Acuña, A.M., Lemaire, C., van Grondelle, R., Robert, B., van Stokkum, I.H.M., 2018b. Energy transfer and trapping in* Synechococcus *WH 7803. Photosynth. Res. 135, 115–124.)*

EE harvested by the PBS to both PSI and PSII on the cytosolic (n)-side of the TM. The peripheral "rods" project radially from the central core and contain stacked hexameric $(\alpha\beta)_6$ discs of PC (emitting with a peak at 650 nm) and eventually PE; they transfer EE to the core of the PBS. The PBS structure of *Synechocystis* sp. PCC 6803, which has six rods and a three-cylindrical core, was established by Arteni et al. (2009) (see Fig. 3). Each rod contains three PC hexamers, while in the core, the upper cylinder contains four APC660 trimers, and each of the two basal cylinders contain two APC660 and two APC680 (see Fig. 3C); in addition, we note that the width of the two basal APC core cylinders is equal to that of a single PSII dimer within the TM.

The APC660 trimers contain three α^{APC}-β^{APC} monomers, while in one long-wavelength emitter APC680 trimer, an α^{APC} is replaced by $\alpha^{AP\text{-}B}$ (i.e., the AP-B coded by *apcD*), and in the other long-wavelength emitter APC680 trimer, a β^{APC} is replaced by $\beta^{18.5}$ (coded by *apcF*) and an α^{APC} is replaced by $\alpha^{L}{}_{CM}$, which is the α domain of the multidomain core-membrane linker L_{CM} (with L_{CM} coded by *apcE*) (see Fig. 3). The ApcD, ApcF, and ApcE in the APC680 are "terminal emitters" that

are essential for the final EET from PBS toward PSII and/or PSI. ApcD and ApcF are necessary for the EET from PBS to PSI (Ashby and Mullineaux, 1999; Dong et al., 2009). On the other hand, ApcE (or L_{CM}) predominantly transfers energy to PSII (Chang et al., 2015; Tang et al., 2015), but its relation with PSI is not yet known. Since ApcE functions as an "anchor" of the PBS to the TM (Glazer, 1989), studies of energy transfer from PBS to the PSs in mutants without ApcE cannot be done.

When present, the PEs are located at the end of the peripheral rods, extending the light-harvesting capability of the PBS to the green region; they are followed by PCs. The EE harvested in the peripheral rods is transferred to APCs in the core and then to the PSs in the TM via the APC680 trimers. These specific chromophore locations in the PBS are responsible for the unidirectional EET (Glazer, 1989): PE → PC → APC660 → APC680 → Chl *a*. Experimental data show that, even if there are hundreds of PBPs in a PBS, the PSs receive light energy absorbed anywhere within the PBS quite efficiently (Glazer, 1989). Moreover, energy transfer within stabilized PBSs is independent of the mode of rod-core assembly (David et al., 2014).

2.1.3 Interaction of Phycobilisomes With Photosystem I and Photosystem II

Here, we will mainly discuss the role played by PBS, which harvests light that is very weakly absorbed by the two PSs (see Table 1), as a sensitizer of ChlF in PSII, as well as in PSI. Its participation in "feeding" energy to PSI has been proven, as the excitation of PBS leads to emission at 715–730 nm, attributed to PSI Chls (see Section 2.3), as well as those at 685 and 695 nm from PSII (see Section 2.2); also, the PSI fluorescence excitation spectrum has peaks due to PBPs (Ghosh and Govindjee, 1966; Rijgersberg and Amesz, 1980). Further, time-resolved 77 K fluorescence spectra of cyanobacteria show an increase of both PSI and PSII emission in parallel with a decrease in PBS fluorescence with time (Bruce et al., 1985; Yamazaki et al., 1984). Moreover, in cyanobacteria, P700 oxidation is observed when PBS is excited, confirming EET from PBS to the Chls of PSI (Glazer et al., 1994).

The mechanism of PBS interaction with the PSs, especially with PSI, is not yet fully understood. Several models have been proposed in which: (1) PBSs connect either with PSII dimer through the core, or with PSI trimers or monomers, also through the core, or through the rods (Harris et al., 2018; Joshua and Mullineaux, 2004; Mullineaux, 2008; Watanabe et al., 2014; Zlenko et al., 2016); (2) PBSs have been shown to connect simultaneously with both PSII and PSI, forming a supercomplex of a PBS, a PSII dimer, and a PSI trimer, that is, PBS-PSII-PSI (Liu et al., 2013); (3) PSII, in a PBS-PSII supercomplex, may also transfer EE to PSI via a so-called "spillover" mechanism, PBS → PSII → PSI (Biggins and Bruce, 1989; Federman et al., 2000; Lia et al., 2004; Ueno et al., 2017); and (4) the PBSs partly (energetically) uncouple from PSI during a dark-to-light transition (Chukhutsina et al., 2015). Since different modes of PBS interaction with the PSs are important in the regulation of EE distribution between PSII and PSI through *state transitions*, we will discuss these in greater detail in Section 4.1.

2.1.4 On the Rates of Excitation Energy Transfer From Phycobilisomes to Photosystem I and Photosystem II

Acuña et al. (2018a) estimated the rate of EET from PBS to PSII in a PBS-PSII complex by measuring ultrafast time-resolved emission spectra of whole cells of a PSI-deficient mutant of *Synechocystis* sp. PCC 6803 (Shen et al., 1993). They made a series of measurements with a streak camera (van Stokkum et al., 2008), providing several sequences of images for which they used two different wavelengths of light (400 nm for Chl excitation and 590 nm for PBS excitation) at different time range(s). Further, Acuña et al. (2018a) analyzed their data on the PBS-PSII complex by means of target analysis (Holzwarth, 1996; van Stokkum et al., 2004) using a functional model for the PBS in *Synechocystis* sp. PCC 6803 (van Stokkum et al., 2018), which was based on the structure determined by Arteni et al. (2009) (see above and Fig. 3A). The following fractions of three different complexes (using 590 nm excitation) were considered in the model: (1) 86% PBS-PSII with open PSII RCs (i.e., with oxidized Q_A, where Q_A is the primary PQ electron acceptor of PSII; see Section 2.2); (2) 8% PBS-PSII with closed RCs (i.e., with all Q_A reduced to Q_A^-); and (3) 6% nontransferring PBSs. The EET rate from the terminal emitter APC680 to PSII, calculated by Acuña et al. (2018a), was 50 ns^{-1} (corresponding to a time constant of 20 ps), which is faster than the PBS internal EET rates between a peripheral rod and a core cylinder (time constant: 68–115 ps) or between the core cylinders (time constant: 115–145 ps) (van Stokkum et al., 2018).

Working on *Synechococcus* sp. WH 7803 cells and with isolated PSI complexes, Acuña et al. (2018b) (1) characterized the EET between different PBPs in the PBS, and from APC680 to both PSI and PSII, by time-resolved emission spectroscopy at room temperature and at 77 K; and then (2) interpreted their results in terms of a target model by using the structure of the PBS-PSII-PSI supercomplex (Liu et al., 2013) and of the PBS from *Synechococcus* sp. WH 7803 (Six et al., 2007). The PBSs of *Synechococcus* sp. WH 7803 have a tricylindrical core and six peripheral rods (see Fig. 3B), as in *Synechocystis* sp. PCC 6803. Here, each rod has five stacked hexamer discs: (i) the first two discs from the tip contain PE hexamers binding the red-colored PEB and the yellow-colored PUB chromophores in a ratio of 5:1 (Six et al., 2007); (ii) the next two discs contain PE hexamers binding only PEB chromophores; and (iii) the fifth disc, connected to the core,

is a PC hexamer. For the target model (excitation, 550 nm): open PSII RCs were 79%; nontransferring PBSs were 14%; and nontransferring PEs were 7%. With this model, they estimated that the EET rate at room temperature was 90 ns^{-1} from APC_{680} to PSI and 50 ns^{-1} from APC_{680} to PSII, while the intra-PBS rates ranged from 11 to 68 ns^{-1}.

2.2 Photosystem II

2.2.1 Crystal Structure of Photosystem II

PSII, with a total molecular mass of 350 kDa per monomer, is a multisubunit protein complex embedded in the TM (Fig. 1). As a light-driven water/PQ oxidoreductase, PSII is the heart of oxygenic photosynthesis (see chapters in Wydrzynski and Satoh, 2005 and reviews by Barber, 2014, 2016; Govindjee et al., 2010; Nelson and Junge, 2015; Nelson and Yocum, 2006; Shen, 2015; Young et al., 2016). The $\{Mn_4CaO_5\}$ complex, at the water splitting site, is situated very close to the lumen (the p-side), but the PQ-binding site is close to the cytosolic phase (the n-side). Similar to other membrane protein complexes (e.g., Cyt b_6f complex; Kurisu et al., 2003; Cramer and Kallas, 2016), the native functional form of the PSII complex in plants, green algae, and cyanobacteria is a dimer in which the two PSII monomers may exchange EE (see a review on PSII excitonic connectivity by Stirbet, 2013).

The very first three-dimensional (3D) structure of PSII, from the thermophilic cyanobacterium *Thermosynechococcus elongatus*, was determined by Zouni et al. (2001) with a resolution of 3.8 Å. Other X-ray crystal structures, at higher resolutions, are now available (e.g., Ferreira et al., 2004; Guskov et al., 2009, 2010; Loll et al., 2005). In addition, structures of PSII from *Thermosynechococcus vulcanus* were also obtained by, for example, Kamyia and Shen (2003) and Umena et al. (2011). We now know that the PSII monomer contains more than 20 different polypeptides, out of which 17 are integral membrane-protein subunits and 3 are extrinsic subunits on the lumen side; in addition, there are ~90 different cofactors in this monomer. We note that the molecular structure of the dimeric PSII complex of the *T. elongatus* is available at a resolution of 2.9 Å (Guskov et al., 2009) and at 1.9 Å (Umena et al., 2011). The main components of the PSII core monomer are: (1) two homologous proteins D1 (PsbA) and D2 (PsbD) that form a heterodimer D1/D2 binding the redox-active cofactors that participate in the primary photochemical events as well as in subsequent PSII ET (see Sections 2.2.5 and 2.2.6); (2) α- and β-subunits of Cytb559; (3) the inner core antenna of PSII, which has two homologous Chl-binding proteins CP43 (PsbC) and CP47 (PsbB), where CP stands for chlorophyll protein complex and the number is the molecular mass in kDa; and (4) three extrinsic membrane proteins (PsbO, PsbV, and PsbU), attached to the lumenal surface; these are essential for the protection of the oxygen evolving complex (OEC) from the outside redox components as well as for the optimization of the ionic environment (see, e.g., Bricker et al., 2012). Furthermore, these are important for the maintenance of channels for water to come to the $\{Mn_4CaO_5\}$ cluster (which has the shape of a distorted chair) and for molecular oxygen and protons to go out of the membrane (see, e.g., Vogt et al., 2015).

PSII core in plants shows an almost identical structure with that of cyanobacteria, but there are also some differences; for example, there are 27 subunits in plants compared to 20 in cyanobacteria (Wei et al., 2016). In addition, the PsbU and PsbV subunits (in cyanobacteria) are replaced by PsbP and PsbQ, and a protein complex PsbW mediates the association of LHCII with the core (in plants); thus, there are many differences between plants and cyanobacteria (cf. Thornton et al., 2004). As mentioned earlier, cyanobacteria lack the Chl-containing peripheral antenna complexes of higher plants, which are replaced by water-soluble PBSs.

2.2.2 The Redox-Active Cofactors of Photosystem II

The D1 and D2 proteins are located symmetrically with respect to the transmembrane region, forming a D1/D2 heterodimer with two branches that together provide the ligands for redox-active cofactors positioned along the pseudo-twofold D1/D2 axis (see Section 2.2.6): (1) six Chls *a* (i.e., P_{D1}, P_{D2}, Chl_{D1}, Chl_{D2}, Chl_{ZD1}, and Chl_{ZD2}; here, the subscripts D1 and D2 refer to the branch on which the specific Chl is attached); (2) two pheophytins, $Pheo_{D1}$ and $Pheo_{D2}$; (3) Q_A (on D2), and Q_B, (on D1), PQ molecules bound to specific amino acids in their respective proteins (see Section 2.2.6 for further information); (4) a nonheme iron situated at equal distance between Q_A and Q_B; (5) two β-Cars; (6) four Mn ions; (7) three or four Ca^{2+} ions (one of which is included in the Mn-cluster); (8) three Cl^- ions; and (9) one carbonate (CO_3^{2-}) or hydrogen carbonate (HCO_3^-) ion bound to the nonheme iron, which is involved in the Q_B protonation during its reduction by Q_A (see Section 2.2.6, and a review by Shevela et al., 2012). Important for the coordination of PSII cofactors are the amino acids with ionic side chains (i.e., Asp, Glu, and His).

2.2.3 The Inner Antenna of Photosystem II

The inner PSII antenna proteins CP43 and CP47 are positioned on each side of the D1/D2 heterodimer, forming a CP43/D1/D2/CP47 cluster, and contain 13 and 16 Chls *a* (ligated mainly to histidine residues), as well as 4 and 5 β-Cars; these

pigments are located in two layers toward both surfaces of the TM, each with one Chl *a* placed in the middle between the layers (see, e.g., Barber, 2014; Ferreira et al., 2004). Under the pseudo-twofold symmetry, 13 of the 16 Chls of CP47 have a symmetry partner in CP43, while the additional Chls with no analog in CP43 are in the main lumenal domain: Chl 612(11), Chl 613(12), and Chl 617(16), with the Chls labeled with the numbering system used by Umena et al. (2011); the numbering in parentheses are those of Loll et al. (2005). The function of Chls in this inner antenna is to "capture" photons, as well as to receive EE from the PBS, and direct this energy to the Chls in the RC, where the primary photochemistry takes place (see Section 2.2.4).

The Chls in CP43 and CP47 are located at an optimum distance from the Chls in the PSII RC (e.g., ~25 Å for CP47; Zouni et al., 2001), the latter being highly oxidizing after charge separation; they are sufficiently close to accept EE from the antenna Chls, but distant enough to prevent oxidation of Chl in the antenna (van Amerongen and Croce, 2013). Due to this relatively long distance, the EET from CP43/CP47 to the RC occurs with time constants of 40–50 ps (Pawlowicz et al., 2007; van der Weij-de Wit et al., 2011). In models used to determine the RC trapping kinetics, the average trapping time (τ) of excitation is taken as $\tau_{mig} + \tau_{trap}$ (see, e.g., van Amerongen and Croce, 2013). The τ_{mig} is the overall migration time (i.e., the time taken for an excitation created somewhere in PSII to reach the RC), while τ_{trap} is the overall trapping time. The τ_{trap} equals $N \cdot \tau_{iCS}$ (if charge recombination is neglected), where τ_{iCS} represents the intrinsic charge separation time and N is the number of isoenergetic light-harvesting pigments, including the primary (electron) donor. In trap-limited models, τ_{mig} is short enough to be neglected, and thus $\tau = \tau_{trap}$; a well-known example is the exciton/radical pair equilibrium model of Schatz et al. (1987, 1988), which also includes charge recombination and secondary charge separation. Several authors (e.g., Baake and Schlöder, 1992; Belyaeva et al., 2011; Lazár, 2003; see a review by Lazár and Schansker, 2009) have used the above information in models to simulate ChlFI transients. However, τ_{mig} cannot be neglected if Chls in the antenna are at a relative large distance from the RC. Picosecond fluorescence kinetics of PSII in different mutants of *Synechocystis* PCC 6803 have indeed been fitted either with a trap-limited or an energy migration-limited model (Tian et al., 2013).

The carotenoids (Cars) in PSII inner antenna absorb light in the blue-green region of the solar spectrum (see, e.g., Goedheer, 1961 and reviews by Govindjee, 1999; Berera et al., 2009). Studies using ultrafast time-resolved spectroscopy show that although β-Cars transfer EE to Chls of the PSII core, they do so with a lower efficiency than in the PSI core (de Weerd et al., 2003b; Holt et al., 2004). In this regard, by exciting β-Car and by measuring photoinduced ET to and from the PQ pool, Stamatakis et al. (2014) found that, although β-Cars transfer EE to Chl *a* molecules in both the PSs of *Synechococcus* sp. PCC 7942, they lead only to the oxidation of the PQ pool by PSI, but not its reduction by PSII. This shows that β-Cars in PSI do play a role in light harvesting, by widening its absorption cross section, but not those in PSII. In PSII, β-Cars have rather a photoprotective function, through quenching or by preventing the formation of Chl triplet excited states (^{3}Chl*) (which are potential singlet oxygen sensitizers), as well as by scavenging singlet oxygen ($^1O_2$) and other ROSs near the RC (Siefermann-Harms, 1987; Britton, 2008).

2.2.4 Spectral Characteristics of Chlorophyll-Protein Complexes of the Photosystem II Core

At room temperature, Chl fluorescence in cyanobacteria, green algae, and plants is mostly due to PSII. Steady-state emission spectrum shows a main band with a fluorescence maximum (F_{max}) at 685 nm (F685), which is mostly from PSII, and a small shoulder at $\lambda > 700$ nm, which is due to both PSII and PSI. (Note that in cyanobacteria, the PSI to PSII ratio is often 3–5:1 instead of 1:1, as it is in plants and algae; thus, the contribution of room temperature PSI fluorescence is higher in cyanobacteria than in plants.) At very low temperatures (e.g., 77 K), the absorption and fluorescence bands are much more clearly resolved. The resulting higher spectral resolution allows us to observe new emission bands at 720–730 nm and at 693–698 nm that are not at all obvious at room temperature: (1) the fluorescence band at 720 nm, discovered in the green alga *Chlorella* (Brody, 1958), is from PSI, originating from long-wavelength Chls (LWCs) in the core antenna, absorbing in the 698–705 nm region (Boardman et al., 1966; Das and Govindjee, 1967; Fromme et al., 2003); and (2) the fluorescence between 693 and 698 nm from PSII (Bergeron, 1963; Govindjee and Yang, 1966; Kok, 1963; Krey and Govindjee, 1964), which was shown later to originate from LWCs in CP47 (see discussion below). Brody (1958) was the first to measure Chl fluorescence at 77 K on any photosynthetic samples, and found that the new fluorescence band at 720 nm in *Chlorella* cells was much higher than the one at 685 nm, which predominates at room temperature. Furthermore, in their study of EET at different temperatures, Cho and Govindjee (1970a,b) measured both fluorescence emission and excitation spectra in *Chlorella* and in the cyanobacterium *A. nidulans* (*Synechococcus* PCC7942) from 77 K down to 4 K (see Fig. 4 for some of the results on *A. nidulans*).

We also note that measurements of Chl fluorescence spectra at cryogenic temperatures (i.e., <100 K) indicate light-induced PSII fluorescence quenching that is most probably due to Chl_{ZD1} oxidation (Schweitzer and Brudvig, 1997; Schweitzer et al., 1998). At these low temperatures, following the primary charge separation, Chl_{ZD1} and Cyt b559 compete

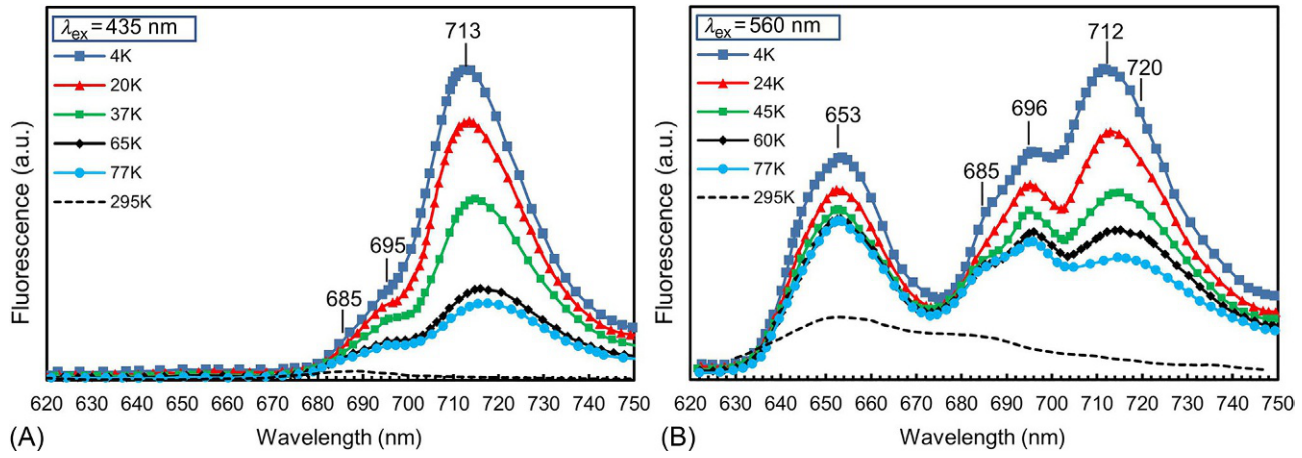

FIG. 4 Steady-state emission spectra of *Anacystis nidulans* in the 4–77 K temperature range. (A) Emission spectra for excitation at 435 nm (absorption by Chl *a*, which in cyanobacteria are more numerous in PSI than in PSII; Jordan et al., 2001; Umena et al., 2011); the 295 K fluorescence spectrum *(the black dashed curve)* is also shown for comparison. (B) Emission spectra for excitation at 560 nm (absorption by phycocyanin from phycobilisomes, which are attached preferentially to PSII); the 295 K fluorescence spectrum *(the black dashed curve)* is also shown for comparison. *a.u.*, arbitrary units. *(Modified from Cho, F., Govindjee, 1970b. Low temperature (4-77 K) spectroscopy of* Anacystis*: temperature dependence of energy transfer efficiency. Biochim. Biophys. Acta 216, 151–161.)*

to reduce $P680^+$ (de Paula et al., 1985; Okayama and Butler, 1972), instead of the tyrosine residue 161 of the D1 protein (i.e., Y_Z) via the S-states of the OEC (see Section 2.2.6). Schweitzer and Brudvig (1997) suggested that even a small fraction of 15% Chl_{ZD1}^+ can quench 70% of the low-temperature fluorescence due to excitonic connectivity between PSIIs in the TM.

The assignment of various Chl emission bands of low-temperature fluorescence spectra to specific Chl *a*-protein complexes and Chls has been useful in the study of EET in the antenna and primary charge separation (see, e.g., Karapetyan et al., 2014). Chl *a*-protein complexes of the PSII core (i.e., D1, D2, CP47, and CP43) have, in addition to a large Soret band at 440 nm, several absorption bands between 660 and 690 nm and fluorescence maxima (at 77 K) between 683 and 780 nm (see Table 2).

The Q_y absorption region of isolated D1/D2/cytb559 particles at room temperature has a maximum at 675.5 nm that splits into two peaks at about 670 and 679 nm at cryogenic temperatures (see, e.g., Tetenkin et al., 1989); the first peak is generally assigned to the accessory Chls and the second one mainly to P680. D1/D2/cytb559 has a broad fluorescence band with a peak near 684 nm (i.e., F684; Groot et al., 1994) that was attributed to P680 (i.e., the pair P_{D1}/P_{D2}); however, F684 in these preparations was recently assigned only to P_{D1} (see discussion in Section 2.2.5). At 77 K, the CP43 complex shows absorption bands in the Q_y region at 660, 669, and ~679 nm, and a small band at ~682.5 nm (see, e.g., de Weerd et al., 2002; Groot et al., 1999), while the CP47 complex displays bands at ~661, ~670, ~677, and ~683, and a small one at ~690 nm (de Weerd et al., 2002; Groot et al., 1995). The 695 nm fluorescence band (F695), as well as a low-energy fluorescence band near 690–691 nm, have been assigned to Chl *a* molecules in the CP47 complex (see, e.g., Gasanov et al., 1979; Dekker et al., 1995; Groot et al., 1995; Reppert et al., 2010). Also, a low-energy fluorescence band at ~683 nm was attributed to Chls in the CP43 complex (see, e.g., Dang et al., 2008). Furthermore, a very weak emission band near 740 and 780 nm was

TABLE 2 Absorption and Fluorescence Band Maxima of Core Chl *a*-Protein Complexes of PSII at 4–77 K

Complex	A_{max} (nm)	F_{max} (nm)
CP43	660, 669, 679, 682.5[a]	683
CP47	661, 670, 677, 683, 690[a]	690, 695, 753[a]
D1/D2/$Cytb_{559}$	671[a], 679	684, 740[a], 780[a]
P680	680	684

[a]*Minor bands.*

also observed by several authors (Hughes et al., 2007; Krausz et al., 2005; Morton et al., 2014); it has been assigned to emission from a charge-transfer state in the PSII core.

Fluorescence spectra of photosynthetic organisms at low temperatures (see, e.g., Cho and Govindjee, 1970a,b; Murata et al., 1966; Rijgersberg and Amesz, 1980) are quite complex and still not completely understood. The assignment of fluorescence bands at 685–689, 693–698, and 710–740 nm to specific Chl *a* molecules in the two PSs is still being debated. Identification of the low-energy (i.e., lower than that of the primary electron donor) absorption and/or emission from Chls in PSII and PSI cores are important for the understanding of energy transfer kinetics in the PSs (see a review by Chen et al., 2015a); some of the involved Chls are termed "red Chls" or LWCs. LWC can be one of the following (see a review by Reimers et al., 2016 and references therein): (1) Chls in specific locations that have low-energy excited states due to their interaction with the protein scaffold; (2) excitonically coupled assemblies of Chls giving rise to low-energy excited states; (3) low-energy excited states arising from charge transfer transitions; and (4) excitation of a species that was already in an excited state. The location of LWC in CP43 and CP47 is still a matter of debate due to issues related to the purity of isolated complexes (see reviews by, e.g., Hall et al., 2016; Reimers et al., 2016; Reinot et al., 2016 and references therein). CP43 has two Chls with absorption bands centered at ~683 nm (see Table 2); in all likelihood, they are Chl (43) and Chl (45) [Chl *a* numbering is from Loll et al., 2005]. However, CP47 has Chl (29), which has an H-bond to the PsbH subunit; in all probability, it is the best candidate for being the major contributor to the lowest energy trap in this complex (and hence the origin of the F695 emission band of PSII), but Chl (24) and Chl (26) have also been suggested to give F695 (Reinot et al., 2016). Since Chl (29) is close to Car_{D2} and Chl_{ZD2}, it has the potential to dissipate excess energy in the antenna under high light conditions, while since Chl (24) and Chl (26) are located close to the RC, they could efficiently transfer energy to it (Reinot et al., 2016).

2.2.5 Primary Charge Separation in Photosystem II

The pseudo-twofold D1/D2 axis of PSII RC passes through the nonheme iron and the $P_{D1}/P_{D2}/Chl_{D1}/Chl_{D2}$ cluster (see Fig. 5B). Only the D1 branch is active during the initial charge separation processes (Diner and Rappaport, 2002), and this asymmetry seems to be highly influenced by the surrounding protein scaffold (van Amerongen and Croce, 2013). The EE harvested by the inner PSII antenna is funneled to the RC where it oxidizes a Chl *a* species absorbing at 680 nm (P680), considered to be the primary PSII electron donor. In analogy with P870 in the purple bacterial RC, which has a pair of BChl molecules, the pair (P_{D1}/P_{D2}) of Chl molecules here had been assumed to be P680 (see, e.g., Barber and Archer, 2001). However, compared with the pair of BChls in P870, the pyrrole rings of P_{D1} and P_{D2} are less parallel and this disrupts

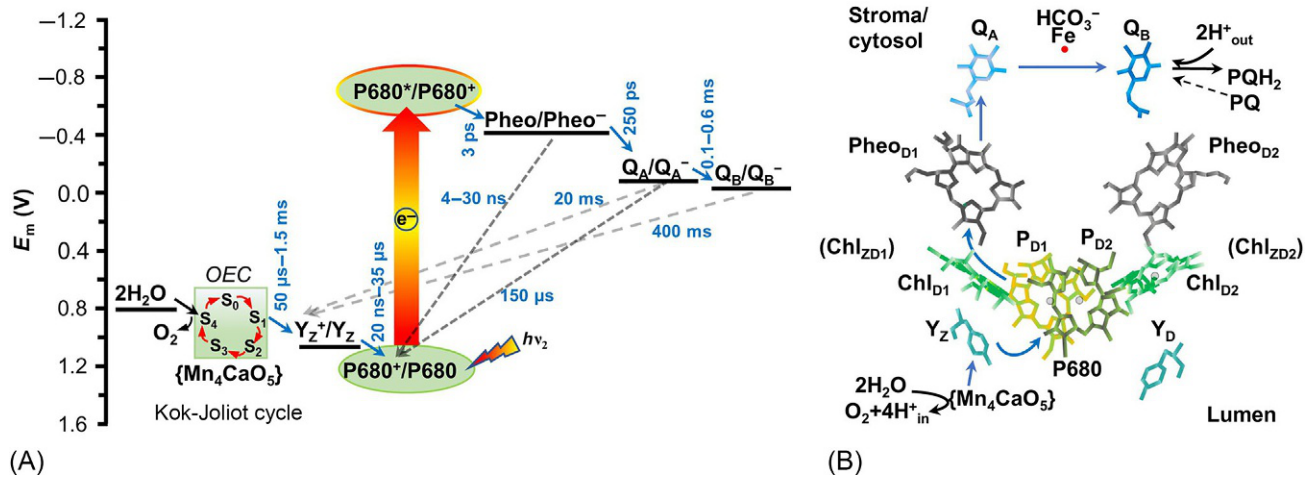

FIG. 5 A schematic diagram of electron transport (ET) reactions in the PSII RC. (A) A scheme for light-induced ET from water to plastoquinone *(plain arrows)*, as well as a simplified diagram of the oxidative water splitting (the Kok-Joliot cycle) and some dark recombination reactions *(dashed gray arrows)*. For standard redox potential (E_m) and rate constant values, see, e.g., Antal et al. (2013). (B) ET between the redox components of PSII shown on a simplified 3D presentation; the locations of Chl_{ZD1} and Chl_{ZD2} are only indicated in parentheses. Chl is chlorophyll; Fe is non-heme iron; HCO_3^- is hydrogen carbonate ion bound to the nonheme iron Fe; OEC is oxygen-evolving complex; P680 and P680* is the chlorophyll pair (P_{D1}/P_{D2}) in the ground and excited electronic states; Pheo is pheophytin; PQ and PQH_2 are plastoquinone and plastoquinol; Q_A and Q_B are primary and secondary (bound) plastoquinone electron acceptors of PSII; S_0, S_1, S_2, S_3, and S_4 are the S-states of the OEC, as defined by Kok et al. (1970); Y_Z and Y_D are redox-active tyrosine residues of the D1 and D2 proteins, respectively. *(The 3D presentation of PSII redox factors was modified from Tikhonov, A.N., 2013. pH-dependent regulation of electron transport and ATP synthesis in chloroplasts. Photosynth. Res. 116, 511–534.)*

the overlap of their wave functions, thus having consequences for the primary charge separation processes (Renger and Schlodder, 2010). Theoretical calculations based on the molecular structure of the PSII core have suggested a coupling between the six adjacent central chlorins in the PSII RC; therefore, multimeric models for the excited state of P680 have been proposed (see, e.g., Novoderezhkin et al., 2007; Prokhorenko and Holzwarth, 2000; Raszewski et al., 2008), in which the exciton transitions are delocalized over the entire cluster of these six molecules: P_{D1}, P_{D2}, Chl_{D1}, Chl_{D2}, Phe_{D1}, and Phe_{D2}.

Over the years, various spectroscopic techniques have been used to study the EET and charge separation in PSII (see reviews by Mamedov et al. 2015; Mirkovic et al., 2017 and references therein). In the very first experiments with time-resolved pump-probe absorption spectrometry, Wasielewski et al. (1989) used a 610 nm (500 fs) laser light, and inferred from their data that the formation of the radical pair $P680^+ Pheo_{D1}^-$ and disappearance of $P680^*$ in the PSII RC at 4°C took place within ~3 ps (see also Govindjee and Wasielewski, 1989). Prokhorenko and Holzwarth (2000) using both photon-echo and transient absorption measurements to measure the same charge separation in the PSII RC suggested a slightly faster (1.5 ps) charge separation step $\left(Chl_{D1}Pheo_{D1}\right)^* \rightarrow Chl_{D1}^+ Pheo_{D1}^-$ and a much slower (25 ps) secondary charge separation process ($Chl_{D1}^+ Pheo_{D1}^- \rightarrow P_{D1}^+ Pheo_{D1}^-$). Later, based on precise information about the PSII core structure coupled with transient absorption spectroscopy data, Holzwarth et al. (2006a) reported a 5.5 ps initial charge separation, $Chl_{D1}^+ Pheo_{D1}^-$, followed by a slower (35 ps) secondary charge separation $P_{D1}^+ Pheo_{D1}^-$. In both these studies, Chl_{D1} was suggested to be the primary electron donor. Subsequently, low-temperature studies by Novoderezhkin et al. (2005, 2007) and by Romero et al. (2010), where experimental data were analyzed by global and target analysis, indicated that multiple pathways for charge separation are possible (due to the disorder produced by slow protein motions). Romero et al. (2010) found that charge separation processes start with the excited states $(Chl_{D1}Phe_{D1})^*$ or $(P_{D1}P_{D2}Chl_{D1})^*$, which give rise to two different pathways for charge separation with time constants of 400 fs and 1.8 ps, respectively. However, Shelaev et al. (2008, 2011) proposed an alternative model, in which $P680^+Chl_{D1}^-$ is the initial radical pair (instead of $Chl_{D1}^+ Phe_{D1}^-$), followed by the reduction of $Pheo_{D1}$ (reviewed by Mamedov et al., 2015).

Recently, Duan et al. (2018) used two-dimensional (2D) optical photon echo spectroscopy and theoretical calculations to separate the charge transfer dynamics from the energy transfer dynamics. They used four primary charge separated states in their theoretical modeling: $P_{D2}^+ P_{D1}^-$, $Chl_{D1}^+ Pheo_{D1}^-$, $P_{D1}^+ Chl_{D1}^-$, and $P_{D1}^+ Pheo_{D1}^-$ (cf. Novoderezhkin et al., 2011). Duan et al. (2018) concluded that a charge separation component with the time constant of 1.5 ps is clearly resolved at ambient temperatures and corresponds to $\left(Chl_{D1}Pheo_{D1}\right)^* \rightarrow Chl_{D1}^+ Pheo_{D1}^-$. The suggested secondary charge separation processes are: $Chl_{D1}^+ Pheo_{D1}^- \rightarrow P_{D1}^+ Pheo_{D1}^-$, and $\left(P_{D1}P_{D2}\right)^* \rightarrow \left(P_{D2}^+ P_{D1}^-\right) \rightarrow P_{D1}^+ Chl_{D1}^- \rightarrow P_{D1}^+ Pheo_{D1}^-$.

2.2.6 *Electron Transport in Photosystem II*

The charge separation events in the PSII RC generate a strong oxidant ($P680^+/P680$; $E_m = +1.2$ V) and a weak reductant ($Pheo^-/Pheo$; $E_m = -0.536$ V); the redox potentials, noted here, had been measured in *Synechocystis* sp. PCC 6803 by Allakhverdiev et al. (2010).

Let us not forget that the efficiency of exciton trapping in PSII RC depends strongly on the redox states of the chromophores in the RC and of the secondary electron acceptor Q_A.

The ET pathway in PSII is shown in Fig. 5, with water oxidation on the lumenal (p) side of the membrane and PQ reduction on the cytosolic (n) side of PSII, that is, on the stromal side of the membrane. We will now summarize these reactions [see also Barber, 2008 and references therein], which have often been studied using ChlF measurements [see, e.g., chapters in Papageorgiou and Govindjee, 2004]. After the generation of the radical pair $P680^+Pheo^-$, $Pheo^-$ reduces Q_A in ~250 ps, producing $P680^+ PheoQ_A^-$. Then, $P680^+$ is reduced back to P680, in the time range of 20 ns–35 µs, by ET from the tyrosine residue 161 of the D1 protein (Y_Z); thus, $Y_Z^{\bullet} P680PheoQ_A^-$ is formed, where $Y_Z^{\bullet}$ is a neutral radical generated through proton transfer most likely to His 190 of D1 (Hays et al., 1999). We note here that both $P680^+$ and $Pheo^-$ are quenchers of ChlF (see, e.g., for $P680^+$: Butler et al., 1973; Shinkarev and Govindjee, 1993; Bruce et al., 1997; and for $Pheo^-$: Klimov et al., 1977). Longer fluorescence lifetimes and higher fluorescence yields are obtained only after the reduction of $P680^+$ as well as the oxidation of $Pheo^-$ (i.e., $Y_Z^{\bullet} P680PheoQ_A^-$). Finally, Q_A^- reduces Q_B within 0.1–0.6 ms, forming $Y_Z^{\bullet} P680PheoQ_A Q_B^-$, while $Y_Z^{\bullet}$ extracts an electron from the $\{Mn_4CaO_5\}$ cluster that is known to bind two H_2O molecules.

For the reactions on the (electron) donor side of PSII, Kok et al. (1970) developed a model of water oxidation based on their experiments, as well as on those of Joliot (1965) and Joliot et al. (1969), in which OEC is suggested to exist in one of the five oxidation states, labeled S_0, S_1, S_2, S_3, and S_4 (see Fig. 5A). In this model, after each photochemical reaction at PSII RC, a single electron is transferred from the OEC to it, advancing OEC to the next higher S-state (see Joliot and Kok, 1975; Mar and Govindjee, 1972). Thus, after four such reactions, two water molecules are oxidized to one molecule of oxygen. Since Mn is the redox-active metal in the $\{Mn_4CaO_5\}$ cluster, extensive effort has been made to study its behavior. Identifying the steps of this essential process in oxygenic photosynthesis at the molecular level has proven to be a

challenging problem, and structural and functional data on the $\{Mn_4CaO_5\}$ cluster obtained with various techniques have been important in the recent progress on this problem (see, e.g., Cox et al., 2008; Pushkar et al., 2008; Retegan et al., 2014; Shen, 2015; Shinkarev et al., 1997; Siegbabahn, 2011).

Of the two electron acceptors Q_A and Q_B in PSII, Q_A (a one-electron acceptor) is permanently bound to D2, whereas Q_B (a two-electron acceptor) is weakly bound to the D1 protein. After the primary charge separation, $Pheo^-$ reduces Q_A, forming $P680^+ PheoQ_A^-$. Then, the Q_A^- reduces Q_B to Q_B^- (that remains tightly bound to D1); but once Q_B has been fully reduced by the addition of two electrons (after two "light" reactions) and two protons have been added (see below for further information), the resulted weakly bound Q_BH_2 (which is nothing else but a PQH_2) is released in the membrane and is replaced by a PQ molecule from the PQ pool. This process is known as the "two-electron gate" (Velthuys and Amesz, 1974), since two electrons are needed for the reduction of Q_B; the kinetics of this reaction has been measured through ChlF decay after brief saturating light flashes (see, e.g., Robinson and Crofts, 1983). In Fig. 5A, we also show the recombination reactions between $Pheo^-$ or Q_A^- with $P680^+$, and between Q_A^- or Q_B^- with Y_Z^+. These are often measured using ChlF and thermoluminescence (see, e.g., DeVault et al., 1983; DeVault and Govindjee, 1990; Rose et al., 2008; Rutherford et al., 1984; Vass and Govindjee, 1996), providing valuable information on the redox properties of the above-mentioned components.

As mentioned earlier (see Section 2.2.2), a bicarbonate ion (HCO_3^-) is bound on the nonheme iron located between Q_A and the Q_B-site (Umena et al., 2011); it is essential for the functioning of the "two-electron gate" (see Govindjee et al., 1976) and the formation of PQH_2 (for this "bicarbonate" effect, see the review by Shevela et al., 2012 and papers by Cao and Govindjee, 1988; Cao et al., 1991, 1992; Eaton-Rye and Govindjee, 1988; Khanna et al., 1977; Vermaas et al., 1982). This unique bound bicarbonate ion has been suggested to play a critical role in the reduction of Q_B with it functioning as a proton donor to Q_B^{2-}. In addition to this, there are effects of HCO_3^- on the donor side of PSII (see a review by Stemler, 1982), and the mechanism of this action is under active discussion (Ananyev et al., 2018).

2.3 Photosystem I

2.3.1 Crystal Structure of Photosystem I

PSI functions as a Pc/Fd (photo)-oxidoreductase, which, in cooperation with PSII, leads to a linear ET from H_2O to $NADP^+$, where Pc and Fd are water-soluble, one electron redox carriers (see Croce et al., 2018; Golbeck, 2006; Fromme and Grotjohann, 2011; Kargul et al., 2012; Nelson and Junge, 2015; Nelson and Yocum, 2006). The most remarkable property of PSI is its high efficiency; it operates with a quantum yield close to 1.0 (Nelson and Yocum, 2006). PSI complexes in cyanobacteria form trimers that are in equilibrium with PSI monomers, which vary as a function of concentration of cations (Kruip et al., 1994) or protons (Schwabe et al., 2001); this aspect of cyanobacteria is quite different from that in plants and green algae, where PSIs exist only as monomers. PSI is much larger in size than PSII, but its protein subunit composition is a bit less complex. The crystal structure of the trimeric PSI complex of the thermophilic cyanobacterium *T. elongatus* was solved at a resolution of 2.5Å (Fromme et al., 2001; Jordan et al., 2001); a PSI monomer was shown to contain 12 protein subunits (PsaA-F, PsaI-M, and PsaX) and 127 cofactors: 96 Chls and 22 Cars; 2 phylloquinones (A_{1A} and A_{1B}); 3 [4Fe-4S] clusters; 1 putative Ca^{2+} ion; and 4 lipid molecules. The largest two transmembrane subunits PsaA and PsaB are highly homologous, a product of gene duplication; they form a PsaA/B heterodimer, with their two branches arranged in a pseudo-C2 symmetry providing His ligands that coordinate antenna Chl *a* molecules and the RC chromophores (P700 and A_0), as well as Cys ligands that coordinate the [4Fe-4S] center F_X. On the other hand, PsaC, another PSI protein, binds the [4Fe-4S] centers F_A and F_B. The main function of the small integral subunits PsaF, PsaI, PsaJ, PsaK, and PsaL is the stabilization of the core PSI antenna system.

Although the crystal structure of PSI core complex of *T. elongatus* is quite similar to those of plants (Ben-Shem et al., 2003), there are several differences, for example, the subunit PsaL is quite different in the two systems. Furthermore, subunits PsaX and PsaM are only present in cyanobacteria, whereas, plants contain subunits PsaG and PsaH. The PsaG subunit in plants forms an anchoring point for the Lhca subunits of the PSI peripheral antenna, while the subunit PsaH, together with PsaL and PsaK, have been shown to play important roles in state transitions in plants and green algae (see, e.g., Kouřil et al., 2005; Zhang and Scheller, 2004). In cyanobacteria, PsaM and PsaL are responsible for PSI trimer formation (Jordan et al., 2001; Schluchter et al., 1996); in addition, a different PsaL structure and the absence of PsaM explain why PSIs are only monomeric in plants. Moreover, on the lumenal side of the membrane in plants, the subunit PsaF facilitates a better Pc binding, which increases by two orders of magnitude the rate of ET from Pc to P700 compared to that in cyanobacteria (Hippler et al., 1996; Ueda et al., 2012).

As mentioned earlier, PSI in cyanobacteria is generally assumed to interact with PBS mainly during *state transitions*, but there is no detailed information available on their direct interaction. A special PBS-PSI supercomplex has been found in *Anabaena* sp. PCC 7120, in which PSI is a tetramer (Watanabe et al., 2014). In addition, a mutant of *Synechocystis* sp.

PCC 6803, with an inactivated (or knockout) gene of the rod-core linker PcpG2 (see Section 4.1.1), has a unique type of PBS without a core. Although this PBS, known as CpcG2-PBS, interacts with PSI through rods (Kondo et al., 2007), it is not involved in state transitions (Kondo et al., 2009). Recently, Gwizdala et al. (2018b) measured spectral dynamics of PC rods (also without any core) isolated from the ΔAB mutant of *Synechocystis*; this mutant has PBS with rods, but without core (Ajlani et al., 1995). In addition, these rods have been shown to switch between two spectrally different conformations (with maxima at 651 or at 672 nm). This switch has been attributed to the interaction of PC with the linker polypeptides. Gwizdala et al. (2018b) have suggested that the red-shifted chromophores (i.e., those with maxima at 672 nm) may be involved in direct EET to PSI in the PBS-PSI supercomplexes, as reported by Kondo et al. (2007, 2009) and Watanabe et al. (2014).

2.3.2 Arrangement of the Redox-Active Cofactors of Photosystem I

The redox-active cofactors in PSI are arranged on two branches along the pseudo-C2 axis of the PsaA/B heterodimer (see Section 2.3.6), which consists of 22 transmembrane helices (Nelson and Junge, 2015). We now provide information on the names and location of all the cofactors involved: (1) on the lumenal side of the membrane, there are two chlorins (at 6.3 Å distance) that form the P700 (Kok, 1957), which is a heterodimer of Chl *a* and Chl *a′* (where Chl *a′* is the C-10 epimer of Chl *a*); this arrangement is slightly different from that in P680 of PSII, where P_{D1} and P_{D2} are both identical Chl *a* molecules; (2) two monomeric Chls, labeled as A_{accA} and A_{accB}, are situated at ~12 Å from P700; (3) two more monomeric Chls, labeled as A_{0A} and A_{0B}, are situated still further from P700, at 20–21 Å; (4) two molecules of phylloquinone, PhQ (2-methyl-3-phytyl-1,4-naphthaquinone), A_{1A} and A_{1B}, are located still farther from P700; and (5) there is a [4Fe-4S] cluster (known as F_X), situated on the top of the pseudo-C2 axis, that receives electrons from either of the two phylloquinones A_1. As already mentioned, the PsaC subunit (on the cytosolic side of the membrane) binds two terminal [4Fe-4S] clusters, F_A and F_B, which participate in ET toward Fd/flavodoxin.

2.3.3 The Inner Photosystem I Antenna

In the PSI core, the majority of antenna Chl *a* molecules are situated in the N-terminal six helix domain of PsaA and PsaB subunits, playing a light-harvesting role (just as Chls do in CP47 and CP43 in PSII). In addition, 10 Chl *a* molecules are associated with the subunits PsaG, PsaL, PsaM, PsaK, and PsaX, as well as a phosphatidylglycerol molecule. With the exception of two Chl *a* molecules that seems to form a "bridge" between the RC and the antenna, the distance between adjacent Chls *a* in the PSI inner antenna is in the range of 6–16 Å and the distance between any of the antenna Chls *a* to the RC cofactors is >18 Å. The Chl network in the PSI core forms a rather random array surrounding the RC; this is in contrast to that of BChls in the purple bacteria, where the chromophores are organized in a highly symmetric ring-like structure (Hu et al., 1997). In a study of EE migration in the trimeric cyanobacterial PSI, Şener et al. (2004) suggested the existence of excitonic connectivity between the antennas of PSI monomers. As shown for PSII (see Section 2.2.3), the excited-state decay kinetics of PSI in cyanobacteria was also found to be neither purely trap limited, nor purely (transfer to the trap) limited (Byrdin et al., 2000).

Since cyanobacteria have a high stoichiometric ratio of PSI to PSII (usually 2–6), 80%–95% of total Chls *a* and 73%–93% of Cars are located in PSI (Fujita et al., 1994). In all 60 of the 90 Chls in the PSI inner antenna are in immediate contact with Cars, with the majority of β-Cars located near the long wavelength Chls *a* (i.e., LWC); no carotenoid molecule is situated close to P700. Besides their role in light harvesting and photoprotection, mentioned earlier for PSII, Cars are known to be necessary for the assembly and stabilization of pigment-protein complexes (Wang et al., 2004).

2.3.4 Spectral Characteristics of Chlorophyll-Protein Complexes, and of Long-Wavelength Chls of Photosystem I

The inner antenna of PSI in cyanobacteria (as well as of green algae and plants) is heterogeneous, both spectrally and kinetically. In addition to Chl680 (i.e., Chl molecules with a broad absorption band centered around 680 nm), which makes up the bulk Chls, a minor (3%–10%) pool of Chls *a* (LWCs) absorbing at longer wavelengths of light (i.e., 710–750 nm) also exist (see reviews by Gobets and van Grondelle, 2001; Karapetyan et al., 1999, 2014; Schlodder et al., 2005, 2011). The number of Chls *a* contained in the LWC pool, as well as their absorption maxima, are highly species dependent. An LWC absorbing at 708 nm (Chl708), with the fluorescence maximum at ~720 nm, was identified in both PSI monomers as well as in trimers of *Synechocystis* PCC 6803 (van der Lee et al., 1993; Gobets et al., 1994). Other LWCs are: Chl710, Chl715, and Chl719 located, for example, in PSI trimers of *Synechococcus elongatus* (Pålsson et al., 1996) as well as Chl710 in PSI monomers and Chl740 in PSI trimers in *Arthrospira platensis*, also called *Spirulina* (Schlodder et al., 2005; Shubin et al., 1993; see Fig. 6A).

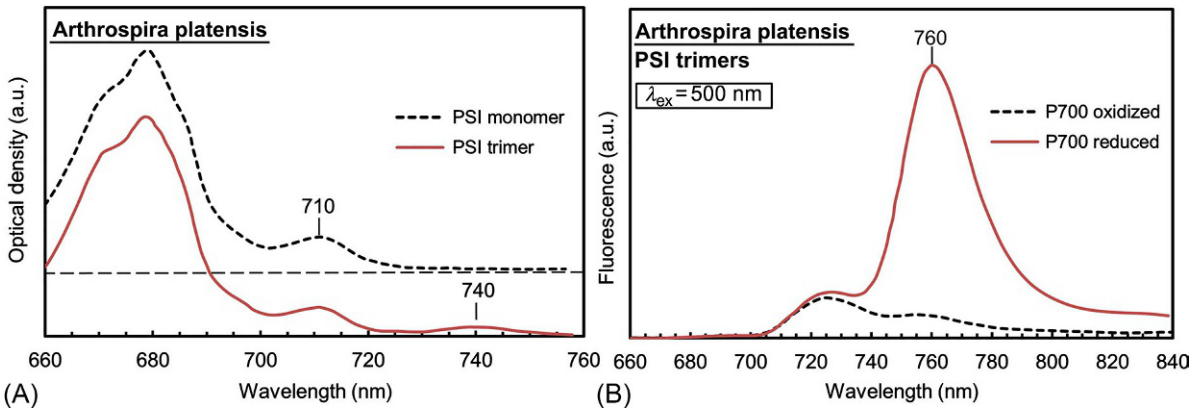

FIG. 6 Steady-state absorption and emission spectra of PSI complexes from *Arthrospira platensis*. (A) 6 K absorption spectra of PSI trimers *(plain line)* and PSI monomers *(dashed line)*. See the absorption bands of the low-wavelength chlorophylls Chl710 and Chl740. (B) 77 K fluorescence spectra (excitation $\lambda = 500$ nm) of PSI trimers with reduced P700 (i.e., P700; *solid line*) and oxidized P700 (i.e., $P700^+$; *dashed line*). See how the F760 from Chl740 is quenched in the PSI trimer with oxidized P700. *a.u.*, arbitrary units. *((A) Modified from Gobets, B., van Grondelle R., 2001. Energy transfer and trapping in photosystem I. Biochim. Biophys. Acta 1507, 80–99; (B) modified from Schlodder, E., Hussels, M., Cetin, M., Karapetyan, N.V., Brecht, M., 2011. Fluorescence of the various red antenna states in photosystem I complexes from cyanobacteria is affected differently by the redox state of P700. Biochim. Biophys. Acta 1807, 1423–1431.)*

In the PSI trimer of *S. elongatus*, the location of Chl719 was suggested to be at the trimeric interface region, as it is missing in the monomeric unit (Pålsson et al., 1998). Furthermore, an LWC called P750 was long ago observed in *A. nidulans* (*Synechococcus*) by Govindjee (1963), which has a 760-nm fluorescence band at 77 K similar to that of Chl740 in PSI trimers of *A. platensis* (see Fig. 6B); thus, P750 may have, as Chl740, a photoprotective role in photosynthesis (see below for discussion on Chl740), but other possible functions of P750 that are not related to PSI have also been suggested (Govindjee and Shevela, 2011).

The number of LWCs depends on the PSI aggregation state (Gobets and van Grondelle, 2001): in monomeric PSI preparations, there are fewer LWCs than in trimers. Changes in pigment-protein and pigment-pigment interactions are responsible for differences in Chl *a* absorption bands. LWCs in the PSI inner antenna often consist of closely coupled dimers or larger aggregates of three to seven Chls in which the excitonic and charge transfer states are mixed (Gobets et al., 1994; Jordan et al., 2001; Romero et al., 2008). When the LWCs are excited directly, their fluorescence is much more anisotropic than when the main pool of Chls is excited (Wittmershaus et al., 1992); this shows that these LWCs have a higher degree of orientation. Karapetyan et al. (2014) showed that the presence of LWCs in the PSI inner antenna not only decreases the quantum yield of exciton trapping, but also the number of energy transfers between the bulk Chl680 molecules, while there is an increase in the PSI absorption cross section (CS_{abs}), promoting EET between the monomers within a trimer and protecting the RC against excess energy when it is inactive. Such a photoprotective role is played, for example, by Chl740 in PSI trimers of *Spirulina* cells (which live in alkaline lakes under high light conditions). Karapetyan et al. (1999) have discussed that fluorescence at 760 nm (F760), from Chl740, depends on the redox state of P700; it is strongly quenched when PSI RCs are closed (i.e., with $P700^+$) (see Fig. 6B). This quenching has been ascribed to EE migration from Chl740 (that consists of several excitonically coupled Chls at the trimeric interface region, which are located on different monomers) to $P700^+$ (Shubin et al., 1991, 1993). Therefore, when one PSI monomer is "closed," the EE from the other monomers migrates via Chl740 to the antenna of the monomer with PSI RC closed, which is then quenched (i.e., dissipated as heat) by $P700^+$ (see Fig. 7).

At room temperature, the fluorescence spectrum of the PSI complex from *Synechocystis* PCC 6803 has a 685-nm band and a shoulder at 712 nm (Wittmershaus et al., 1992), while the fluorescence spectrum of PSI trimers from *A. platensis* has a band between 730 and 735 nm that is even more intense than the 685 nm band (Schlodder et al., 2005). PSI fluorescence spectra, especially at low temperatures, are greatly influenced by the presence of LWCs (Golbeck, 1987). This is because there is a fast (few ps) EET from the bulk Chls to LWCs, which significantly increases the fluorescence quantum yield of the LWCs (see reviews by Gobets and van Grondelle, 2001; Karapetyan et al., 2006); ChlF in PSI is emitted mainly from the LWCs (Brecht et al., 2012). Absorption and fluorescence band maxima of core Chl *a*-protein complexes of PSI from *Synechocystis* PCC 6803 at 4–77 K are listed in Table 3.

Byrdin et al. (2000) observed that the quantum yield of Chl *a* fluorescence of PSI RC in the thermophilic cyanobacterium *T. elongatus* increases at room temperature by ~12% when the PSI RCs are closed (i.e., with $P700^+$), as was subsequently

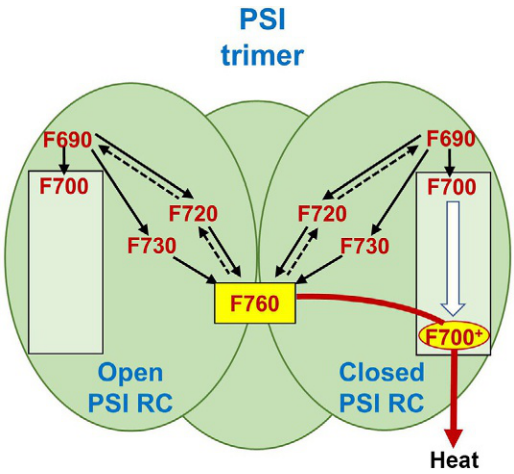

FIG. 7 A diagram of excitation energy (EE) migration between different Chl pools of the core antenna of PSI monomers in a PSI trimer of *Arthrospira platensis*, and energy exchange between the antenna of a monomer with open reaction center (RC) and another with closed RC. The Chl pools are represented by their fluorescence bands: F690, emission of the bulk Chl; F720 and F730 emission of the intermediary longwave Chls; F760, emission of the extremely longwave Chl740, originating from excitonically coupled Chls located on different PSI monomers, which makes possible energy exchange between them. Energy transfer between the pigment pools are indicated by *solid arrows* for downhill transfer, and *dashed arrows* for uphill transfer. The *bold arrow* indicates the dissipation of EE into heat by $P700^+$. *(Modified from Karapetyan, N.V., Holzwarth, A.R., Rögner M., 1999. The photosystem I trimer of cyanobacteria: molecular organization, excitation dynamics and physiological significance. FEBS Lett. 460, 395–400.)*

TABLE 3 Absorption and Fluorescence Band Maxima of Core Chl *a*-Protein Complexes of PSI in *Synechocystis* PCC 6803 at 4–77 K

Complex	A_{max} (nm)	F_{max} (nm)
PsaA/PsaB (main Chl pool)	682	692
PsaA/PsaB (LWC pool)	708	720
P700	698	703

predicted by Lazár (2013) on theoretical grounds (see Section 3). However, Wientjes and Croce (2012) measured only a 4% (±0.7%) increase in the fluorescence quantum yield at room temperature in closed PSI-LHCI from *Arabidopsis thaliana*.

2.3.5 Primary Charge Separation in Photosystem I

The primary radical pair in PSI RC, that is, $P700^+ A_0^-$, is formed within a few ps after P700 receives an exciton (or a photon). In the very first measurements of this primary charge separation in isolated PSI from spinach (Fenton et al., 1979; also see Wasielewski et al., 1987), the time for this reaction was observed to be in the range of 3–14 ps. However, the crystal structure of PSI in *T. elongatus* (Jordan et al., 2001) revealed that the heads of the two chlorins in the Chl *a*/Chl *a′* pair are not perfectly on top of each other, implying that the excitonic coupling in P700 may not be very strong, even if stronger than in P680. Based on this information, Di Donato et al. (2011), Holzwarth et al. (2006b), and Müller et al. (2010) concluded that $A_{acc}^+ A_0^-$ must be the first radical pair in PSI, which can be photogenerated within <1 ps on both the PsaA and PsaB branches (see discussion below), while the time constant for the transfer of the positive charge to P700 would be in the 6–20 ps range. However, the idea that $A_{acc}^+ A_0^-$ is the primary radical pair in PSI is not generally accepted; Shelaev et al. (2010) have, instead, proposed that an excited state delocalized on P700 and A_0 would generate very quickly (within 100 fs) the classical first radical pair $P700^+ A_0^-$ (cf. a review by Mamedov et al., 2015).

2.3.6 Electron Transport in Photosystem I

PSI RCs function over a much more reducing range of redox potentials than the PSII RCs, as they need to generate a sufficiently low redox potential for the reduction of $NADP^+$. In PSI, the redox potential of $P700/P700^+$ is +0.43 V, of A_0 / A_0^- is −1.0 V, and of F_X / F_X^-, F_A / F_A^-, and F_B / F_B^- is ~ −0.7, −0.52, and −0.58 V, respectively (Nelson and Yocum, 2006; for

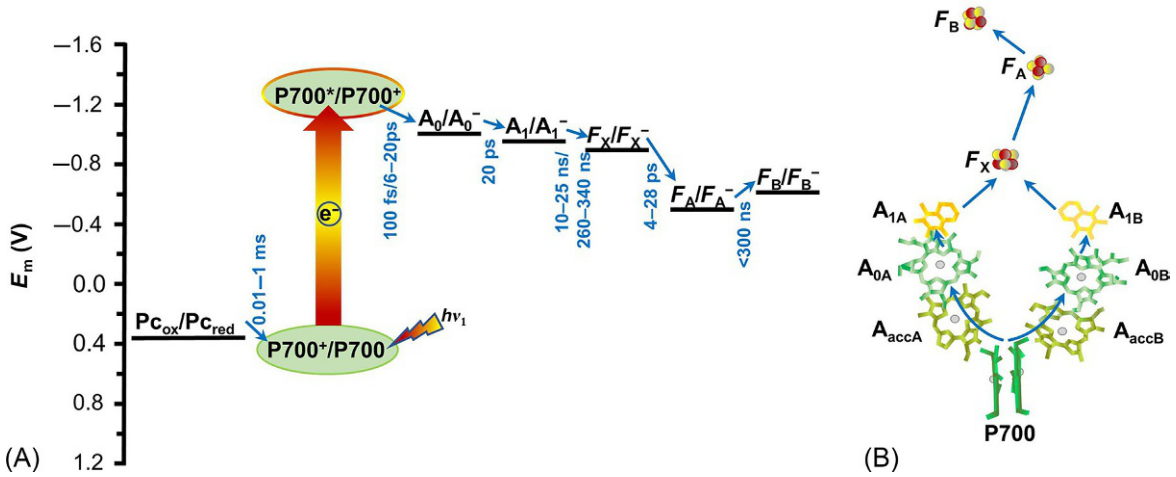

FIG. 8 A schematic diagram of electron transport (ET) reactions in the PSI RC. (A) A scheme for light-induced ET from plastocyanin (Pc) to ferredoxin (Fd) *(plain arrows)*. For standard redox potential (E_m) and rate constant values, see, for example, Antal et al. (2013). (B) ET pathway in PSI shown on a simplified 3D presentation. A_{acc} and A_0 are monomeric Chls; A_1 is a phyloquinone; F_X, F_A, and F_B are [4Fe-4S] clusters; P700 is a (Chl *a*/Chl *a*′) heterodimer in the ground state, where Chl *a*′ is the C-10 epimer of Chl *a*, while P700* represents the excited electronic state. *(The 3D presentation of PSII redox factors was modified from Sun, J., Hao, S., Radle, M., Xu, W., Shelaev, I., Nadtochenko, V., Shuvalov, V., Semenov, A., Gordone, H., van der Est, A., Golbeck J.H., 2014. Evidence that histidine forms a coordination bond to the A_{0A} and A_{0B} chlorophylls and a second H-bond to the A_{1A} and A_{1B} phylloquinones in $M688H_{PsaA}$ and $M668H_{PsaB}$ variants of* Synechocystis *sp. PCC 6803. Biochim. Biophys. Acta 1837, 1362–1375.)*

abbreviations see Section 2.3.2). Note that the ET in PsaC takes place against the redox potential gradient, as F_A is more electropositive than F_B (Heathcote et al., 1978).

Fig. 8 shows a scheme of ET in PSI (Govindjee et al., 2017; Makita and Hastings, 2016). After EET to the PSI RC from its antenna, the radical pair $P700^+A_0^-$ is formed either directly (in 100 fs) or after secondary reactions (in 6–20 ps; see above). Then, A_0^- reduces the phylloquinone A_1 within ~20 ps, which then reduces F_X following biexponential kinetics (Joliot and Joliot, 1999) characterized by time constants of 10–25 ns and 260–340 ns. From F_X, the electron is transferred within 1 ns to the terminal carriers F_A and F_B, and then within ~1 ms to the water-soluble Fd (or flavodoxin) on the cytosolic (n) side of the TM. At about the same time, $P700^+$ is reduced on the lumenal (p) side by Pc (or Cyt c_6) within 0.01–1 ms. When no water-soluble electron acceptors or donors are present, $[F_A/F_B]^-$ and $P700^+$ recombine (via the repopulation of A_1^-) within less than 1 s (Brettel, 1997); however, if electrons from $[F_A/F_B]^-$ are transferred to oxygen (Rousseau et al., 1993), all P700s are rapidly blocked in their closed state (Savikhin et al., 2001).

In contrast to PSII, where only the D1 branch of the D1/D2 heterodimer is known to be redox active, data on PSI have shown that charge separation and ET can take place through both branches of the PsaA/B heterodimer until F_X (see, e.g., Giera et al., 2009; Li et al., 2006). Measurements of PSI ET, by difference absorption spectroscopy, on a mutant of the green alga *Chlorella sorokiniana* lacking most of the PSII and its peripheral antenna, showed biexponential kinetics of the reoxidation of A_1^- (Joliot and Joliot, 1999); these were the first experimental data correlated to a possible bidirectional ET in PSI RC: that is, parallel reoxidation (at different rates) of A_{1A}^- and A_{1B}^- by F_X. This bidirectionality is asymmetric (in favor of branch A over branch B), with ratios at room temperature of, for example, 70:30 (Milanovsky et al., 2014) or 77:23 (Makita and Hastings, 2015). However, a much more symmetrical ratio (i.e., closer to 50:50) could be obtained, depending on the kinetic model used (Makita and Hastings, 2016).

2.3.7 Photosystem I Antenna Under Stress Conditions, Especially Iron Stress

Different types of abiotic stress are common in cyanobacterial habitats, but these organisms have evolved for a very long time and have strategies to overcome many severe environmental conditions. For example, iron limitation is a common nutrient stress for cyanobacteria (Guikema and Sherman, 1984; Martin and Fitzwater, 1988; Singh and Sherman, 2007). Under these conditions, as PSI contains more iron, it decreases even more than PSII (leading to a lower PSI:PSII ratio). In addition, PBSs, Cyts, and Fd (see, e.g., Fraser et al., 2013; Chen et al., 2018) also decrease, with Fd being replaced by flavodoxin (encoded by *isiB*; Fitzgerald et al., 1977). Furthermore, the CP43′ complex (or IsiA, encoded by *isiA*), a homolog of the PsaC subunit of PSII (i.e., CP43), becomes the dominant Chl-binding protein in a number of cyanobacteria, including *Synechocystis* PCC 6803 and *Synechococcus* PCC 7942 (Burnap et al., 1993; Öquist, 1971). IsiA contains 13–16 Chl *a* molecules (see, e.g., Feng et al., 2011), while CP43 has 13 Chl *a*, and the loop connecting helices V and VI of CP43 on the

lumenal side of PSII is missing in IsiA, which thus has ~100 less amino acid residues (Bibby et al., 2001a). However, the IsiA gene was also shown to be induced by other stress factors, such as high salt, high light, high temperature (heat), and oxidizing compounds (Havaux et al., 2005; Kojima et al., 2006; Vinnemeier et al., 1998; Yousef et al., 2003).

Iron deficiency in cyanobacteria has also been shown to cause increased monomerization of PSI trimers, which reduces the effective CS_{abs} of PSI, and lowers the capacity for state transitions (Ivanov et al., 2006). The effect of this stress seems to be relieved by the presence of 18 IsiA complexes surrounding the trimeric PSI core, which act as additional PSI antenna (Bibby et al., 2001b; Boekema et al., 2001); this, of course, increases the light-harvesting cross section (Andrizhiyevskaya et al., 2002; Melkozernov et al., 2003). Furthermore, Wang et al. (2010) have shown the presence of an IsiA-PSI-PSII supercomplex both under iron-deficient and high light conditions. The energy transfer and trapping processes in trimeric PSI and PSI-IsiA supercomplexes from *Synechococcus* PCC 7942, studied by time-resolved absorption difference and fluorescence spectroscopy, showed that EE equilibration in IsiA-PSI supercomplexes is somewhat lengthened compared with that in trimeric PSI (Andrizhiyevskaya et al., 2004). The take home message was that the IsiA ring is an effective light-harvesting antenna for PSI trimers; here, the EE is equilibrated among the IsiA and PSI core antenna chlorophylls before exciton trapping, and the intrinsic time constant for energy transfer from IsiA to PSI is 2 ± 1 ps.

Under long-term iron deficiency, different numbers of IsiA or empty IsiA rings have been observed (see a review by Chen et al., 2018 and references therein). Ihalainen et al. (2005) and Ma et al. (2017) have measured significant excitation quenching in isolated IsiA, and in certain IsiA-PSI complexes, respectively. This fluorescence quenching was suggested to be induced by carotenoids (Berera et al., 2009, 2010), as in Chl-protein complexes in higher plants (see a review by Magdaong and Blankenship, 2018, and chapters in Demmig-Adams et al., 2014). However, a different quenching mechanism was recently proposed by Chen et al. (2017) that involves pigment-protein interaction (i.e., ET from an excited Chl *a* to a Cys residue), as has been reported for bacteriochlorophyll *a*-containing Fenna-Mathews-Olson protein from *Chlorobium limicola*, a green sulfur bacterium (Orf et al., 2016).

3. ANALYSIS OF CHLOROPHYLL *A* FLUORESCENCE INDUCTION IN CYANOBACTERIA: MEASUREMENTS WITH CONTINUOUS AND MODULATED LIGHT

3.1 Chlorophyll *a* Fluorescence Induction and Measuring Techniques

The major use of the light absorbed by the photosynthetic pigments in the antenna of PSII and PSI is for photochemistry, that is, conversion of EE into chemical energy, as initiated by the primary charge separation in the RCs and subsequent ET. However, the excited states of the pigments are also de-excited by at least two other major competing processes: non-radiative dissipation as heat (which can be spontaneous or due to other processes; see Section 4.2) and fluorescence emission (i.e., the radiative deactivation of the first singlet excited state of a molecule to its ground state; Rabinowitch and Govindjee, 1969). Since changes in ChlF reflect changes not only in photochemical, but also in non-photochemical (e.g., heat dissipation) processes, ChlF of photosynthetic organisms (including cyanobacteria) is being used as a highly sensitive and noninvasive tool to monitor various aspects of photosynthesis (see Govindjee et al., 1986; Kalaji et al., 2014, 2017; Papageorgiou and Govindjee, 2004).

Although PBs emit fluorescence (see Section 2.1.1), this is not in direct competition with photochemistry, and thus it provides information mainly on the efficiency of EET from them to the Chls in the two PSs (see, e.g., Acuña et al., 2018a,b; Bruce et al., 1985; Ghosh and Govindjee, 1966). On the other hand, ChlF of plants, algae, and cyanobacteria during a dark-to-light transition is variable in time and carries information about the dynamics of photochemical events, as well as other types of processes, such as NPQ of Chl *a* excited state, state transitions, and photoinhibition. The very first observation of changes in ChlFI, during illumination of a photosynthetic sample, was published by Kautsky and Hirsch (1931); they had used green leaves and observed changes in ChlF intensity using their eyes! The phenomenon has been called the Kautsky effect, ChlF transient, or ChlFI (see a review by Govindjee, 1995) and has important applications in photosynthesis research (see, e.g., Kalaji et al., 2012, 2014, 2017).

To measure ChlFI, samples are initially kept in dark for a fixed time and fluorescence is often measured at wavelengths longer than 700 nm to avoid overlap with the exciting light. In dark-adapted plants, algae, and cyanobacteria, the ChlFI curve shows a fast (hundreds of ms) polyphasic rise to a peak P, the OJIP transient (see Fig. 9A and C), where O is for origin, the minimum fluorescence F_O, while J and I are inflection points between "O" and "P." The initial fast OJIP phase is followed by a slow (minutes) PS(M)T phase, where the fluorescence ultimately reaches a terminal steady-state T (after 5–10 min) at a level close to F_O, depending on the past physiological condition of the organism and the intensity of the excitation light; from "P" there is a decrease in fluorescence to the "S" level, and then there is a rise to a maximum M before fluorescence goes down to the T level (see Fig. 9B and D). The shape of the PS(M)T phase greatly depends on the nature

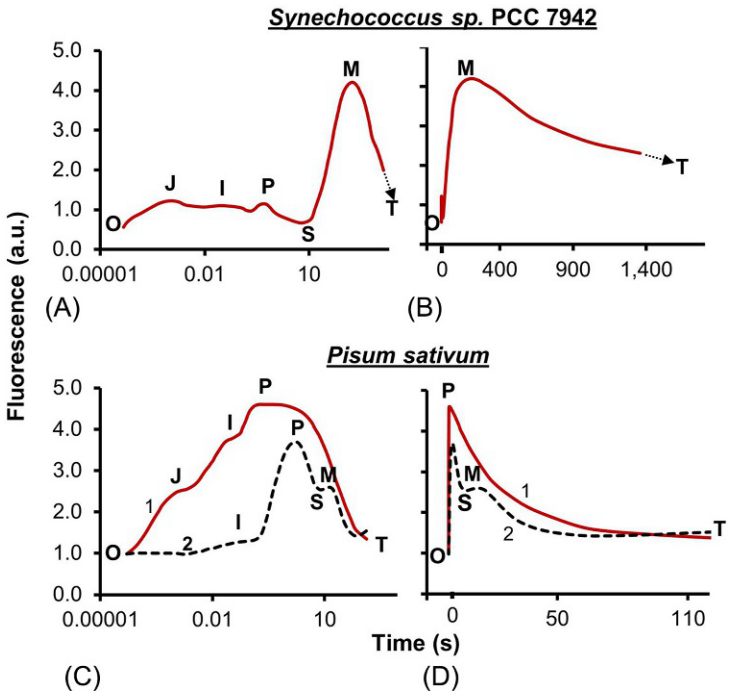

FIG. 9 Chl fluorescence transients measured from *Synechococcus* sp. PCC 7942 cells (A and B) and *Pisum sativum* leaves (C and D). Marked in the diagram are the O, J, I, P, S, M, and T steps, where: O (origin) is minimum fluorescence level; P is the peak; S stands for semi-steady state; M is a maximum; and T is terminal steady-state level. Note that after the M-step, the fluorescence decreases towards T. *All curves* were measured with the PEA (Photosynthetic Efficiency Analyser, Hansatech) instrument under red light of 3000 μmol photons $m^{-2} s^{-1}$, with the exception of *Pisum sativum (curve 2)*, which was measured with 30 μmol photons $m^{-2} s^{-1}$. The *curves* in (A) and (C) are on log (time) scales, whereas the curves in (B) and (D) are on linear (time) scales. *a.u.*, arbitrary units. *(Curves from* Synechococcus *sp. PCC 7942 have been modified from Tsimilli-Michael, M., Stamatakis, K., Papageorgiou, G.C., 2009. Dark-to-light transition in* Synechococcus *sp. PCC 7942 cells studied by fluorescence kinetics assesses plastoquinone redox poise in the dark and photosystem II fluorescence component and dynamics during State 2 to State 1 transition. Photosynth. Res. 99, 243–255; and for* Pisum sativum *from Strasser, R.J., Srivastava, A., Govindjee, 1995. Polyphasic chlorophyll a fluorescence transient in plants and cyanobacteria. Photochem. Photobiol. 61, 32–42.)*

and history of the photosynthetic organism. For general information on ChlFI, see reviews by several authors (Govindjee and Papageorgiou, 1971; Govindjee, 1995, 2004; Krause and Weis, 1991; Lazár, 1999, 2006; Papageorgiou and Govindjee, 2011; Papageorgiou et al., 2007; Schreiber, 2004; Stamatakis et al., 2007; Stirbet and Govindjee, 2012; Stirbet et al., 2014; Strasser et al., 2004).

Today, many types of fluorometers are in use, differing in modes of ChlFI measurement. Apart from some special techniques, such as the pump-and-probe (France et al., 1992; Valkunas et al., 1991), the fast repetition rate method, also called the light-induced fluorescence transient (Kolber et al., 1998; Osmond et al., 2017), and the flash fluorescence induction (Koblížek et al., 2001; Nedbal et al., 1999), ChlFI is mostly measured by two methods. In the first one, after a brief dark period, continuous light is turned on for both fluorescence excitation and induction of photosynthesis (Delosme, 1967; Strasser and Govindjee, 1991; Strasser et al., 2004); here, the ChlFI magnitude, as well as its shape, depend(s) on the light intensity of excitation. One commercial fluorometer often used to measure ChlFI with this technique is the *Plant Efficiency Analyzer* (*PEA*; Hansatech, Norfolk, United Kingdom), which has a high signal to noise ratio and a 10-μs time resolution. The second method is the pulse amplitude modulation (PAM) technique, in which photosynthesis is driven by continuous actinic light while the ChlF is "excited" by very short (few microsecond duration) measuring flashes, fired at a given frequency (i.e., modulated) that is locked in synchronization with a detector cycling at the same frequency (Schreiber, 1986; Neubauer and Schreiber, 1987; Schreiber and Neubauer, 1987). The ChlF signal is detected during the short flash and also a few microseconds after the flash, and both signals are subtracted to find the ChlF signal. One advantage of this technique is that the ChlF signal is proportional to the quantum yield of ChlF by the measuring flashes only. The PAM technique is generally used in the so-called saturating pulse (SP) mode (Bradbury and Baker, 1981; see a review by Schreiber, 2004), in which additional strong saturating light pulses (<1 s) are applied at different time intervals during the ChlFI measurement and subsequent dark relaxation (i.e., when the actinic light is turned off); this PAM-SP technique was first introduced by the Walz company (Effeltrich, Germany), followed by others, for example, Photon Systems Instruments (Brno, Czech Republic).

3.1.1 *Basic Chlorophyll* a *Fluorescence Levels* F_O *and* F_M*: Problems and Concerns*

Changes in fluorescence intensity during the ChlF transient are generally ascribed only to the emission from PSII (see Section 2.2.4), whereas the contribution to ChlF from PSI is generally assumed to be constant (Franck et al., 2002; Pfündel et al., 2013; Trissl et al., 1993; but see Lazár, 2013 and references therein). For reviews presenting ChlFI studies in cyanobacteria, see, for example, Campbell et al. (1998), Campbell and Öquist (1996), Govindjee and Shevela (2011), Ogawa and Sonoike (2016), Papageorgiou (1996), and Papageorgiou et al. (2007).

Two important ChlF levels are defined, F_O and F_M (see Fig. 9), which, however, are not easily measured in cyanobacteria as in plants and algae (see below). The first is the minimum fluorescence, the F_O level, expected to reflect the state in which all PSII RCs are open (i.e., with all Q_A in the oxidized sate). Basically, this level is the result of the so-called transfer equilibrium (Laible et al., 1994), that is, equilibrium of the excited states within all the pigments in the antenna and in the RC before the charge separation occurs. The other level is the maximum fluorescence, the F_M level, which reflects the state in which all PSII RCs are closed (i.e., with all Q_A in the reduced state, Q_A^-). This relationship between ChlF and the redox state of Q_A was first described by Duysens and Sweers (1963) (see a review by Stirbet and Govindjee, 2012). In this hypothesis, fluorescence intensity is related to the fraction of $[Q_A^-]$, but there are alternative views (see, e.g., Schansker et al., 2014). In cyanobacteria, there is an obvious difficulty in getting the F_O due to PSII alone since the contribution of PSI fluorescence is very high due to high (usually 3–5) PSI:PSII ratio. Thus, upfront, we know that there is the measured (apparent) F_O, and the true F_O (corrected for PSI fluorescence); at the same time, PSI fluorescence must be subtracted from the F_M level also. Even after this correction, we need to be sure that all PSIIs are open, at F_O, and no light-induced non-photochemical processes are present, and the sample is in State 1 (i.e., all antenna pigments belonging to PSII are in it), and only then could the initial fluorescence level be taken as the "true" F_O and, consequently, under saturating actinic light, the F_P would be F_M. However, when light-induced non-photochemical processes (that are different in different samples) cause changes in the basic fluorescence levels, we then label them as F_O' and F_M'. Furthermore, the maximum fluorescence during dark recovery (after the actinic light illumination is turned off and closed PSIIs are transitioning to open centers) is labeled as F_M''.

When using a PAM instrument, the F_O level is usually obtained in sufficiently (~10 min) dark-adapted plants and algae. On the other hand, much longer dark adaptation (hours, or even days) is necessary following high light or other stress treatments (Adams and Demmig-Adams 2014 and references therein); the problem is further complex in a cyanobacterial lichen (Demmig-Adams et al., 1990b,c). However, the dark period of about 10 min, in most cases, ensures that Q_A in all the PSII RCs is in the oxidized state. In ChlFI measurements with the continuous-light technique, the F_O in a dark-adapted sample is measured at the beginning of illumination, at a time ranging from 20 to 50 µs. However, a caveat must be given: it is essential that the dark-adapted samples have only Q_B and not Q_B^-, as this is not the case in some samples. If Q_B^- is present, or when PQH_2 remains in the dark, Q_A^- is formed as soon as the light is turned on, raising the F_O level (see, e.g., thermoluminescence experiments in spinach leaves by Feild et al., 1998; Rutherford et al., 1984). On the other hand, if a strong saturating light pulse (thousands of µmol photons $m^{-2} s^{-1}$) is applied to a dark-adapted plant, the F_M level is achieved in few hundreds of ms. The difference between F_M and F_O is the maximum variable ChlF F_V ($=F_M - F_O$), referred to as variable fluorescence.

In cyanobacteria, the real F_O and F_M levels are not as easy to get as in green algae or in higher plants. Since the photosynthetic and respiratory ET chains in cyanobacteria are on the same membrane and share several components (see Fig. 1), the PQ pool is reduced in darkness by, for example, NDH-1 and SDH (Mullineaux and Allen, 1986; Schreiber et al., 1995). The reduced PQ pool causes two opposite effects. As explained above, the presence of PQH_2 in darkness leads to a "false" high F_O level; this fact has been often overlooked in the literature. Also, the reduced PQ pool shifts cells to State 2 in darkness: that is, the CS_{abs} of PSI increases and that of PSII decreases (see Section 4.1). However, the quantum yield of ChlF of PSI is much lower than that of PSII: for example, for plants, it is only 20%–25% of that of PSII at the F_O level (Trissl et al., 1993). Therefore, the transition to State 2 results in a decreased F_O as compared to that in State 1. However, it is difficult, *a priori*, to know which of the two opposing effects would predominate, and the measured F_O in dark-adapted cyanobacteria reflects the interplay of the above two processes. Experiments show that the F_O in dark-adapted cyanobacteria is lower than the "real" F_O mainly due to the State 2 effect (Schreiber et al., 1995; Jallet et al., 2012) and Q_A reduction (due to equilibration with PQH_2) is of lesser importance. As for the F_M level, even if the dark-adapted cyanobacteria are in State 2, as explained earlier, this does not prevent the full reduction of Q_A by a saturating flash. However, since the CS_{abs} of PSII in State 2 is lower than that of PSI, the F_P level reached in this case is lower than that attained when the cells are initially in State 1, which is the real F_M (Schreiber et al., 1995). In addition, it was found that the measured F_O and F_M levels depend on PB:Chl ratio, both levels being higher when this ratio is higher (Campbell et al., 1998; El Bissati and Kirilovsky, 2001). By assuming that PBSs contribute to the fluorescence signal measured by PAM, Acuña et al. (2016a,b) and Ogawa and Sonoike (2016) found that fluorescence from free PBSs is not negligible. Finally, as explained earlier, the contribution of PSI fluorescence

to the fluorescence signal is much higher in cyanobacteria than in plants, because of the higher PSI:PSII ratio. Thus, the "true" value of the ratio $F_V/F_M=(F_M-F_O)/F_M$, relating to the maximum quantum yield of PSII photochemistry (see below) cannot be easily obtained in cyanobacteria.

In view of the above, we need to find ways to evaluate the true ChlF levels for F_O and F_M. To determine a correct F_O value, preillumination of the sample with weak far-red light can be used, as in plants and algae. In addition, weak (~30 μmol photons $m^{-2} s^{-1}$) blue light can be also used to oxidize the PQ pool in cyanobacteria (Schreiber et al., 1995). The reason is that, while blue light is absorbed by Chls in both PSII and PSI, the high Chl content of PSI and high PSI:PSII ratio in cyanobacteria leads to higher absorption of the blue light by PSI. Thus, the PQ fraction reduced during darkness is oxidized by PSI, and leads to a transition from State 2 to State 1, which enables the measurement of a more correct F_O level. However, the F_O obtained in such a way is still higher than the true F_O, due to the PSI contribution. [We also emphasize that the blue light used in the F_O measurement must be weak enough, otherwise it will induce OCP-dependent NPQ (see Section 4.2.1)].

We must remember that to keep the State 1 status when measuring F_M, the saturating light pulse must be short enough, that is, about 30 ms, to avoid a State 1-to-State 2 transition induced by rapid PQ reduction during this strong illumination (Schreiber et al., 1995). However, DCMU treatment is more often used for the measurement of a correct F_M level, since it keeps all Q_A in the reduced state as Q_A^- (Campbell et al., 1998; Campbell and Öquist, 1996). Finally, the correction of both F_O and F_M levels for constant fluorescence emitted by PSI and/or free PBS (Ogawa and Sonoike, 2016) must be also made to obtain correct F_O and F_M levels.

3.2 The Maximum Quantum Yield of Photosystem II Photochemistry

3.2.1 The F_V/F_M Ratio: A Proxy of the Maximum Quantum Yield of Photosystem II Photochemistry

The two basic fluorescence levels, F_O and F_M, are enough to estimate the maximum quantum yield of PSII photochemistry of a photosynthetic sample, $\Phi(P_0)$. Kitajima and Butler (1975) presented simple derivations, which were confirmed by experimental measurements, showing that the ratio $(F_M-F_O)/F_M=F_V/F_M$ is a proxy for $\Phi(P_0)$. Since it is quickly and easily measured in dark-adapted plants and green algae, the F_V/F_M ratio is the most frequently used ChlF parameter to characterize the efficiency of photosynthesis. However, as discussed above, we need to deal differently with cyanobacteria than with plants and algae to correctly obtain the quantum yield of PSII (see below).

3.2.2 The F_V/F_M Values in Cyanobacteria: Comparison With Plants and Green Algae

Fluorescence measurements on a large number of C3 plants, grown under nonstressed conditions, gave a mean F_V/F_M value of 0.832 (Björkman and Demmig, 1987). However, if the apparent F_O and F_M values of dark-adapted cyanobacteria are used, the estimated F_V/F_M ratio is only 0.3–0.4, which is clearly too low (Gao et al., 2007). Using the DCMU method for the F_M determination, improves a bit the F_V/F_M value, which reaches a value between 0.45 and 0.6 (Allahverdiyeva et al., 2013; Ogawa et al., 2013; Schuurmans et al., 2015). Working on six cyanobacterial species, Misumi et al. (2016) found that the F_V/F_M ratios in marine cyanobacteria with a low PB to Chl ratio are higher than in freshwater cyanobacteria, which have higher PB to Chl ratios. On the other hand, Zhang et al. (2017) found that if F_M is measured without DCMU, and F_O evaluated using a weak blue light (see Section 3.1.1), the F_V/F_M is about 0.45, and the use of DCMU for F_M determination increases the F_V/F_M to about 0.6, which is still too low to reflect efficient photosynthesis. In addition, Demmig-Adams et al. (1990c) found that F_V/F_M, in cyanobacterial lichens, ranged from 0.52 to 0.7 under certain conditions. However, when Ogawa and Sonoike (2016) measured F_O and F_M, in cyanobacteria, under illumination with weak blue light and upon DCMU treatment, respectively, and corrected for the constant fluorescence coming from PSI and/or free PBSs, they obtained a value of ~0.82 for F_V/F_M, which is very close to the 0.83 value reported by Björkman and Demmig (1987) for C3 plants. This shows that the efficiency of PSII photochemistry in cyanobacteria is similar to that of higher plants, and it is important to use special protocols and corrections in ChlF measurements for cyanobacteria.

3.3 The OJIP Transient Analysis

During the OJIP transient, measured under saturating light, the ChlF increases from F_O, when all Q_A are oxidized, to a maximum F_M level, when all Q_A are reduced (Duysens and Sweers, 1963). At the F_M level, there is a bottleneck in the ET on the acceptor side of PSI (Munday and Govindjee, 1969a,b); this is due to a transient inactivation of the FNR and the Calvin-Benson cycle, which limits the consumption of NADPH. In order to understand the mechanisms behind the ChlFI, the OJIP curve has been analyzed using theoretical simulations (e.g., Belyaeva et al., 2011; Lazár, 2003, 2009; Stirbet et al., 1998, 2001; Tomek et al., 2001; Zhu et al., 2005). Initially, only PSII was considered in these models, but the simulated

OJIP curves were significantly improved when PSI-driven ET was also considered (see, e.g., Lazár, 2009); these theoretical studies support the conclusions of Munday and Govindjee (1969a,b) and Schansker et al. (2005) regarding the effects of PSI activity on the ChlFI.

During the O-P rise, there are usually two inflections (see Fig. 9A and C): J (at ~2 ms) and I (at ~30 ms). However, there are other inflections under certain conditions. These include an inflection "K"(at ~0.3 ms) observed in heat-stressed samples (Guissé et al., 1995) that was attributed to the inactivation of OEC (Strasser, 1997). The rapid OJ rise (observed in ChlF curves plotted on a logarithmic time scale) is the "photochemical" phase of the OJIP transient, since its initial slope and relative height depend strongly on the light intensity, and is insensitive to temperature variations (Delosme, 1967; Neubauer and Schreiber, 1987; Strasser et al., 1995). The relative J-level increases and appears earlier when the light intensity is increased (Strasser et al., 1995). However, at very high light intensities, a dip is formed after J due to a transient ET limitation on the (electron) donor side of PSII that leads to a transient reoxidation of Q_A^- and accumulation of $P680^+$ (Schreiber and Neubauer, 1990); the latter is also a quencher of Chl fluorescence (see Section 2.2.6). The JIP rise is a "thermal" phase since it is less affected by changes in light intensity but is sensitive to changes in temperature, in contrast to the photochemical OJ phase; it is absent at subfreezing temperatures (see reviews by Stirbet and Govindjee, 2012; Stirbet et al., 2014). We further note that the JIP phase is correlated with the reduction of the PQ pool by PSII-driven ET, but it is also influenced by the oxidation of PQH_2 as driven by PSI activity (Munday and Govindjee, 1969a,b; Schansker et al., 2005). The amplitude of the IP rise in higher plants has been correlated with the PSI/PSII ratio (Ceppi et al., 2012; Oukarroum et al., 2009). We also mention that in samples with a reduced PQ pool during darkness (such as cyanobacteria, or plants and algae kept in anaerobic conditions), not only is the F_O level increased (see earlier), but also the F_J level (Tóth et al., 2007; Tsimilli-Michael et al., 2009); as discussed later (Section 4.1.1), these changes in the OJ rise can be used to evaluate the redox poise of the PQ pool in cyanobacteria during darkness (Tsimilli-Michael et al., 2009).

Besides the F_V/F_M ratio, a proxy for PSII photochemical efficiency (see Section 3.2), other parameters have been also defined based on the OJIP transient, which are assumed to be related to the activity of PSII and the efficiency of ET to the PQ pool and PSI electron acceptors during the OJIP transient; these are part of the so-called "JIP-test" (Strasser and Strasser, 1995), and have been defined using not only the F_O and F_M values, but also the intermediate fluorescence levels F_K, F_J, and F_I (see reviews by Stirbet and Govindjee, 2011; Strasser et al., 2004; Tsimilli-Michael and Strasser, 2008). These parameters were shown to be very sensitive to the effects of biotic and abiotic stress on photosynthesis, mainly in plants and algae (Kalaji et al., 2016; Stirbet et al., 2018). Here, we mention similar ChlFI studies on the effects of diverse stress factors in cyanobacteria (see also a book on stress in cyanobacteria by Srivastava et al., 2013): (1) salt (Hu et al., 2014; Lu and Vonshak, 1999; Sudhir et al., 2005; Zhang et al., 2010); (2) Cu^{2+} (Deng et al., 2014); (3) Sb (V) (Wang and Pan, 2012); (4) As(III) (arsenic) (Wang et al., 2012); (5) nitrite (Zhang et al., 2017); (6) pyrogallol (Wang et al., 2016); (7) pyrene (Shao et al., 2010); (8) artemisinin (Ni et al., 2012); and (9) ultrasonics (Duan et al., 2017).

3.4 Chlorophyll *a* Fluorescence Induction Analysis Using the PAM-Saturation Pulse Method

As described in Section 3.1, in ChlFI measurements using the PAM-SP method, consecutive saturation light pulses are applied to the sample during the actinic illumination that drives photosynthesis, and sometimes also during the subsequent dark recovery (see Fig. 10). The fluorescence data collected during actinic illumination allow the evaluation of several parameters (see a review by Lazár, 2015) of photochemical quenching and of different types of processes that decrease Chl fluorescence without involving photochemical quenching, that is, energy-dependent NPQ of the Chl excited state (e.g., qE in plants), state transition qT (i.e., State 1-to-State 2), and photoinhibitory quenching qI, which characterize the light-adapted state of the sample; on the other hand, the data obtained during dark recovery enable separation and evaluation of these types of fluorescence quenching (Müller et al., 2001; see Fig. 10). For a detailed discussion of NPQ of Chl excited state and state transitions in cyanobacteria, see later sections in this chapter (Section 4.2). Below, we present the PAM-SP method.

Originally, for the analysis of PAM-SP data, the following three parameters were used (see, e.g., Bilger and Björkman, 1990; Schreiber et al., 1986): (1) coefficient of photochemical quenching, $qP=(F_M'-F(t))/(F_M'-F_O')$, which has values between 0 and 1, and is routinely used as an estimate for the fraction of open PSII RCs (i.e., with Q_A oxidized); (2) coefficient of NPQ, $qN=((F_M-F_O)-(F_M'-F_O'))/(F_M-F_O)$; and (3) the NPQ parameter, $NPQ=(F_M-F_M')/F_M'$, which also reflects the light-induced NPQ. In the above equations, $F(t)$ is the fluorescence at time "t" of actinic illumination, and F_M' is the maximum fluorescence reached during the SP fired just after the determination of $F(t)$. The F_O' is, however, measured by switching off the actinic light and switching on a low intensity far-red ($\lambda \sim 740$ nm) light, predominantly absorbed by PSI, which leads to the oxidation of the PQ pool (and, thus, indirectly of Q_A^-); however, F_O' may eventually be calculated as $F_O'=(F_O/((1/F_O)-(1/F_M)+(1/F_M')$, according to Oxborough and Baker (1997; see also Pfündel et al., 2013). Furthermore,

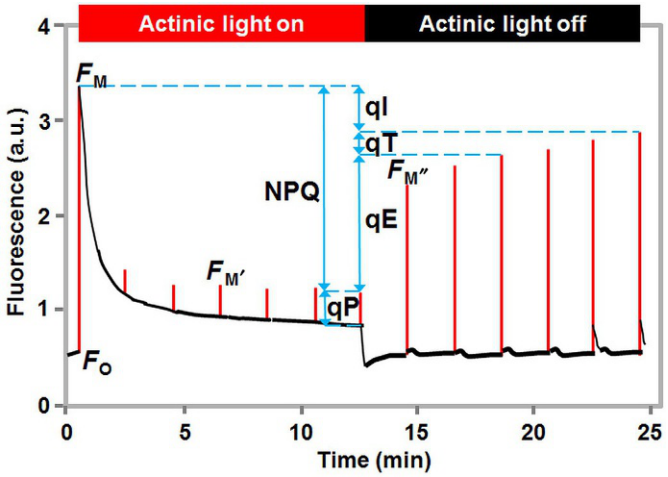

FIG. 10 Measurement of NPQ using the PAM-SP method. After application of a saturating pulse on a dark-adapted sample (e.g., leaf), ChlF rises from the minimum (F_O) to the maximum (F_M) level. Under continuous moderate actinic light, fluorescence decreases due to a combination of photochemical quenching (qP) and different types of NPQ. The difference between F_M measured after dark-adaptation and the maximal fluorescence under actinic light after a saturating light pulse (F_M') is a measure of NPQ (i.e., qE, qT, and qI, where qE is the energy-dependent nonphotochemical quenching of Chl excited states, qT is the state change-dependent NPQ, and qI is photoinhibition-dependent NPQ). F_M' almost recovers in several minutes after the actinic light is switched off, reflecting the relaxation of the qE component of NPQ. Characteristic times for recovery of qE, qT, and qI might be different for different samples and conditions. a.u., arbitrary units. *(Modified from Müller, P., Li, X., Niyogi, K.K., 2001. Nonphotochemical quenching. A response to excess light energy. Plant Physiol. 125, 1558–1566.)*

the untangling of the other types of ChlF quenching that do not involve photochemical quenching (i.e., qE, qT, and qI; see earlier and Fig. 10) by using different relaxation times of F_M'' during the dark recovery was introduced by Hodges et al. (1989) and Quick and Stitt (1989). However, we warn the readers that the problem is quite complex in view of basic differences in the quenching processes involved.

In addition, methods to calculate the quantum yield of processes occurring during actinic illumination are now available. The advantage of these methods is that the sum of the quantum yields of all the possible processes equals unity, which is not true for the coefficients qP and qN; this way, the relative contribution of each process can be calculated and compared. Different theories have been developed (see a review by Lazár, 2015), but the following three quantum yields are generally used (Hendrickson et al., 2004): (1) the effective quantum yield of PSII photochemistry during actinic illumination, $\Phi_{PSII}=(F_M'-F(t))/F_M'$; (2) the quantum yield of the nonregulatory (basal) NPQ, $\Phi_{f,D}=F(t)/F_M$; and (3) the quantum yield of the regulatory light-induced NPQ, $\Phi_{NPQ}=(F(t)/F_M')-(F(t)/F_M)$. As mentioned above, $\Phi_{PSII}+\Phi_{f,D}+\Phi_{NPQ}=1$.

One of the most used parameters for samples in the light-adapted state is $\Phi_{PSII}=(F_M'-F(t))/F_M'=qP\,F_V'/F_M'$ (Genty et al., 1989), where F_V'/F_M' is the maximum quantum yield of PSII photochemistry in the light-adapted state. This quantum yield, as well as all the above PAM-SP parameters, can be measured at any time during actinic illumination, but are mostly measured under steady state. Genty et al. (1989) showed that Φ_{PSII} is linearly correlated with the quantum yield of CO_2 assimilation in several higher plants, although this is not always true (see, e.g., Cheeseman et al., 1991, 1997).

In higher plants, where PSII participates only in photosynthetic ET, Φ_{PSII} reflects more or less true photosynthetic electron flow. However, in cyanobacteria, electrons from PSII can be used in both photosynthetic and respiratory electron flows. Thus, Φ_{PSII} in cyanobacteria generally reflects an apparent photosynthetic flow. For example, a mutant of *Synechocystis* sp. PCC 6803 lacking the gene encoding NDH-1 had a higher Φ_{PSII} than the wild type (Ogawa et al., 2013). The higher Φ_{PSII} in the mutant reflects a higher photosynthetic electron flow, which is closer to the true photosynthetic electron flow, as the respiratory reactions are more or less inhibited in this mutant. On the other hand, the lower value of Φ_{PSII} in the wild type reflects an apparent photosynthetic electron flow, since a portion of electrons available from PSII is used by respiration. This agrees with the fact that, when a weak blue light is used as a background illumination in the wild-type cyanobacteria, Φ_{PSII} increases (Ogawa and Sonoike, 2016), since the light stimulates the PSI reactions (see earlier) and, in turn, the photosynthetic electron flow. Thus, when measuring and interpreting values and changes of Φ_{PSII} in cyanobacteria, the experimental conditions must be considered with care.

In order to learn about the early investigations on cyanobacteria using the PAM-SP method, we refer the readers to Campbell et al. (1998), Campbell and Öquist (1996), Clarke et al. (1993, 1995), Miller et al. (1991), and Schreiber et al. (1995). In these studies, F_O was mostly determined in dark-adapted samples (as in plants), F_O' was measured after switching off the actinic light or by turning off the light coupled with illumination with far-red light, and F_M was determined by

treatment with DCMU during the light-induced steady state. Under these conditions, Φ_{PSII} and F_V'/F_M', obtained under optimal illumination, were usually between 0.4–0.5 and 0.42–0.55, respectively. In other studies (see, e.g., El Bissati et al., 2000; El Bissati and Kirilovsky, 2001), the minimum and maximum fluorescence levels were measured for the dark-adapted state, as well as upon illumination with blue or orange actinic light, and under DCMU treatment (for F_M only). These studies served to discriminate between what is now known as the OCP-related NPQ (induced by strong blue light; see Section 4.2) and state transition (induced by weak orange light; see Section 4.1). PAM-SP measurements in cyanobacteria were also used to visualize qualitative differences between measured curves in different cyanobacteria, or changes caused by particular treatments, without evaluation of related parameters (see, e.g., Boulay et al., 2008; Jallet et al., 2012; Joshua et al., 2005; Wilson et al., 2006). We refer the readers to Boulay et al. (2008) who discuss the occurrence and function of OCP in photoprotective mechanisms in various cyanobacteria.

A series of theoretical studies of ChlF transients, measured in cyanobacteria, have been published by Acuña et al. (2016a,b, 2018c,d). Acuña et al. (2016a) used a functional model including OCP-dependent NPQ quenching (see Section 4.2) to fit the fluorescence data obtained with the PAM-SP method in the wild-type *Synechocystis* PCC6803, as well as in mutants lacking the PBS core terminal emitters ApcD and ApcF (see Section 2.1.2); they described the OCP-dependent NPQ as in the model proposed by Gorbunov et al. (2011). For the fitting of the above data, the authors considered time-dependent contributions of the following photosynthetic complexes: (1) PBS-PSII; (2) PSIs alone; (3) PSIIs alone; and (4) free PBSs. They found that the amount of free PBSs contributing to the fluorescence signal was greater in the mutants lacking ApcD and ApcF. Moreover, this increase was positively correlated with the rate constant of the binding of photoactivated OCP to PBS.

In another study, Acuña et al. (2016b) measured spectrally resolved fluorescence transients (see Kaňa et al., 2009) in control and DCMU-treated wild-type *Synechocystis* PCC6803, as well as in its mutants lacking either PSII or PSI. They used a mathematical procedure to decompose the measured signal to contributions of different photosynthetic complexes based on the characteristic spectral features of the complexes. The measured fluorescence data were described by a sum of signals attributed to: (1) unquenched free PBSs, and quenched (probably by PSI) PBSs—for the mutant cells lacking PSII; (2) PBS-PSII$_{closed}$ complexes, and quenched (probably by HliP; see Section 1) PBS-PSII complexes—for the mutant cells lacking PSI; and (3) PBS-PSII$_{closed}$ complexes mildly quenched by PSI, and PBS-PSII$_{closed}$ complexes strongly quenched by PSI (by assuming PBS-PSII-PSI megacomplexes formed in both cases; Liu et al., 2013)—for the wild-type cells. In the case (3) of wild-type cells, Acuña et al. (2016b) assumed state transitions involving the PBS-PSII-PSI megacomplex, but also considered PSII energy spillover to PSI as a possible alternative mechanism. Acuña et al. (2016b) also confirmed that the SM rise in the ChlF transient of the wild-type cells is due to a State 2-to-State 1 transition, which is accelerated in cells treated with DCMU, as reported earlier by Kaňa et al. (2012).

In a subsequent study by Acuña et al. (2018c), spectrally resolved PAM-SP fluorescence transients of *Synechocystis* PCC6803 mutant cells lacking PSI were measured under different conditions affecting respiratory activity. They applied the same mathematical procedure to determine the photosynthetic complexes contributing to the fluorescence signal as in Acuña et al. (2016b), and the results were used to simulate the fluorescence transients based on a minimal model inspired by the one proposed by Ebenhöh et al. (2014). The photosynthetic complexes involved were identified as: (1) PBS-PSII complexes in which the PSII dimer has both RCs closed; (2) PBS-PSII complexes with both the RCs open; and (3) PBS-PSII complexes with both RCs closed, but whose fluorescence was assumed to be quenched by an unknown HliP-type quencher (see Section 1) active only in the presence of oxygen. In addition, Acuña et al. (2018d) studied spectrally resolved PAM-SP fluorescence transients of the wild-type *Synechocystis* PCC6803 and mutants lacking either PSI or NDH-1 complexes, measured after different dark-adaptation periods. Acuña et al. (2018c) found that the measured fluorescence signal was a sum of three signals that were attributed to: (1) PBS-PSII-PSI complexes with moderate EET from PBS to PSI, and fully closed PSII RCs; (2) PBS-PSII-PSI complexes with fast EET to PSI, and partially closed PSII RCs; and (3) PBS-PSII(-PSI) complexes with fully open PSII RCs. Also, Acuña et al. (2018c) suggested that the molecular mechanism underlying the State 2-to-State 1 transition is a deceleration of the energy transfer from PBS to PSI (see the next section).

4. SHORT-TERM REGULATORY PROCESSES OF PHOTOSYNTHESIS

4.1 State Transitions

4.1.1 State Transitions in Cyanobacteria, Compared to Plants and Algae

State transitions are short-time light-adaptive phenomena that optimize photosynthesis by synchronizing the turnover rates of PSII RC and PSI RC when there is an excitation imbalance in their PSs, which are usually due to variations in color and intensity of the incident light and to differences in photosynthetic pigments in the antenna (see reviews by Allen and

Mullineaux, 2004; Govindjee and Papageorgiou, 1971; Harris et al., 2018; Kirilovsky, 2015; Mullineaux and Emlyn-Jones, 2005; Papageorgiou, 1975, 1996; Papageorgiou and Govindjee, 2011, 2014; Rochaix, 2014). However, note that differential energy transfer by PBS to either PSI or PSII has also been shown to be induced by changes in osmolality (Papageorgiou and Alygizaki-Zorba, 1997; Papageorgiou et al., 1998, 1999; Stamatakis and Papageorgiou, 1999, 2001; Stamatakis et al., 2005, 2007): in hyperosmotic cell suspension, PBSs deliver more EE to PSI than to PSII, while in hypoosmotic suspension they deliver less excitation to PSI than to PSII.

The concept of state transition remains similar for different photosynthetic organisms, basically consisting of reciprocal changes in the CS_{abs} of PSI and PSII through adjustment in the amount of EE transferred to the two RCs from their respective peripheral antenna (i.e., LHC subunits in plants and green algae, and PBS in cyanobacteria). Fluorescence measurements, both fluorescence transients and emission spectra, are the main diagnostic tools with which these changes have been identified (Lamb et al., 2018; Papageorgiou, 1996; Papageorgiou and Govindjee, 2011, 2014; Papageorgiou et al., 2007). The best way to recognize state transitions is to measure fluorescence spectra at 77 K, where changes in the relative intensity of the major PSI and PSII bands (i.e., the F685/F730 ratio) reflect the distribution of EE between the PSs (see, e.g., Kaňa et al., 2012; Lamb et al., 2018). Since PSII fluorescence yield at ambient temperature is significantly higher compared to that of PSI (see Sections 2.2 and 2.3), state transitions at room temperature lead to a decrease or increase in ChlF, mainly due to variations in PSII CS_{abs}. For example, ChlF in State 2, when the CS_{abs} of PSII is smaller than that of PSI, is weaker at room temperature (see Fig. 11A) and the ratio F685/F730 at 77 K is lower, as expected (see Fig. 11B).

To recapitulate history, state transitions were discovered by Bonaventura and Myers (1969) in the green alga *Chlorella pyrenoidosa* and independently by Murata (1969a,b) in the red alga *Porphyridium cruentum* and spinach chloroplasts. Prolonged illumination with light absorbed predominantly by PSI pigments (also called light 1) resulted in enhanced ChlF, while prolonged illumination with light absorbed predominantly by PSII pigments (light 2) resulted in decreased ChlF. These light-adaptive transitions have been discussed using the terminology of Myers (1971), who called State 1 and State 2 the states induced after light adaptation to lights 1 and 2, respectively: after a State 2-to-State 1 transition, PSII CS_{abs} > PSI CS_{abs} and ChlF at ambient temperature is high, while after a State 1-to-State 2 transition, PSII CS_{abs} < PSI CS_{abs} and ChlF is low. Similar phenomena take place regardless of the type of peripheral pigment complexes involved in the light harvesting of other oxygenic photosynthetic organisms: for example, in the cyanobacterium *Synechococcus* (Fork and Satoh, 1983; Mohanty and Govindjee, 1973; Mullineaux et al., 1986; Papageorgiou and Govindjee, 1967, 1968a), green algae (Delepelaire and Wollman, 1985; Papageorgiou and Govindjee, 1968b), red algae (Ley and Butler, 1980; Mohanty et al., 1971; Murata, 1970; Ried and Reinhardt, 1980), cryptomonads (Snyder and Biggins, 1987), and higher plant leaves (Canaani et al., 1984; Chow et al., 1981; Malkin et al., 1986). However, the extent of state transition differs between various organisms, being more pronounced in cyanobacteria, for which state transitions play a prominent role in the regulation of

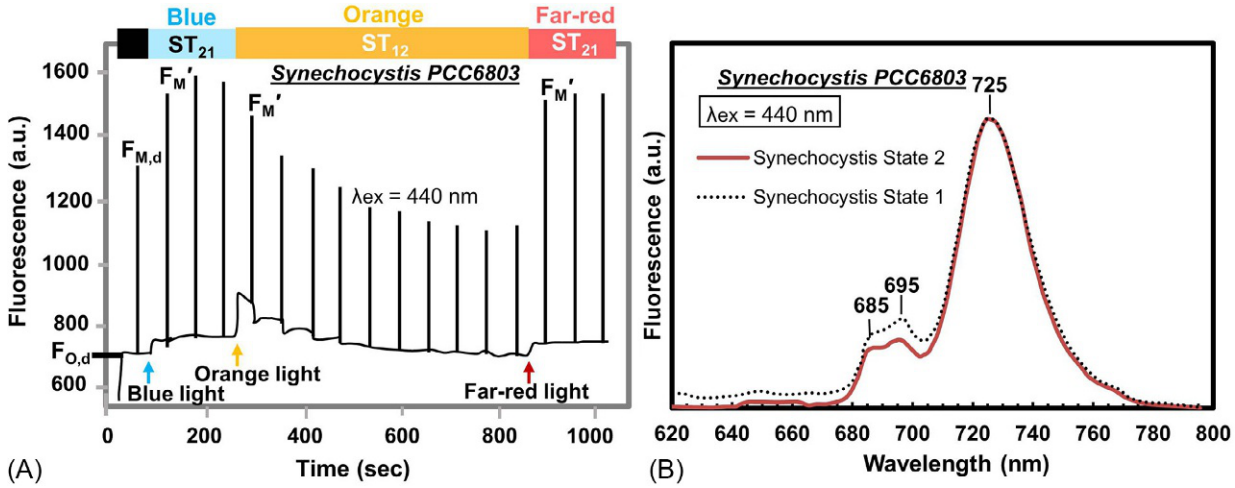

FIG. 11 Fluorescence changes during state transitions. (A) Measurements of fluorescence yield by a PAM fluorometer during different types of illumination in wild-type *Synechocystis* sp. PCC 6803 cells. Dark-adapted cells for 5 min were successively illuminated with *blue* (30 μmol photons $m^{-2} s^{-1}$), *orange* (30 μmol photons $m^{-2} s^{-1}$), and *far-red* (30 μmol photons $m^{-2} s^{-1}$) light. Saturating pulses (3200 μmol photons $m^{-2} s^{-1}$, 800 ms duration) were applied to assess F_M dark ($F_{M,d}$), and F_M'. (B) 77 K emission spectra of dark-adapted (5 min) cells illuminated 30 min with orange light *(solid line)* and then 30 min with blue light *(dotted line)* at room temperature. The excitation wavelength was 440 nm. The spectra were normalized to the PSI fluorescence peak at 725 nm. *a.u.*, arbitrary units. *(Modified from El Bissati, K., Kirilovsky, D., 2001. Regulation of psbA and psaE expression by light quality in* Synechocystis *species PCC 6803. A redox control mechanism. Plant Physiol. 125, 1988–2000.)*

photosynthesis, probably due to frequently lower light fluxes in the aquatic environment, in which most of these are living, than those of terrestrial plants (Falkowski et al., 2004).

State transitions are initiated in all oxygenic photosynthetic organisms by redox changes in the PQ pool, with the transition to State 2 being triggered by PQ pool reduction, and the transition to State 1 being triggered by PQ pool oxidation (Allen et al., 2011; Mullineaux and Allen, 1990; Vernotte et al., 1990). Moreover, state transitions can be naturally induced not only during illumination, but also by non-photochemical oxidation or reduction of the PQ pool in darkness due to metabolic processes involving, for example, respiration in cyanobacteria (Aoki and Katoh, 1982; Mullineaux and Allen, 1986) and chlororespiration in green algae (Bulté et al., 1990; Wollman and Delepelaire, 1984).

Plants and algae are usually in State 1 after dark adaptation and are shifted to State 2 upon illumination. However, many dark-adapted cyanobacteria are in State 2 under prolonged darkness due to a high metabolically induced ET to the PQ pool (see Section 3.3, and Ogawa et al., 2013), and subsequently undergo a very large State 2-to-State 1 transition upon illumination, because of their high PSI:PSII ratio (Mullineaux and Allen, 1986). State transitions in *Synechocystis* sp. PCC 6803 wild type (which is usually in State 1 after dark adaptation), as well as its mutants deficient in oxidases (Ox^-) or SDH^-, have been studied by Bolychevtseva et al. (2015): the PQ pool was reduced in the Ox^- mutant and oxidized in the SDH^- mutant after dark adaptation. Analysis of both variable Chl fluorescence and 77 K fluorescence spectra showed that the WT and SDH^- mutant were in State 1 after dark adaptation, while the Ox^- mutant was in State 2. The State 2 was characterized by ~1.5 times lower photochemical activity of PSII and a higher reduction rate of P700. Further, based on ChlFI measurements from *Synechococcus* sp. PCC 7942 cells, Tsimilli-Michael et al. (2009) proposed that the $(F_M - F_O)/F_O$ $(=F_V/F_O)$ ratio, and the relative height of the J-level $(V_J = (F_J - F_O)/F_V)$, can be used as indices reflecting the redox poise of the PQ pool and the established state during darkness. They also used a special light protocol for the study of the dark-to-light transition in order to assess the PSII dynamics during the State 2-to-State 1 change and to determine the fluorescence component not originating from PSII.

On the other hand, the redox state of the PQ pool in plants and algae was found to be "sensed" at the Qo site (lumenal) of the Cyt b_6f complex (Vener et al., 1997; Zito et al., 1999), and the processes involved in state transitions are better known here (see, e.g., Rochaix, 2014) than in cyanobacteria. The most accepted view of the events taking place in plants and algae during state transitions is the following. Under illumination with light 2, the PQ pool is reduced, which triggers a State 1-to-State 2 transition through the activation of a thylakoid protein kinase; then, mobile LHCIIs of PSII are phosphorylated (Bennett, 1980), which then dissociate from PSII and associate with PSI (Andersson et al., 1982; Kouřil et al., 2005). On the other hand, under illumination with light 1, the PQ pool is oxidized, which triggers a State 2-to-State 1 transition through the deactivation of the kinase; this allows the redox-independent phosphatases (Silverstein et al., 1993; Shapiguzov et al., 2010) to dephosphorylate the mobile LHCIIs, which then dissociate from PSI and associate with PSII. At the end of a state transition, the PQ pool reaches a new redox poise, and the imbalance between PSI and PSII activities is corrected (see, e.g., an in silico study of state transitions in *Chlamydomonas reinhardtii* by Stirbet and Govindjee, 2016).

A few studies suggest that Cyt b_6/f is involved in processes that also trigger state transitions in cyanobacteria (Huang et al., 2003; Mao et al., 2002), but the exact mechanism is not clear. Allen et al. (1985) have proposed the involvement of a protein kinase to trigger state transitions in cyanobacteria, as in plants and green algae, but the existence of this kinase remains elusive. Chen et al. (2015b) found that β subunits of PCs (CpcBs) in *Synechocystis* sp. PCC 6803 are phosphorylated on Ser22, Ser49, Thr94, and Ser154, and have used these to construct four non-phosphorylated mutants. These mutants showed a lower level of fluorescence quenching, a less efficient energy transfer inside the PBS, a slower state transition, and slower growth under high light conditions than in the wild-type cyanobacteria. Chen et al. (2015b) have speculated that PBS phosphorylation may modify its interactions with the PSs during state transitions.

Two possible mechanisms that can lead to changes in PSII and PSI CS_{abs} have been suggested to be involved in state transitions in cyanobacteria, which are not mutually incompatible: (1) changes in the energetic coupling of PBS with PSII and PSI (e.g., Harris et al., 2018; Liu et al., 2013; Mullineaux, 2008); and (2) spillover of energy from PSII to PSI (see, e.g., Biggins and Bruce, 1989; Federman et al., 2000; Lia et al., 2004; Ueno et al., 2017). Further research is needed to decide on the role of these two mechanisms.

The PBSs have been found to be more mobile on the cytosolic side of the TM than the PSs within the membrane (see, e.g., Mullineaux et al., 1997), and it was assumed that PBS mobility is essential for state transitions in a manner similar to LHCII mobility in plants and green algae (Wientjes et al., 2013). On the other hand, Schluchter et al. (1996) showed that the mutant $psaL^-$ of *Synechococcus* sp. PCC 7002 (in which PSI trimers cannot be formed) was capable of performing a State 2-to-State 1 transition three times faster than the wild type; considering that this was due to an increased diffusion rate in the membrane of monomeric compared to trimeric PSI complexes, it was suggested that the mobility of PSI complexes during state transitions in cyanobacteria plays an important role in state transitions.

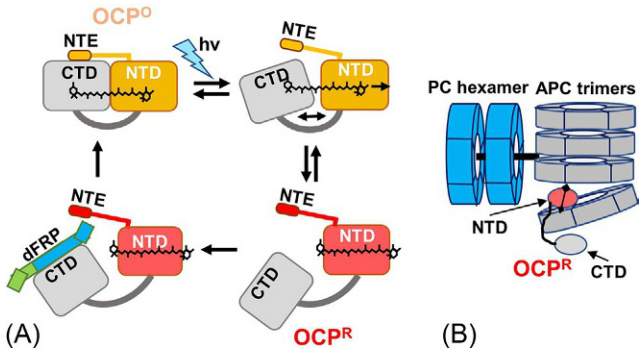

FIG. 12 OCP-related NPQ. (A) Proposed mechanism for OCP-NPQ: strong blue light absorption by inactive OCP^O induces conformational changes in the ketocarotenoid and domain interfaces, including the breaking of a conserved salt bridge, Arg155-Glu244. Translocation of the ketocarotenoid entirely into the N-terminal domain (NTD) and detachment of the N-terminal extension (NTE) from the C-terminal domain (CTD) allows the complete dissociation of the two domains. The photoactivated OCP^R reverts to inactive OCP^O in darkness. In vivo, the interaction between the fluorescence recovery protein (FRP) and CTD accelerates the process. (B) The interaction of OCP^R with the PBS through APC trimers of the core to mediate the dissipation of excess EE as heat. *(Modified from Bao, H., Melnicki, M.R., Kerfeld, C.A., 2017. Structure and functions of orange carotenoid protein homologs in cyanobacteria. Curr. Opin. Plant Biol. 37, 1–9; Harris, D., Tal, O., Jallet, D., Wilson, A., Kirilovsky, D., Adir, N., 2016. Orange carotenoid protein burrows into the phycobilisome to provide photoprotection. Proc. Natl. Acad. Sci. U.S.A. 113, E1655–E1662.)*

After the isolation of a functional PBS-PSII-PSI supercomplex in *Synechocystis* sp. PCC 6803 by Liu et al. (2013), the involvement of PBS mobility in state transitions was questioned, as in this case, minor adjustment of the PBSs would be sufficient. The nature of PBS interaction with PSII and PSI during state transitions in different strains of cyanobacteria is thus an important issue that needs to be resolved. As we mentioned earlier (see Section 2 on the PBS, and Fig. 12A and B), in *Synechococcus* sp. PCC 7002, as well as *Synechocystis* sp. PCC 6701 and PCC 6803, light energy absorbed by the PBS is transferred to PSs via the terminal APC emitters of the PBS core ApcD, ApcF, and ApcE, and these may thus play a special role in state transitions. The PBSs are functionally associated mainly with PSIIs through ApcE (see, e.g., Mimuro et al., 1986), which explains why a lower number of PSII RCs (with 35 Chls per RC) can maintain ET (via Cyt b_6f) to the more numerous PSI RCs (with 96 Chls per RC). Studies on *Synechocystis* sp. PCC 6803 mutants, in which the genes of the rod-core linkers PcpG1 and/or PcpG2 are disruptant, that is, inoperative, showed that the cpcG1 disruptant and the cpcG2/cpcG1 double mutant have a severe defect in state transitions, while the cpcG2 disruptant does not (Kondo et al., 2007, 2009). Since the PBS core is missing from the CpcG2-PBS, while CpcG1-PBS is equivalent to a normal PBS, Kondo et al. (2009) concluded that the PBS core plays an essential role in state transitions. We also note that in the *Synechocystis* mutant lacking the membrane protein RpaC ($RpaC^-$), which is involved in the stability of the PBS-PSII interaction (Joshua and Mullineaux, 2005), state transitions were inhibited, the cells being locked in State 1 (Emlyn-Jones et al., 1999; Kaňa et al., 2012; Mullineaux and Emlyn-Jones, 2005).

Changes in EET to PSI are often found to modulate the relative CS_{abs} of the PSs during state transitions (see, e.g., Ashby and Mullineaux, 1999; Chukhutsina et al., 2015). By using fluorescence spectra, Ashby and Mullineaux (1999) showed that ApcF and ApcE are involved in energy transfer from PBS to PSI in *Synechocystis* sp. PCC 6803, while in *Synechococcus* sp. PCC 7002 it was shown that the terminal emitter ApcD was predominantly involved in the process (e.g., Dong et al., 2009); nevertheless, state transitions were inhibited in mutants of *Synechocystis* sp. PCC 6803 and *Synechococcus* sp. PCC 7002 lacking both ApcD and ApcF. On the other hand, as stated earlier, a functional supercomplex consisting of a PBS, a PSII dimer, and a PSI trimer has been isolated from *Synechocystis* sp. PCC 6803 (Liu et al., 2013) by using cross-linking stabilization in vivo (Papageorgiou, 1977). The EET rates from APC680 to PSI and PSII, calculated assuming such a PBS-PSII-PSI supercomplex (Acuña et al., 2018b), were significantly different: that is, $50\,ns^{-1}$ for PSII and $90\,ns^{-1}$ for PSI (see Section 2.1.4). Thus, in principle, it is possible that modulations of the PBS-PSII-PSI supercomplex can provide a basis for state transitions in cyanobacteria (Harris et al., 2018), but this hypothesis is not generally accepted. Chukhutsina et al. (2015) have proposed another type of mechanism for state transitions in cyanobacteria after studying changes in EET from PBSs to PSs during dark-light transitions by using ps fluorescence spectroscopy. These authors suggest that the PBSs partially energetically uncouple from PSI during the State 2-to-State 1 transition and state that their experimental data does not support a role of PBS-PSII-PSI supercomplexes or the spillover mechanism in state transitions. In conclusion, despite the intensive research on state transitions in cyanobacteria, important details of this process still remain unresolved, especially the essential issue of how changes in the redox state of the PQ pool trigger energy redistribution between PSI and PSII.

4.1.2 On the Origin of the S-M and M-T Phases of the OJIPSMT Transient

As discussed earlier, the ChlFI curve shows an initial fast (hundreds of milliseconds) OJIP phase. In plants and green algae, fluorescence emission decreases monotonically after the maximum P, first to a semi-steady state, S, and then rises to a maximum M after 2–10 s, and then decreases to a terminal steady-state T (reached after few minutes) at a level that is close to F_O (see, e.g., Papageorgiou et al., 2007; Strasser et al., 1995). However, in cyanobacteria containing PBS (with both rods and core), the peak P is only a minor maximum, and after a short decrease to an S-plateau (a semi-steady state), the fluorescence increases to a much higher maximum (M), and then slowly decreases to a terminal steady-state T (see, e.g., Campbell and Öquist, 1996; Govindjee and Papageorgiou, 1971; Papageorgiou and Govindjee, 1968a; Papageorgiou et al., 2007). Furthermore, cells of the green alga *C. reinhardtii* (hereafter Chlamydomonas) also show a fluorescence maximum M (reached in 100–200 s) as high (or higher) than the peak P, if they are preilluminated with high light for a few hours (Allorent et al., 2013) or kept in anoxic conditions under very low light or during darkness (Bulté et al., 1990; Ebenhöh et al., 2014; Kodru et al., 2015). Below, we will discuss relevant studies on the origin of the slow SM rise and MT decline phases in the ChlFI curves. A summary of these studies, published since 1968, is presented in Table 4.

The slow SMT fluorescence phase observed in different photosynthetic organisms was first systematically investigated in the Photosynthesis Lab at the University of Illinois, Urbana-Champaign (see, e.g., Govindjee and Papageorgiou, 1971; Mohanty and Govindjee, 1973, 1974; Mohanty et al., 1971; Papageorgiou, 1975; Papageorgiou and Govindjee, 1968a,b). In a Chl fluorescence induction study of *S. elongatus* (previously known as *A. nidulans*), Papageorgiou and Govindjee (1968a) observed that the O_2 evolution rate increases during the slow SM fluorescence rise, indicating a parallel increase in PSII activity. Since Bonaventura and Myers (1969) found a similar correlation between O_2 evolution and ChlF during the State 2-to-State 1 transition in *Chlorella* cells, it was suggested that the SM rise in cyanobacteria is possibly due to a State 2-to-State 1 transition (Govindjee and Papageorgiou, 1971). Papageorgiou and Govindjee (1968a) also showed that the SM rise is maximized after treatment with DCMU, which was later shown to occupy the Q_B-binding site of PSII (Velthuys, 1981; Wraight, 1981), leading to the oxidation of the PQ pool by PSI. This treatment is now used in ChlF studies to determine the F_M level in cyanobacteria (see Section 3). The hypothesis that the SM fluorescence rise in cyanobacteria is due to a State 2-to-State 1 transition was established without doubt by Kaňa et al. (2012), as they measured an increased PSII fluorescence emission over that from PSI at 77 K, while fluorescence yield of the PBs remained constant (see Table 4). Also, more importantly, they showed that the SM rise was missing in ChlFI curves of State 1-locked RpaC$^-$ mutant cells of *Synechocystis* sp. PCC 6803, as well as of State 2-locked wild-type *Synechocystis* sp. PCC 6803 cells suspended in hyperosmotic solution. Other fluorescence measurements on different cyanobacterial species presented by Kaňa et al. (2012) showed a similar SM rise in cyanobacteria containing PBS with both rods and core, such as *Synechocystis*, *Synechococcus* (PCC7942, WH5701), and the diazotrophic cyanobacterium (*Cyanothece* ATCC51142); however, the SM rise was absent in the PBS rod-containing *Acaryochloris marina* (MBIC 11017).

Working on the wild-type cells of the green alga Chlamydomonas, kept in anoxic conditions during darkness, Kodru et al. (2015) observed that the SM fluorescence rise is modified after treatment with various chemicals (i.e., *n*-propyl gallate PG, salicylhydroxamic acid SHAM, and carbonyl cyanide *p*-trifluoromethoxyphenylhydrazone FCCP) that indirectly influence the redox state of the PQ pool. More importantly, Kodru et al. (2015) found that the SM rise was absent in the State 1-locked *stt7* mutant of Chlamydomonas (Depege et al., 2003) (see Table 4). Therefore, the SM fluorescence rise can be used as an efficient and quick method to monitor state transitions in both cyanobacteria and green algae. In addition, a high SM rise (reached in ~100 s) was recently observed in ChlFI curves of *A. thaliana* plants acclimated to chilling temperatures (~2°C) that was also correlated with a State 2-to-State 1 transition (Mishra et al., 2018).

The origin of the MT fluorescence decline is hardly understood. Results obtained by Bernát et al. (2018) on *Synechocystis* sp. PCC 6803 and its ΔapcD and ΔOCP mutants, which cannot perform either state transitions or OCP-related NPQ (see Section 4.2.1), showed that the OCP-related NPQ is not involved in this fluorescence decrease, while the extent of photoinhibition is low. The authors therefore assumed that other quenching mechanisms are implicated, that is, those involving excitonic decoupling of PBS from PSII (Stoitchkova et al., 2007; Tamary et al., 2012) or flavodiiron (Flv)-related quenching (see a review by Allahverdiyeva et al., 2015). On the other hand, parallel measurements of ChlFI and NADPH fluorescence induction in *Synechocystis* sp. PCC 6803 cells showed that the MT decline observed in both curves was abolished in conditions of low intracellular CO_2 concentration that limits CO_2 assimilation, or during the inhibition of CO_2 assimilation (Holland et al., 2015); the MT decrease in the Chl fluorescence was thus assigned by these authors to the photochemical quenching (i.e., by oxidized Q_A) occurring during the activation of the Calvin Benson cycle. Here, we also mention another study of the SMT fluorescence phase in cyanobacteria by Stamatakis et al. (2007), who found that the slow SM rise in *Synechococcus* sp. PC 7942 was replaced by a continuous P to T fluorescence decrease after the cells had been: (1) treated with *N*-ethyl-maleimide (NEM), which inhibits the PBS → PSI EET (Glazer et al., 1994); or (2) kept in hyperosmotic

TABLE 4 **Possible Origins Suggested for the SM Rise and the MT Decline During the Slow ChlF Transient in Algae and Cyanobacteria**

Organism	Origin of the SM Rise	Origin of the MT Decline	References
Chlorella pyrenoidosa (a green alga)	State 2 (low fluorescence)-to-State 1 (high fluorescence) transition (due, possibly, to a decrease in energy transfer from PSII to PSI, leading to an increase in ChlF from PSII). Note: oxygen evolution increased in parallel with the SM fluorescence rise	State 1-to-State 2 transition, or due to increased rate of internal conversion (heat loss) in PSII antenna (perhaps, indirectly influenced by changes in the rate of CO_2 assimilation and photo-phosphorylation)	Govindjee and Papageorgiou (1971) and Mohanty and Govindjee (1974) Also see: Papageorgiou and Govindjee (1968b) for the discovery and the first experiments, and Papageorgiou et al. (2007) for a detailed discussion on the SM rise and MT decline in plants and algae
Porphyridium cruentum (a red alga)	SM rise and MT decline are linked to both ET and the energy-dependent structural changes in the TM (fixation with glutaraldehyde abolishes these "slow" fluorescence changes)		Mohanty et al. (1971)
Synechococcus sp. *PCC 7942* *Synechocystis* sp. *PCC 6803 and its mutant RpaC*$^{-}$ (cyanobacteria)	State 2-to-State 1 transition was shown by increased PSII emission over that from PSI, measured at 77 K (fluorescence yield of the phycobilins remained constant; most importantly, the RpaC^{-} mutant, blocked in "state changes" had no SM rise). Note: in cyanobacteria, hyper-osmotic suspension media block the SM rise	Probably due to photoinhibition (Papageorgiou et al., 2007; measurements on *Synechococcus* PCC7942); data on the MT decline by Bernát et al. (2018) show a small photoinhibition and that OCP-related NPQ is not involved; Note: Holland et al. (2015) suggest photochemical quenching for the MT decline, as is abolished during C_i limitation	See Papageorgiou et al. (2007) for discussion on the SMT phase in cyanobacteria; Kaňa et al. (2012) for experiments on the SM rise in *Synechocystis* PCC6803, its mutant RpaC^{-}, and *Synechococcus*; Holland et al. (2015) and Bernát et al. (2018) for experiments on the MT decline in *Synechocystis* PCC6803) Also see: Govindjee and Papageorgiou (1971) and Papageorgiou and Govindjee (2011)
Chlamydomonas reinhardtii (a green alga)			
(A) Preilluminated for 4 h under high light (initially in State 2)	State 2-to-State 1 transition; Chl *a* spectra at 77 K confirmed the existence of State 2 after dark-adaptation; observed LHCII de-phosphorylation during the State 2-to-State 1 transition	NPQ induced by LHCSR3, which moves from PSI to PSII during State 2-to-State 1 transition (Note: LHCII de-phosphorylation takes place during MT)	Allorent et al. (2013)
(B) Grown in low light; dark (or low light) adapted under anaerobic condition (initially in State 2)	SM rise was assumed due to State 2-to-State 1 transition		Ebenhöh et al. (2014)
(C) Grown in low light; dark-adapted under low oxygen (initially in State 2); the *stt7* mutant	SM rise is due to State 2-to-State 1 transition since the *stt7* mutant lacking "state changes" has no SM rise	The MT decay was discussed in terms of photoinhibition and energy-dependent quenching (qE)	Kodru et al. (2015)
Haematococcus pluvialis (a green alga) (initially in State 1)	Partial release of qE (due to ΔpH decrease)	Due to adjustment of mutually controlled processes (e.g., ET, photophosphorylation, qE, CO_2 assimilation)	Fratamico et al. (2016) See also Papageorgiou et al. (2007) for a detailed discussion of the SM rise and the MT decline in plants and algae

From the poster of Stirbet and Govindjee, presented in 2016 at the 17th International Congress of Photosynthesis Research, Maastricht, The Netherlands.

conditions, which maximizes the PBS → PSI and minimizes PBS → PSII EET (Papageorgiou and Alygizaki-Zorba, 1997); or (3) treated with DCMU (which maximizes the PBS → PSII EET) and maintained at 2°C.

On the other hand, in Chlamydomonas cells preilluminated with high light for a few hours, the MT decline was found to be associated with the energy-dependent NPQ (qE), as it was abolished after treatment with nigericin (Allorent et al., 2013), which dissipates the ΔpH across the TM (see Table 4). An interesting point is that qE and State 2-to-State 1 transition are interrelated in this case, as the light-harvesting complex stress-related (LHCSR3) protein, which in Chlamydomonas induces the qE (Peers et al., 2009), was found to be associated with PSII in State 1, and with PSI in State 2 (Allorent et al., 2013). Experimental results show that the MT decline in Chlamydomonas is relatively faster toward the end of the State 2-to-State 1 transition (Allorent et al., 2013), when the majority of LHCSR3 are reassociated with PSII. However, no experimental data are available to provide information on the origin of the MT decline in Chlamydomonas cells grown under low light and dark adapted in anoxic conditions, when the LHCSR3 content is low. Since ΔpH dissipation by nigericin also inhibits the ATP synthesis necessary for CO_2 assimilation, it is possible that, as suggested for cyanobacteria (Holland et al., 2015), the MT decline in Chlamydomonas is rather due to photochemical quenching during the induction of the Calvin-Benson cycle than to qE quenching (Allorent et al., 2013).

4.2 Nonphotochemical Quenching of Chlorophyll *a* Fluorescence

4.2.1 On the Mechanism of the Orange Carotenoid Protein-Induced Nonphotochemical Quenching of Chlorophyll a *Fluorescence in Cyanobacteria*

Unlike state transition, which is a dark/low light regulatory process of photosynthesis, NPQ of Chl *a* excited state represents a short-term photoprotection phenomenon under excess light (see Demmig-Adams et al., 2006; Magdaong and Blankenship, 2018) to prevent damage to the PSs (see, e.g., Campbell and Tyystjärvi, 2012; Soitamo et al., 2017). In plants and green algae, a very important NPQ process is the energy-dependent quenching (qE). qE is triggered by the ΔpH build-up across the TM during photosynthetic ET (Wraight and Crofts, 1970; Briantais et al., 1979) and consists of adjustments in light harvesting through deactivation of the first excited state of Chl *a* (^{1}Chl*) to the ground state. Diverse mechanisms have been proposed for qE, such as the involvement of carotenoid de-epoxidation, of PsbS protein, and of LHCRS3 and LHCRS1 (see, e.g., Li et al., 2009; Nilkens et al., 2010; Peers et al., 2009; and chapters in Demmig-Adams et al., 2014). [We note that, under conditions of prolonged stress, a sustained NPQ component involving carotenoid de-epoxidation can develop, which was considered to be a photoinhibition (qI) process (see, Demmig-Adams and Adams, 2006).] However, the main photoprotective mechanism against high light in PBS-containing cyanobacteria is the OCP-related NPQ (see Section 1), in which the energy received by PSs is decreased by increasing thermal dissipation of excess energy at the level of PBS, with the OCP acting both as a light sensor and an energy quencher (see, e.g., Harris et al., 2016, 2018; Kirilovsky and Kerfeld, 2016; Magdaong and Blankenship, 2018; Sonani et al., 2018; Thurotte et al., 2015). This type of quenching is very efficient, as it was shown that one OCP per PBS in vitro was sufficient to quench almost all of PBS fluorescence (Gwizdala et al., 2011), while in vivo, quenched *Synechocystis* cells (i.e., with active OCP) grown under low-medium light receive only 65%–70% of the energy absorbed by the PBS (Rakhimberdieva et al., 2007).

OCP is a photoactive water-soluble protein (of ~35 kDa), present in most cyanobacterial strains (Kerfeld and Kirilovsky, 2013), that noncovalently binds a single ketocarotenoid molecule (i.e., 3′-hydroxyechinenone; Holt and Krogmann, 1981), and absorbs blue-green light. OCP homologs have also been found recently (Bao et al., 2017; Kerfeld et al., 2017; Moldenhauer et al., 2017), and the 4-(or 4′-) keto functionality seems to be essential for OCP photoactivation and its fluorescence quenching activity (de Carbon et al., 2015). The OCP involvement in NPQ was shown by Wilson et al. (2006), who found that a ΔOCP *Synechocystis* mutant (i.e., without a functional gene coding the OCP) was unable to develop NPQ under high light. In addition, these authors also showed that PSII activity in nonquenched wild-type *Synechocystis* cells (i.e., with inactive OCP) is saturated at a lower light intensity than in cells in the quenched state. Absorption of strong blue-green light or white high light by the OCP induces carotenoid and protein conformational changes that convert the orange (inactive) state of OCP (OCP^O) into a metastable red (active) state OCP^R; only OCP^R can attach to the PBS and induce EE dissipation and fluorescence quenching (Gwizdala et al., 2011; Wilson et al., 2008). During the OCP^O activation, the high blue or white light induces structural changes that separate its N-terminal (NTD) and C-terminal (CTD) domains (Thurotte et al., 2015). Following this separation, the ketocarotenoid molecule, which initially was crossing both NTD and CTD domains (Kerfeld et al., 2003), becomes disconnected from the CTD and shifts 12 Å deeper into a cavity within the NTD of the now quenching-active OCP^R (see Fig. 12) (Gupta et al., 2015; Gurchiek et al., 2018; Leverenz et al., 2015; Liu et al., 2016; Maksimov et al., 2015b, 2017).

The ketocarotenoid disconnection from the CTD during photoactivation was suggested to involve either the rotation of the β-ionylidene ring (Maksimov et al., 2015b) or a transient keto-enol shift (Bandara et al., 2017), but its global structural rearrangement remains to be studied. Moreover, by using a ΔApcC mutant, Harris et al. (2016) found that the core linker protein ApcC is also shifted within the cylinder cavity, stabilizing the OCP^R-PBS interaction. The ketocarotenoid molecule in the OCP^R is very close (5–10 Å) to the PB chromophores of the PBS core, but the specific interactions that lead to EE dissipation are not yet established. Nonetheless, after the OCP^R burrows into a terminal hexamer of a basal core cylinder, PBS structural alterations themselves would most probably also affect the EET kinetics (Harris et al., 2018). Gwizdala et al. (2018a) observed the presence of quasi-stable intermediate states during the binding and unbinding of OCP to PBS, with a spectroscopic signature that indicates a transient decoupling of some rods of the PBS during OCP docking. Actually, EET modulation, based on changes in PBS aggregation states, has been proposed by Bar Eyal et al. (2017) in desert crust cyanobacteria (see Section 4.2.2).

The active OCP^R is metastable and, under low light conditions or darkness, it converts to the dark-adapted thermodynamically stable OCP^O form. However, as shown by Boulay et al. (2010), a fluorescence recovery protein (FRP) is necessary during the in vivo recovery from the OCP-related NPQ, which accelerates this process (see also, e.g., Gwizdala et al., 2013; Lu et al., 2017; Sluchanko et al., 2017). The FRP is a 13 kDa soluble protein without attached chromophores that exists primarily as a dimeric complex dFRP (Sutter et al., 2013); both FRP and dFRP have high affinity for the CTD domain of OCP^R. The molecular mechanism of FRP functioning is not yet clearly established. Thurotte et al. (2017) showed that, in a first phase, dFRP accelerates the OCP^R detachment from the PBS and then assists in its deactivation to the basic OCP^O; in addition, Thurotte et al. (2017) have suggested that different OCP and FRP amino acids could be involved in these two activities. Lu et al. (2017) have now studied several FRP site-directed mutants and have proposed that, after the initial dFRP attachment to the CTD, dFRP experiences conformational changes that allow it also to bridge with the NTD. Then, a structural rearrangement of the dFRP facilitates the OCP^R reversion to the inactive orange state OCP^O (see also Magdaong and Blankenship, 2018). Moreover, Liu et al. (2018) found that FRP cannot induce the OCP^R detachment and conversion to OCP^O in the presence of excess Cu^{2+} ions due to the formation of a Cu^{2+}-locked OCP^R state; this has positive consequences, as it reduces the EET toward the PSs, and thus increases photoprotection in Cu^{2+} stressed cyanobacteria.

The induction and recovery dynamics of the OCP-related NPQ are usually studied by measuring the fluorescence kinetics with PAM-SP fluorometers (see Section 3); this fluorescence quenching leads to lower F_M' values, due mainly to a smaller PSII antenna size. The amplitude of the fluorescence quenching depends on light intensity, on the concentration of the FRP, as well as on the number of OCP per PBS (Kirilovsky, 2015). The number of OCP per PBS was shown to increase under stress conditions involving an imbalance between the number of PBS and RCs, and/or PSII degradation, like high light, salt stress, or iron starvation (see, e.g., Gorbunov et al., 2011; Kirilovsky, 2015; Wilson et al., 2007). Maksimov et al. (2015a) also found that the rate of fluorescence recovery decreases with an increase in the amplitude of the OCP-related NPQ. Here, we refer the readers to an interesting biophysical model of the induction and recovery of the OCP-related NPQ proposed by Shirshin et al. (2017), which has been applied to describe the experimental fluorescence kinetics in the *Synechocystis* sp. PCC 6803 mutant lacking PSs.

4.2.2 *Other Photoprotective Mechanisms in Cyanobacteria Leading to Quenching of Chlorophyll* a *Fluorescence*

Besides the OCP-related NPQ, other types of photoprotective mechanisms have been observed in cyanobacteria (see, e.g., Kirilovsky et al., 2014; Magdaong and Blankenship, 2018). One of these mechanisms involves HliP proteins (see Section 1), which accumulate under high light conditions (e.g., Daddy et al., 2015; Havaux et al., 2003; He et al., 2001; Komenda and Sobotka, 2016); they contain Chl *a* and β-carotene, and play an important role in Chl synthesis, PSII repair, and photoprotection (Komenda and Sobotka, 2016; Niedzwiedzki et al., 2016; Staleva et al., 2015). Using femtosecond spectroscopy, Staleva et al. (2015) found that energy dissipation in HliPs is achieved via direct energy transfer from the Q_y state of Chl *a* to the S1 state of β-carotene (see also Niedzwiedzki et al., 2016; Llansola-Portoles et al., 2017).

Another non-OCP-related photoprotection mechanism is induced by iron starvation, and involves IsiA proteins that form a ring around PSI trimers (see Section 2.3.7). As mentioned earlier, quenching of ChlF was observed in IsiA uncoupled to PSI, which is due to Chl *a*-protein interactions by cysteine residues in the IsiA protein (Chen et al., 2017), rather than through Chl *a*-β-carotene interactions (Berera et al., 2009, 2010).

Besides the above non-OCP-related photoprotection mechanisms, reversible PBS decoupling from PSII and/or PSI, or detachment of hexamers from the PBS, can also modulate the EET to the PSs under stress conditions (see, e.g., Kirilovsky et al., 2014). Furthermore, based on single-molecule spectroscopy on the cells of *Synechocystis* sp. PCC 6803, Gwizdala et al. (2016) have suggested a rapid light-regulated photoprotection process that provides photoprotection before the OCP

mechanism is activated; while the core is normally the target in this type of quenching, any subunit of a PBS can be quenched. Moreover, a special non-OCP photoprotection mechanism functions in desert crust cyanobacteria *Leptolyngbya ohadii*. When these cyanobacteria become desiccated, they are completely quenched (Bar Eyal et al., 2017). Measurements on desiccated crust cyanobacteria, compared to hydrated ones, showed shorter fluorescence lifetimes, reduced EET between PBS components, and a red shift in the emission spectra, which were attributed to the loss of the ordered PBS structure.

Zeaxanthin, which is involved in thermal energy dissipation in higher plants and algae, has been invoked as possibly playing a photoprotective role in cyanobacteria as well. Although only correlative in nature, the extent of non-photochemical ChlF quenching in cyanobacterial lichens was found to be associated with the zeaxanthin content of the thalli (Demmig-Adams et al., 1990a). Moreover, the zeaxanthin content (as well as those of the ketocarotenoids central to OCP-related energy dissipation—see Section 4.2.1) of thalli was found to be higher in cyanobacterial lichens from more sun-exposed sites compared to those growing in more shaded sites (Adams et al., 1993), and both zeaxanthin and ketocarotenoids have recently been implicated in photoprotection of PSII (Kusama et al., 2015) as well as localized to PSI (Vajravel et al., 2017). That elevated levels of zeaxanthin are involved in the acclimation of cyanobacteria to higher light intensities, and thus likely play a role in photoprotection, has been documented in several studies (e.g., Aigner et al., 2018; Bemal and Anil, 2016; Daddy et al., 2015).

5. CONCLUSIONS

In this chapter we have described several aspects of the photosynthetic process in cyanobacteria, and have focused on the use of ChlF in understanding some of the events related to photosynthesis. We have also provided a general overview of cyanobacteria, pointing out the differences between them and other oxygenic photosynthetic organisms (such as green algae and higher plants).

Some of the salient points of cyanobacteria, as compared to other photosynthetic organisms, are: (1) The TM contains both the photosynthetic and respiratory ET components (Lea-Smith et al., 2016) that leads to a more or less reduced PQ pool after dark adaptation (see, e.g., Ogawa et al., 2013); (2) the PSI/PSII ratios are usually higher (3–5:1) as compared to ~1:1 in other organisms (Kawamura et al., 1979); (3) water-soluble PBSs containing PB chromophores function as accessory antenna, instead of membrane-embedded LHC complexes containing Chl *a* and Chl *b*; (4) cyanobacteria mostly use light-induced OCP-related NPQ instead of energy-dependent quenching qE (Magdaong and Blankenship, 2018) to protect themselves against excess light; (5) they have much more important, and somewhat unique, "state transitions" that are induced by changes in the PQ pool redox state, although understanding of the triggering process needs new experiments (Kirilovsky et al., 2014); and (6) they have complex stress responses that involve adaptive changes in the structure of PBS and/or the involvement of special membrane-embedded complexes IsiA containing Chl *a*/*b* (see, e.g., Fraser et al., 2013).

In this chapter, we have also described briefly the latest structural and functional data on PBS, PSII, and PSI, followed by a theoretical discussion on ChlFI that has been extensively used in obtaining information on several photosynthetic reactions, as well as on the so-called "state transitions" and NPQ of the excited state of Chl. Two main ChlFI measuring techniques were described: continuous-light and PAM-SP techniques, together with problems of their use in research on cyanobacteria. Indeed, when standard measurement protocols (originally developed for higher plants) are applied to cyanobacteria, the measured fluorescence signals are found to be significantly different and often lead to incorrect interpretations. Thus, we have included a discussion on (i) how to obtain the correct values for the initial (F_O) and maximum (F_M) ChlF needed to calculate the maximum quantum yield of PSII photochemistry and (ii) the necessity to reduce or take into account the contribution of PSI and free PBS signals to decipher the PSII ChlF signal; we emphasize that special attention must be paid to obtain correct interpretation of the fluorescence signal. In addition to chapters in this book, readers may also consult the following books on topics—not covered in our chapter: Flores and Herrero (2014) and Los (2017, 2018), listed under "Further Reading."

GLOSSARY

A_{1A} and A_{1B} phylloquinones (2-methyl-3-phytyl-1,4-naphthaquinone) of photosystem I, where the suffixes A and B refer to the PsaA and PsaB protein subunits to which they are attached

A_{accA}, A_{accB}, A_{0A}, A_{0A} specific chlorophyll *a* molecules in the reaction center of photosystem I, where the suffixes A and B refer to the PsaA and PsaB protein subunits to which they are attached

A_{max} absorption band maximum

AP-B allophycocyanin-B

APC allophycocyanin

Car carotenoid (including carotenes)
CEF cyclic electron flow
Chl chlorophyll
^{1}Chl*, ^{3}Chl* singlet and triplet excited state of chlorophyll *a*
ChlF chlorophyll *a* fluorescence
ChlFI chlorophyll *a* fluorescence induction
Chl680, Chl708, Chl710, Chl715, Chl719, Chl740 chlorophyll *a* molecules with absorption maxima given in nm
Cox cytochrome *c* oxidase
CP chlorophyll protein complex
CS_{abs} absorption cross-section
CTD C-terminal domain of orange carotenoid protein
Cyd cytochrome *bd* quinol oxidase
Cyt cytochrome
ΔpH pH difference across the thylakoid membrane
$\Delta\Psi$ electric potential difference across the thylakoid membrane
DCMU 3-(3,4-dichlorophenyl)-1,1-dimethylurea (also known as diuron)
EE excitation energy
EET excitation energy transfer
ET electron transport
F684, F685, F690, F695, F696, F720, F730, F740, F760 fluorescence (F) bands with peaks at wavelengths given in nm
F_K, F_J, F_I, F_P chlorophyll *a* fluorescence intensities at K, J, I, and P steps of chlorophyll *a* fluorescence induction
F_M, F_M', F_M'' maximum chlorophyll *a* fluorescence for dark-adapted state, light-adapted state, and during dark recovery, respectively
F_{max} fluorescence band maximum
F_O, F_O' minimum chlorophyll *a* fluorescence for dark-adapted and light-adapted state, respectively
F(t) chlorophyll *a* fluorescence intensity at time t during actinic illumination
F_V (maximum) variable chlorophyll *a* fluorescence
F_V/F_M ratio of variable to maximum chlorophyll *a* fluorescence, considered to be equivalent of the quantum yield of PSII photochemistry for dark-adapted state
Fd ferredoxin
Flv flavodiiron
FNR ferredoxin-$NADP^+$ oxidoreductase
FRP, dFRP monomer and dimer of fluorescence recovery protein
fs femtosecond
F_X, F_A, F_B three different [4Fe-4S] centers of photosystem I
$\Phi(P_0)$ maximum quantum yield of PSII photochemistry for dark-adapted state
Φ_{PSII} effective quantum yield of PSII photochemistry during actinic illumination
$\Phi_{f,D}$ quantum yield of nonregulatory (basal) nonphotochemical quenching of chlorophyll *a* fluorescence during actinic illumination
Φ_{NPQ} quantum yield of regulatory light-induced nonphotochemical quenching of chlorophyll *a* fluorescence during actinic illumination
HCO_3^- bicarbonate ion bound to the nonheme iron located between Q_A and Q_B sites of photosystem II
HliP high-light-inducible proteins
LEF linear electron flow
LHC light harvesting complex
LHCSR1, LHCSR3 light-harvesting complex stress-related proteins
LWC long wavelength chlorophylls
{Mn_4CaO_5} cluster of 4 manganese, one calcium and five oxygen atoms of the oxygen evolving center (complex)
ms millisecond
μs microsecond
$NADP^+$ nicotinamide adenine dinucleotide phosphate (oxidized form)
NDH-1 NAD(P)H:quinone oxidoreductase
NTD N-terminal domain of orange carotenoid protein
NPQ nonphotochemical quenching (of the excited state of Chl)
ns nanosecond
$^1O_2$ singlet oxygen
OCP orange carotenoid protein
OCP^O, OCP^R orange (o; inactive) and red (R; active) forms of the orange carotenoid protein
OEC oxygen evolving center (or complex)
O, K, J, I, D, P, S, M, T steps of chlorophyll *a* fluorescence induction curve
PAM pulse amplitude modulation
PEA plant efficiency analyzer

P680 chlorophyll *a* dimer, primary electron donor in the reaction center of photosystem II
P700 chlorophyll *a*/*a´* heterodimer, primary electron donor in the reaction center of photosystem I
P870 bacteriochlorophyll dimer, primary electron donor in the reaction center of purple bacteria
PBP phycobiliprotein
PBS phycobilisome
PC phycocyanin
Pc plastocyanin
PCB phycocyanobilin
P_{D1}, P_{D2}, Chl_{D1}, Chl_{D2}, Chl_{ZD1}, and Chl_{ZD2} six chlorophylls *a* in the reaction center of photosystem II, where D1 and D2 denote the protein subunit of photosystem II to which they are attached
PE phycoerythrin
PEB phycoerythrobilin
PEC phycoerythrocyanin
Pgr5 proton gradient regulation 5 protein
$Pheo_{D1}$ and $Pheo_{D2}$ two pheophytins in the reaction center of photosystem II, where D1 and D2 refer to the protein subunit of photosystem II to which they are attached
pmf proton motive force
PQ and PQH_2 plastoquinone and plastoquinol
PS photosystem
ps picosecond
PUB phycourobilin
Q_A primary (the first) plastoquinone electron acceptor of photosystem II: a one-electron acceptor
Q_B secondary (the second) plastoquinone electron acceptor of photosystem II: a two-electron acceptor
qE, qT, qI energy dependent, state transition, and photoinhibitory quenching components of chlorophyll *a* fluorescence
qP, qN coefficients of photochemical and nonphotochemical quenching of chlorophyll *a* fluorescence
RC reaction center
ROS reactive oxygen species
s second
S_0, S_1, S_2, S_3, S_4 redox states of 4-manganese cluster of the oxygen evolving complex
SDH succinate dehydrogenase
SP saturation pulse
TM thylakoid membrane
Y_D tyrosine 160 residue of the D2 protein subunit of photosystem II
Y_Z tyrosine 161 residue of the D1 protein subunit of photosystem II

ACKNOWLEDGMENTS

We are highly grateful to William W. Adams III (University of Colorado) for his valuable suggestions for improving this chapter, particularly for bringing to our attention research on cyanobacteria living among filaments of a fungus, forming lichen. D.L. was supported by a grant # LO1204 (Sustainable Development of Research in the Center of the Region Haná) from the National Program of Sustainability I, Ministry of Education, Youth and Sports, Czech Republic. Govindjee was supported by the Department of Plant Biology and the Department of Biochemistry, University of Illinois at Urbana-Champaign (UIUC), Illinois, United States; he also thanks the wonderful staff members of Information Technology, Life Sciences, UIUC, for their constant valuable help.

REFERENCES

Acuña, A.M., Snellenburg, J.J., Gwizdala, M., Kirilovsky, D., van Grondelle, R., van Stokkum, I.H.M., 2016a. Resolving the contribution of the uncoupled phycobilisomes to cyanobacterial pulse-amplitude modulated (PAM) fluorometry signals. Photosynth. Res. 127, 91–102.

Acuña, A.M., Kaňa, R., Gwizdala, M., Snellenburg, J.J., van Alphen, P., van Oort, B., Kirilovsky, D., van Grondelle, R., van Stokkum, I.H.M., 2016b. A method to decompose spectral changes in *Synechocystis* PCC 6803 during light-induced state transitions. Photosynth. Res. 130, 237–239.

Acuña, A.M., van Alphen, P., van Grondelle, R., van Stokkum, I.H.M., 2018a. The phycobilisome terminal emitter transfers its energy with a rate of $(20\ ps)^{-1}$ to photosystem II. Photosynthetica 56, 265–274.

Acuña, A.M., Lemaire, C., van Grondelle, R., Robert, B., van Stokkum, I.H.M., 2018b. Energy transfer and trapping in *Synechococcus* WH 7803. Photosynth. Res. 135, 115–124.

Acuña, A.M., van Alphen, P., dos Santos, F.B., van Grondelle, R., Hellingwerf, K.J., van Stokkum, I.H.M., 2018c. Spectrally decomposed dark-to-light transitions in a PSI-deficient mutant of *Synechocystis* sp. PCC 6803. Biochim. Biophys. Acta 1859, 57–68.

Acuña, A.M., van Alphen, P., Dos Santos, F.B., van Grondelle, R., Hellingwerf, K.J., van Stokkum, I.H.M., 2018d. Spectrally decomposed dark-to-light transitions in *Synechocystis* sp. PCC 6803. Photosynth. Res. 137, 307–320.

Adams III, W.W., Demmig-Adams, B., 2014. Lessons from nature: a personal perspective. In: Demmig-Adams, B., Garab, G., Adams, W.W. III, Govindjee, Sharkey, T.D. (Eds.), Non-Photochemical Quenching and Energy Dissipation in Plants, Algae and Cyanobacteria. Advances in Photosynthesis and Respiration, vol. 40. Springer, Dordrecht, pp. 45–72.

Adams, W.W. III, Terashima, I. (Eds.), 2018. The leaf: a platform for performing photosynthesis. In: Sharkey, T.D., Eaton-Rye, J. (Eds.), Advances in Photosynthesis and Respiration, vol. 44. Springer, Dordrecht, pp. 610.

Adams III, W.W., Demmig-Adams, B., Lange, O.L., 1993. Carotenoid composition and metabolism in green and blue-green algal lichens in the field. Oecologia 94, 576–584.

Adir, N., 2005. Elucidation of the molecular structures of components of the phycobilisome: reconstructing a giant. Photosynth. Res. 85, 15–32.

Aigner, S., Herburger, K., Holzinger, A., Karsten, U., 2018. Epilithic *Chamaesiphon* (Synechococcales, Cyanobacteria) species in mountain streams of the Alps—interspecific differences in photo-physiological traits. J. Appl. Phycol. 30, 1125–1134.

Ajlani, G., Vernotte, C., DiMagno, L., Haselkorn, R., 1995. Phycobilisome core mutants of *Synechocystis* PCC 6803. Biochim. Biophys. Acta 1231, 189–196.

Akimoto, S., Yokono, M., Aikawa, S., Kondo, A., 2013. Modification of energy-transfer processes in the cyanobacterium, *Arthrospira platensis*, to adapt to light conditions, probed by time-resolved fluorescence spectroscopy. Photosynth. Res. 117, 235–243.

Al-Haj, L., Lui, Y.T., Abed, R.M., Gomaa, M.A., Purton, S., 2016. Cyanobacteria as chassis for industrial biotechnology: progress and prospects. Life 6, 42.

Allahverdiyeva, Y., Ermakova, M., Eisenhut, M., Zhang, P., Richaud, P., Hagemann, M., et al., 2011. Interplay between flavodiiron proteins and photorespiration in *Synechocystis* sp. PCC 6803. J. Biol. Chem. 286, 24007–24014.

Allahverdiyeva, Y., Mustila, H., Ermakova, M., Bersanini, L., Richaud, P., Ajlani, G., Battchikova, N., Cournac, L., Aro, E.M., 2013. Flavodiiron proteins Flv1 and Flv3 enable cyanobacterial growth and photosynthesis under fluctuating light. Proc. Natl. Acad. Sci. U. S. A. 110, 4111–4116.

Allahverdiyeva, Y., Isojarvi, J., Zhang, P., Aro, E.-M., 2015. Cyanobacterial oxygenic photosynthesis is protected by flavodiiron proteins. Life 5, 716–743.

Allakhverdiev, S.I., Tomo, T., Shimada, Y., Kindo, H., Nagao, R., Klimov, V.V., Mimuro, M., 2010. Redox potential of pheophytin a in photosystem II of two cyanobacteria having the different special pair chlorophylls. Proc. Natl. Acad. Sci. U. S. A. 107, 3924–3929.

Allen, J.F., Mullineaux, C.W., 2004. Probing the mechanism of state transitions in oxygenic photosynthesis by chlorophyll fluorescence spectroscopy, kinetics and imaging. In: Papageorgiou, G.C., Govindjee (Eds.), Chlorophyll A Fluorescence: A Signature of Photosynthesis. Advances in Photosynthesis and Respiration. vol. 19. Springer, Dordrecht, pp. 663–678.

Allen, J.F., Sanders, C.E., Holmes, N.G., 1985. Correlation of membrane-protein phosphorylation with excitation-energy distribution in the cyanobacterium *Synechococcus* PCC6301. FEBS Lett. 193, 271–275.

Allen, J.F., Santabarbara, S., Allen, C.A., Puthiyaveetil, S., 2011. Discrete redox signaling pathways regulate photosynthetic light-harvesting and chloroplast gene transcription. PLoS One 6, 1–9.

Allorent, G., Tokutsu, R., Roach, T., Peers, G., Cardol, P., et al., 2013. A dual strategy to cope with high light in *Chlamydomonas reinhardtii*. Plant Cell 25, 545–557.

Ananyev, G., Gates, C., Dismukes, G.C., 2018. The multiplicity of roles for (bi)carbonate in photosystem II operation in the hypercarbonate-requiring cyanobacterium *Arthrospira maxima*. Photosynthetica 56, 217–228.

Andersson, B., Åkerlund, H.E., Jergil, B., Larsson, C., 1982. Differential phosphorylation of the light-harvesting chlorophyll–protein complex in appressed and non-appressed regions of the thylakoid membrane. FEBS Lett. 149, 181–185.

Andrizhiyevskaya, E.G., Schwabe, T.M.E., Germano, M., D'Haene, S., Kruip, J., van Grondelle, R., Dekker, J.P., 2002. Spectroscopic properties of PSI-IsiA supercomplexes from the cyanobacterium *Synechococcus* PCC 7942. Biochim. Biophys. Acta 1556, 265–272.

Andrizhiyevskaya, E.G., Frolov, D., van Grondelle, R., Dekker, J.P., 2004. Energy transfer and trapping in the photosystem I complex of *Synechococcus* PCC 7942 and in its supercomplex with IsiA. Biochim. Biophys. Acta 1656, 104–113.

Antal, T.K., Kovalenko, I.B., Rubin, A.B., Tyystjärvi, E., 2013. Photosynthesis-related quantities for education and modeling. Photosynth Res. 117, 1–30.

Aoki, M., Katoh, S., 1982. Oxidation and reduction of plastoquinone by photosynthetic and respiratory electron transport in a cyanobacterium *Synechococcus* sp. Biochim. Biophys. Acta 682, 307–314.

Armbruster, U., Galvis, V.C., Kunz, H.H., Strand, D.D., 2017. The regulation of the chloroplast proton motive force plays a key role for photosynthesis in fluctuating light. Curr. Opin. Plant Biol. 37, 56–62.

Arteni, A.A., Ajlani, G., Boekema, E.J., 2009. Structural organisation of phycobilisomes from *Synechocystis* sp. strain PCC6803 and their interaction with the membrane. Biochim. Biophys. Acta 1787, 272–279.

Ashby, M.K., Mullineaux, C.W., 1999. The role of ApcD and ApcF in energy transfer from phycobilisomes to PSI and PSII in a cyanobacterium. Photosynth. Res. 61, 169–179.

Baake, E., Schlöder, J.P., 1992. Modelling the fast fluorescence rise of photosynthesis. Bull. Math. Biol. 54, 999–1021.

Bandara, S., Ren, Z., Lu, L., Zeng, X., Shin, H., Zhao, K.-H., Yang, X., 2017. Photoactivation mechanism of a carotenoid-based photoreceptor. Proc. Natl. Acad. Sci. U. S. A. 114, 6286–6291.

Bao, H., Melnicki, M.R., Kerfeld, C.A., 2017. Structure and functions of orange Carotenoid protein homologs in cyanobacteria. Curr. Opin. Plant Biol. 37, 1–9.

Bar Eyal, L., Choubeh, R., Cohen, E., Eisenberg, I., Tamburu, C., Dorogi, M., Ünnep, R., Appavou, M.S., Nevo, R., Raviv, U., Reich, Z., Garab, G., van Amerongen, H., Paltiel, Y., Keren, N., 2017. Changes in aggregation states of light-harvesting complexes as a mechanism for modulating energy transfer in desert crust cyanobacteria. Proc. Natl. Acad. Sci. U. S. A. 114, 9481–9486.

Barber, J., 2008. Photosynthetic generation of oxygen. Philos. Trans. R. Soc. Lond. B Biol. Sci. 363 (1504), 2665–2674.

Barber, J., 2014. Photosystem II: its function, structure, and implications for artificial photosynthesis. Biochemistry (Mosc.) 79, 185–196.

Barber, J., 2016. Photosystem II: the water splitting enzyme of photosynthesis and the origin of oxygen in our atmosphere. Q. Rev. Biophys. 49, e14.
Barber, J., Archer, M.D., 2001. P680, the primary electron donor of photosystem II. J. Photochem. Photobiol. A: Chem. 142, 97–106.
Battchikova, N., Eisenhut, M., Aro, E.-M., 2011. Cyanobacterial NDH-1 complexes: novel insights and remaining puzzles. Biochim. Biophys. Acta 1807, 935–944.
Belyaeva, N.E., Bulychev, A.A., Riznichenko, G.Y., Rubin, A.B., 2011. A model of photosystem II for the analysis of fast fluorescence rise in plant leaves. Biophysics 56, 464–472.
Bemal, S., Anil, A.C., 2016. Genetic and ecophysiological traits of *Synechococcus* strains isolated from coastal and open ocean waters of the Arabian Sea. FEMS Microbiol. Ecol. 92, fiw162.
Bennett, J., 1980. Chloroplast phosphoproteins. Evidence for a thylakoid-bound phosphoprotein phosphatase. Eur. J. Biochem. 104, 85–89.
Ben-Shem, A., Frolow, F., Nelson, N., 2003. Crystal structure of plant photosystem I. Nature 426, 630–635.
Berera, R., van Stokkum, I.H.M., d'Haene, S., Kennis, J.T.M., van Grondelle, R., Dekker, J.P., 2009. A mechanism of energy dissipation in cyanobacteria. Biophys. J. 96, 2261–2267.
Berera, R., van Stokkum, I.H.M., Kennis, J.T.M., van Grondelle, R., Dekker, J.P., 2010. The light harvesting function of carotenoids in the cyanobacterial stress-inducible IsiA complex. Chem. Phys. 373, 65–70.
Bergeron, J.A., 1963. In: Kok, B., Jagendorf, A.T. (Eds.), Photosynthetic Mechanisms of Green Plants. vol. 1145. National Academy of Sciences-National Research Council Publication, Washington, DC, pp. 527.
Bernát, G., Steinbach, G., Kaňa, R., Govindjee, Misra, A.N., Prášil, O., 2018. On the origin of the slow M–T chlorophyll a fluorescence decline in cyanobacteria: interplay of short-term light-responses. Photosynth. Res. 136, 183–198.
Bibby, T.S., Nield, J., Barber, J., 2001a. Three-dimensional model and characterization of the iron stress-induced CP43′-photosystem I supercomplex isolated from the cyanobacterium *Synechocystis* PCC 6803. J. Biol. Chem. 276, 43246–43252.
Bibby, T.S., Nield, J., Barber, J., 2001b. Iron deficiency induces the formation of an antenna ring around trimeric photosystem I in cyanobacteria. Nature 412, 743–745.
Biggins, J., Bruce, D., 1989. Regulation of excitation energy transfer in organisms containing phycobilins. Photosynth. Res. 20, 1–34.
Bilger, W., Björkman, O., 1990. Role of the xanthophyll cycle in photoprotection elucidated by measurements of light-induced absorbance changes, fluorescence and photosynthesis in leaves of *Hedera canariensis*. Photosynth. Res. 25, 173–185.
Björkman, O., Demmig, B., 1987. Photon yield of O_2 evolution of chlorophyll fluorescence characteristics at 77 K among vascular plants of diverse origins. Planta 170, 489–504.
Boardman, N.K., Thorne, S.W., Anderson, J.M., 1966. Fluorescence properties of particles obtained by digitonin fragmentation of spinach chloroplasts. Proc. Natl. Acad. Sci. U. S. A. 56, 586–593.
Boekema, E.J., Hifney, A., Yakushevska, A.E., Piotrowski, M., Keegstra, W., Berry, S., Michel, K.-P., Pistorius, E.K., Kruip, J., 2001. A giant chlorophyll–protein complex induced by iron deficiency in cyanobacteria. Nature 412, 745–748.
Bolychevtseva, Y.V., Kuzminov, F.I., Elanskaya, I.V., Gorbunov, M.Y., Karapetyan, N.V., 2015. Photosystem activity and state transitions of the photosynthetic apparatus in cyanobacterium *Synechocystis* PCC 6803 mutants with different redox state of the plastoquinone pool. Biochemistry (Mosc.) 80, 50–60.
Bonaventura, C., Myers, J., 1969. Fluorescence and oxygen evolution from *Chlorella pyrenoidosa*. Biochim. Biophys. Acta 189, 366–383.
Boulay, C., Abasova, L., Six, C., Vass, I., Kirilovsky, D., 2008. Occurrence and function of the orange carotenoid protein in photoprotective mechanisms in various cyanobacteria. Biochim. Biophys. Acta 1777, 1344–1354.
Boulay, C., Wilson, A., D'Haene, S., Kirilovsky, D., 2010. Identification of a protein required for recovery of full antenna capacity in OCP-related photoprotective mechanism in cyanobacteria. Proc. Natl. Acad. Sci. U. S. A. 107, 11620–11625.
Bradbury, M., Baker, N.R., 1981. Analysis of the slow phases of the in vivo chlorophyll fluorescence induction curve. Changes in the redox state of photosystem II electron acceptors and fluorescence emission from photosystems I and II. Biochim. Biophys. Acta 13, 542–551.
Brecht, M., Hussels, M., Schlodder, E., Karapetyan, N.V., 2012. Red antenna states of photosystem I trimers from *Arthrospira platensis* revealed by single-molecule spectroscopy. Biochim. Biophys. Acta 1817, 445–452.
Brettel, K., 1997. Electron transfer and arrangement of the redox cofactors in photosystem I. Biochim. Biophys. Acta 1318, 322–373.
Briantais, J.-M., Vernotte, C., Picaud, M., Krause, G.H., 1979. A quantitative study of the slow decline of chlorophyll *a* fluorescence in isolated chloroplasts. Biochim. Biophys. Acta 548, 128–138.
Bricker, T.M., Roose, J.L., Fagerlund, R.D., Frankel, L.K., Eaton-Rye, J.J., 2012. The extrinsic proteins of photosystem II. Biochim. Biophys. Acta 1817, 121–142.
Britton, G., 2008. Functions of intact carotenoids. In: Britton, G., Liaaen-Jensen, S., Pfander, H. (Eds.), Carotenoids. Natural Functions, vol. 4. Birkhäuser Verlag AG, Basel, pp. 189–212.
Brody, S.S., 1958. A new excited state of chlorophyll. Science 128, 838–839.
Bruce, D., Biggins, J., Steiner, T., Thewalt, M., 1985. Mechanism of the light state transition in photosynthesis: IV. Picosecond fluorescence spectroscopy of *Anacystis nidulans* and *Porphyridium cruentum* in state 1 and state 2 at 77 K. Biochim. Biophys. Acta 806, 237–246.
Bruce, D., Samson, G., Carpenter, C., 1997. The origins of nonphotochemical quenching of chlorophyll fluorescence in photosynthesis. Direct quenching by $P680^+$ in photosystem II enriched membranes at low pH. Biochemistry 36, 749–775.
Bryant, D.A., 1982. Phycoerythrocyanin and phycoerythrin: properties and occurrence in cyanobacteria. J. Gen. Microbiol. 128, 835–844.
Bryant, D.A. (Ed.), 1994. Molecular Biology of Cyanobacteria. Advances in Photosynthesis and Research, vol. 1. Springer, Dordrecht, pp. 892.
Bulté, L., Gans, P., Rebeillé, F., Wollman, F.A., 1990. ATP control on state transitions in vivo in *Chlamydomonas reinhardtii*. Biochim. Biophys. Acta 1020, 72–80.

Burnap, R.L., Troyan, T., Sherman, L.A., 1993. The highly abundant chlorophyll-protein complex of iron-deficient *Synechococcus* sp. PCC 7942 (CP43) is encoded by the isiA gene. Plant Physiol. 103, 893–902.

Butler, W.L., Visser, J.W.M., Simons, H.L., 1973. The kinetics of light-induced changes of C-550, cytochrome b559 and fluorescence yield in chloroplasts at low temperature. Biochim. Biophys. Acta 292, 140–151.

Byrdin, M., Rimke, I., Schlodder, E., Stehlik, D., Roelofs, T.A., 2000. Decay kinetics and quantum yields of fluorescence in photosystem I from *Synechococcus elongatus* with P700 in the reduced and oxidized state: are the kinetics of excited state decay trap-limited or transfer-limited? Biophys. J. 79, 992–1007.

Campbell, D., Öquist, G., 1996. Predicting light acclimation in cyanobacteria from nonphotochemical quenching of photosystem II fluorescence, which reflects state transitions in these organisms. Plant Physiol. 111, 1293–1298.

Campbell, D.A., Tyystjärvi, E., 2012. Parameterization of photosystem II photoinactivation and repair. Biochim. Biophys. Acta 1817, 258–265.

Campbell, D., Hurry, V., Clarke, A.K., Gustafsson, P., Öquist, G., 1998. Chlorophyll fluorescence analysis of cyanobacterial photosynthesis and acclimation. Microbiol. Mol. Biol. Rev. 62, 667–683.

Canaani, O., Barber, J., Malkin, S., 1984. Evidence that phosphorylation and dephosphorylation regulate the distribution of excitation energy between the two photosystems of photosynthesis in vivo: photoacoustic and fluorimetric study of an intact leaf. Proc. Natl. Acad. Sci. U. S. A. 81, 1614–1618.

Cao, J., Govindjee, 1988. Bicarbonate effect on electron flow in a cyanobacterium *Synechocystis* PCC 6803. Photosynth. Res. 19, 277–285.

Cao, J., Vermaas, W.F.J., Govindjee, 1991. Arginine residues in the D2 polypeptide may stabilize bicarbonate binding in photosystem II of *Synechocystis* sp. PCC 6803. Biochim. Biophys. Acta 1059, 171–180.

Cao, J., Ohad, N., Hirschberg, J., Xiong, J., Govindjee, 1992. Binding affinity of bicarbonate and formate in herbicide-resistant D1 mutants of *Synechococcus* sp. PCC 7942. Photosynth. Res. 34, 397–408.

Carpine, R., Raganati, F., Olivieri, G., Hellingwerf, K.J., Pollio, A., Salatino, P., Marzocchella, A., 2018. Poly-β-hydroxybutyrate (PHB) production by *Synechocystis* PCC6803 from CO_2: model development. Algal Res. 29, 49–60.

Casella, S., Huang, F., Mason, D., Zhao, G.Y., Johnson, G.N., Mullineaux, C.W., Liu, L.N., 2017. Dissecting the native architecture and dynamics of cyanobacterial photosynthetic machinery. Mol. Plant. 10, 1434–1448.

Ceppi, M.G., Oukarroum, A., Nuran, C., Strasser, R.J., Schansker, G., 2012. The IP amplitude of the fluorescence rise OJIP sensitive to changes in the photosystem I content of leaves: a study on plants exposed to magnesium and sulfate deficiencies, drought stress and salt stress. Physiol. Plant. 144, 277–288.

Chang, L., Liu, X., Li, Y., Liu, C.C., Yang, F., Zhao, J., Sui, S.F., 2015. Structural organization of an intact phycobilisome and its association with photosystem II. Cell Res. 25, 726–737.

Cheeseman, J.M., Clough, B.F., Carter, D.R., Lovelock, C.E., Eong, O.J., Sim, R.G., 1991. The analysis of photosynthetic performance in leaves under field conditions: a case study using *Bruguiera mangroves*. Photosynth. Res. 29, 11–22.

Cheeseman, J.M., Herendeen, L.B., Cheeseman, A.T., Clough, B.F., 1997. Photosynthesis and photoprotection in mangroves under field conditions. Plant Cell Environ. 20, 579–588.

Chen, M., Li, Y., Birch, D., Willows, R.D., 2012. A cyanobacterium that contains chlorophyll f—a red-absorbing photopigment. FEBS Lett. 586, 3249–3254.

Chen, J., Kell, A., Acharya, K., Kupitz, C., Fromme, P., Jankowiak, R., 2015a. Critical assessment of the emission spectra of various photosystem II core complexes. Photosynth. Res. 124, 253–265.

Chen, Z., Zhan, J., Chen, Y., Yang, M., He, C., Ge, F., Wang, Q., 2015b. Effects of phosphorylation of β subunits of phycocyanins on state transition in the model cyanobacterium *Synechocystis* sp. PCC 6803. Plant Cell Physiol. 56, 1997–2013.

Chen, H.-Y.S., Michelle Liberton, M., Pakrasi, H.B., Niedzwiedzki, D.M., 2017. Reevaluating the mechanism of excitation energy regulation in iron-starved cyanobacteria. Biochim. Biophys. Acta 1858, 249–258.

Chen, H.-Y.S., Bandyopadhyay, A., Pakrasi, H.B., 2018. Function, regulation and distribution of IsiA, a membrane-bound chlorophyll *a*-antenna protein in cyanobacteria. Photosynthetica 56, 322–333.

Cho, F., Govindjee, 1970a. Low-temperature (4-77 K) spectroscopy of *Chlorella*: temperature dependence of energy transfer efficiency. Biochim. Biophys. Acta 216, 139–150.

Cho, F., Govindjee, 1970b. Low temperature (4-77 K) spectroscopy of *Anacystis*: temperature dependence of energy transfer efficiency. Biochim. Biophys. Acta 216, 151–161.

Chow, W.S., Telfer, A., Chapman, D.J., Barber, J., 1981. State 1-State 2 transition in leaves and its association with ATP induced chlorophyll fluorescence quenching. Biochim. Biophys. Acta 638, 60–68.

Chukhutsina, V.U., Bersanini, L., Aro, E.M., van Amerongen, H., 2015. Cyanobacterial light-harvesting phycobilisomes uncouple from photosystem I during dark-to-light transitions. Sci. Rep. 5, 14193.

Clarke, A.K., Hurry, V.M., Gustafsson, P., Öquist, G., 1993. Two functionally distinct forms of the photosystem II reaction-center protein Dl in the cyanobacterium *Synechococcus* sp. PCC 7942. Proc. Natl. Acad. Sci. U. S. A. 90, 11985–11989.

Clarke, A.K., Campbell, D., Gustafsson, P., Öquist, G., 1995. Dynamic responses of photosystem I1 and phycobilisomes to changing light in the cyanobacterium *Synechococcus* sp. PCC 7942. Planta 197, 553–562.

Clegg, R.M., Sener, M., Govindjee, 2010. From Förster resonance energy transfer (FRET) to coherent resonance energy transfer (CRET) and back-A wheen o'mickles mak's a muckle. In: Alfano, R.R. (Ed.), Optical Biopsy VII. Proceedings of SPIE, vol. 7561. SPIE, Bellingham, WA, pp. 7561–7572. article CID number: 75610C, 2010, 21 pp.).

Cooley, J.W., Vermaas, W.F., 2001. Succinate dehydrogenase and other respiratory pathways in thylakoid membranes of Synechocystis sp. strain PCC 6803: capacity comparisons and physiological function. J. Bacteriol. 183, 4251–4258.

Cox, N., Pushkar, Y., Yano, J., Sauer, K., Boussac, A., Yachandra, V.K., 2008. Structural changes in the Mn4Ca cluster and the mechanism of photosynthetic water splitting. Proc. Natl. Acad. Sci. U. S. A. 105, 1879–1884.

Cramer, W.A., Kallas, T., 2016. Cytochrome complexes: evolution, structures, energy transduction, and signaling. In: Govindjee, Sharkey, T.D. (Eds.), Advances in Photosyntesis and Respiration. vol. 41. Springer, Dordrecht, pp. 754.

Croce, R., van Grondelle, R., van Amerongen, H., van Stokkum, I.H.M. (Eds.), 2018. Light Harvesting in Photosynthesis. Foundations of Biochemistry and Biophysics. Taylor & Francis Group/CRC Press, London, pp. 611.

Daddy, S., Zhan, J., Jantaro, S., He, C., He, Q., Wang, Q., 2015. A novel high light-inducible carotenoid-binding protein complex in the thylakoid membranes of *Synechocystis* PCC 6803. Sci. Rep. 5, 9480.

Dang, N.C., Zazubovich, V., Reppert, M., Neupane, B., Picorel, R., Seibert, M., Jankowiak, R., 2008. The CP43 proximal antenna complex of higher plant photosystem II revisited: modeling and hole burning study. I. J. Phys. Chem. B 112, 9921–9933.

Das, M., Govindjee, 1967. A long-wave absorbing form of chlorophyll *a* responsible for the red drop in fluorescence at 298 K and the F723 band at 77 K. Biochim. Biophys. Acta 143, 570–576.

David, L., Prado, M., Arteni, A.A., Elmlund, D.A., Blankenship, R.E., Adir, N., 2014. Structural studies show energy transfer within stabilized phycobilisomes independent of the mode of rod–core assembly. Biochim. Biophys. Acta 1837, 385–395.

de Carbon, C.B., Thurotte, A., Wilson, A., Perreau, F., Kirilovsky, D., 2015. Biosynthesis of soluble carotenoid holoproteins in *Escherichia coli*. Sci. Rep. 5, 9085.

de Paula, J.C., Innes, J.B., Brudvig, G.W., 1985. Electron transfer in photosystem II at cryogenic temperatures. Biochemistry 24, 8114–8120.

de Weerd, F.L., van Stokkum, I.H.M., van Amerongen, H., Dekker, J.P., van Grondelle, R., 2002. Pathways for energy transfer in the core light-harvesting complexes CP43 and CP47 of photosystem II. Biophys. J. 82, 1586–1597.

de Weerd, F.L., Dekker, J.P., van Grondelle, R., 2003a. Dynamics of β-carotene-to-chlorophyll singlet energy transfer in the core of photosystem II. J. Phys. Chem. B 107, 6214–6220.

de Weerd, F.L., Kennis, J.T.M., Dekker, J.P., van Grondelle, R., 2003b. β-Carotene to chlorophyll singlet energy transfer in the photosystem I core of *Synechococcus elongatus* proceeds via the β-carotene S2 and S1 states. J. Phys. Chem. B 107, 5995–6002.

Dekker, J.P., Hassoldt, A., Pettersson, Å., van Roon, H., Groot, M.-L., van Grondelle, R., 1995. On the nature of the F695 and F685 emission of photosystem II. In: Mathis, P. (Ed.), Photosynthesis: From Light to Biosphere. Kluwer Academic Publishers, Dordrecht, pp. 53–56.

Delepelaire, P., Wollman, F.A., 1985. Correlations between fluorescence and phosphorylation changes in thylakoid membranes of *Chlamydomonas reinhardtii* in vivo: a kinetic analysis. Biochim. Biophys. Acta 809, 277–283.

Delosme, R., 1967. Étude de l'induction de fluorescence des algues vertes et des chloroplastes au début d'une illumination intense. Biochim. Biophys. Acta 143, 108–128.

Demmig-Adams, B., Adams III, W.W., 2006. Photoprotection in an ecological context: the remarkable complexity of thermal energy dissipation. New Phytol. 172, 11–21.

Demmig-Adams, B., Adams III, W.W., Czygan, F.-C., Schreiber, U., Lange, O.L., 1990a. Differences in the capacity for radiationless energy dissipation in the photochemical apparatus of green and blue-green algal lichens associated with differences in carotenoid composition. Planta 180, 582–589.

Demmig-Adams, B., Adams III, W.W., Green, T.G.A., Czygan, F.-C., Lange, O.L., 1990b. Differences in the susceptibility to light stress in two lichens forming a phycosymbiodeme, one partner possessing and one lacking the xanthophyll cycle. Oecologia 84 (4), 451–456.

Demmig-Adams, B., Máguas, C., Adams III, W.W., Meyer, A., Kilian, E., Lange, O.L., 1990c. Effect of high light on the efficiency of energy conversion in a variety of lichen species with green and blue-green phycobionts. Planta 180, 400–409.

Demmig-Adams, B., Adams, W.W. III, Mattoo, A. (Eds.), 2006. Photoprotection, Photoinhibition, Gene Regulation, and Environment. Advances in Photosynthesis and Respiration, vol. 21, Springer, Dordrecht, pp. 580.

Demmig-Adams, B., Garab, G., Adams III, W.W., 2014. Non-photochemical quenching and energy dissipation in plants, algae and cyanobacteria. In: Govindjee, Sharkey, T.D. (Eds.), Advances in Photosynthesis and Respiration. vol. 40. Springer, Dordrecht, pp. 649.

Deng, C., Pan, X., Wang, S., Zhang, D., 2014. Cu(2+) inhibits photosystem II activities but enhances photosystem I quantum yield of *Microcystis aeruginosa*. Biol. Trace Elem. Res. 160, 268–725.

Depege, N., Bellafiore, S., Rochaix, J.D., 2003. Role of chloroplast protein kinase *Stt7* in LHCII phosphorylation and state transition in *Chlamydomonas*. Science 299, 1572–1575.

DeVault, D., Govindjee, 1990. Photosynthetic glow peaks and their relationship with the free energy changes. Photosynth. Res. 24, 175–181.

DeVault, D., Govindjee, Arnold, W., 1983. Energetics of photosynthesis glow peaks. Proc. Natl. Acad. Sci. U. S. A. 80, 983–987.

Di Donato, M., Stahl, A.D., van Stokkum, I.H.M., van Grondelle, R., Groot, M.L., 2011. Cofactors Involved in light-driven charge separation in photosystem I identified by subpicosecond infrared spectroscopy. Biochemistry 50, 480–490.

Diner, B.A., Rappaport, F., 2002. Structure, dynamics, and energetics of the primary photochemistry of Photosystem II of oxygenic photosynthesis. Annu. Rev. Plant Biol. 53, 551–580.

Dolganov, N.A., Bhaya, D., Grossman, A.R., 1995. Cyanobacterial protein with similarity to the chlorophyll a/b binding proteins of higher plants: evolution and regulation. Proc. Natl. Acad. Sci. U. S. A. 92, 636–640.

Dong, C., Tang, A., Zhao, J., Mullineaux, C.W., Shen, G., Bryant, D.A., 2009. ApcD is necessary for efficient energy transfer from phycobilisomes to photosystem I and helps to prevent photoinhibition in the cyanobacterium *Synechococcus* sp. PCC 7002. Biochim. Biophys. Acta 1787, 1122–1128.

Douglas, S.E., 1994. Chloroplast origins and evolution. In: Bryant, D.A. (Ed.), The Molecular Biology of Cyanobacteria, Advances in Photosynthesis and Respiration. vol. 1. Springer, Dordrecht, pp. 91–118.

Duan, Z., Tan, X., Li, N., 2017. Ultrasonic selectivity on depressing photosynthesis of cyanobacteria and green algae probed by chlorophyll-A fluorescence transient. Water Sci. Technol. 76, 2085–2094.

Duan, H.G., Prokhorenko, V.I., Wientjes, E., Croce, R., 2018. Primary charge separation in the photosystem II reaction center revealed by a global analysis of the two-dimensional electronic spectra. Sci. Rep. 7, 12347.

Duysens, L.N.M., 1952. Transfer of Excitation Energy in Photosynthesis. (Doctoral thesis). State University, Utrecht.

Duysens, L.N.M., Sweers, H.E., 1963. Mechanism of the two photochemical reactions in algae as studied by means of fluorescence. In: Japanese Society of Plant Physiologists (Eds.), Studies on Microalgae and Photosynthetic Bacteria. University of Tokyo Press, Tokyo, pp. 353–372.

Eaton-Rye, J.J., Govindjee, 1988. Electron transfer through the quinone acceptor complex of photosystem II in bicarbonate depleted spinach thylakoid membranes as a function of actinic flash number and frequency. Biochim. Biophys. Acta 935, 237–247.

Ebenhöh, O., Fucile, G., Finazzi, G., Rochaix, J.-D., Goldschmidt-Clermont, M., 2014. Short-term acclimation of the photosynthetic electron transfer chain to changing light: a mathematical model. Philos. Trans. R. Soc. B 369, 20130223.

El Bissati, K., Kirilovsky, D., 2001. Regulation of psbA and psaE expression by light quality in *Synechocystis* species PCC 6803. A redox control mechanism. Plant Physiol. 125, 1988–2000.

El Bissati, K., Delphin, E., Murata, N., Etienne, A.-L., Kirilovsky, D., 2000. Photosystem II fluorescence quenching in the cyanobacterium *Synechocystis* PCC 6803: involvement of two different mechanisms. Biochim. Biophys. Acta 1457, 229–242.

Emlyn-Jones, D., Ashby, M.K., Mullineaux, C.W., 1999. A gene required for the regulation of photosynthetic light harvesting in the cyanobacterium *Synechocystis* 6803. Mol. Microbiol. 33 (5), 1050–1058.

Engelken, J., Funk, C., Adamska, I., 2012. The extended light-harvesting complex (LHC) protein superfamily: classification and evolutionary dynamics. In: Burnap, R., Vermaas, W. (Eds.), Functional Genomics and Evolution of Photosynthetic Systems. Springer, Dordrecht, pp. 265–284.

Ermakova, M., Huokko, T., Richaud, P., Bersanini, L., Howe, C.J., Lea-Smith, D.J., Peltier, G., Allahverdiyeva, Y., 2016. Distinguishing the roles of thylakoid respiratory terminal oxidases in the cyanobacterium *Synechocystis* sp. PCC 6803. Plant Physiol. 171, 1307–1319.

Falkowski, P.G., Raven, J.A., 2007. Aquatic Photosynthesis, second ed. Princeton University Press, Princeton. 484 pp.

Falkowski, P.G., Katz, M.E., Knoll, A.H., Quigg, A., Raven, J.A., Schofield, O., Taylor, F.R.J., 2004. The evolution of modern phytoplankton. Science 305, 354–360.

Federman, S., Malkin, S., Scherz, A., 2000. Excitation energy transfer in aggregates of photosystem I and photosystem II of the cyanobacterium *Synechocystis* sp. PCC 6803: can assembly of the pigment-protein complexes control the extent of spillover? Photosynth. Res. 64, 199–207.

Feild, T.S., Nedbal, L., Ort, D.R., 1998. Nonphotochemical reduction of the plastoquinone pool in sunflower leaves originates from chlororespiration. Plant Physiol. 116, 1209–1218.

Feng, X., Neupane, B., Acharya, K., et al., 2011. Spectroscopic study of the CP43′ complex and the PSI-CP43′ supercomplex of the cyanobacterium *Synechocystis* PCC 6803. J. Phys. Chem. B 115, 13339–13349.

Fenton, J.M., Pellin, M.J., Govindjee, Kaufmann, K., 1979. Primary photochemistry of the reaction center of photosystem I. FEBS Lett. 100, 1–4.

Ferreira, K.N., Iverson, T.M., Maghlaoui, K., Barber, J., Iwata, S., 2004. Architecture of the photosynthetic oxygen-evolving center. Science 303, 1831–1838.

Fitzgerald, M.P., Husain, A., Hutber, G.N., et al., 1977. Studies on the flavodoxins from a cyanobacterium and a red alga. Biochem. Soc. Trans. 5, 1505–1506.

Fleming, G.R., 2018. The contributions of 49ers to the measurements and models of ultrafast photosynthetic energy transfer. Photosynth. Res. 135, 3–8.

Flombaum, P., Gallegos, J.L., Gordillo, R.A., Rincón, J., Zabala, L.L., Jiao, N., Karl, D.M., Li, W.K.W., Lomas, M.W., Veneziano, D., Vera, C.S., Vrugt, J.A., Martiny, A.C., 2013. Present and future global distributions of the marine cyanobacteria *Prochlorococcus* and *Synechococcus*. Proc. Natl. Acad. Sci. U. S. A. 110, 9824–9829.

Fork, D.C., Mohanty, P., 1986. Fluorescence and other characteristics of blue-green algae (Cyanobacteria), red algae and cryptomonad. In: Govindjee, Amesz, J., Fork, D.C. (Eds.), Light Emission by Plants and Bacteria. Academic Press, London, pp. 451–496.

Fork, D.C., Satoh, K., 1983. State I-State II transitions in the thermophilic blue-green alga (cyanobacterium) *Synechococcus lividus*. Photochem. Photobiol. 37, 421–427.

France, L.L., Geacintov, N.E., Breton, J., Valkunas, L., 1992. The dependence of the degrees of sigmoidicities of fluorescence induction curves in spinach-chloroplasts on the duration of actinic pulses in pump-probe experiments. Biochim. Biophys. Acta 1101, 105–119.

Franck, F., Juneau, P., Popovic, R., 2002. Resolution of the photosystem I and photosystem II contributions to chlorophyll fluorescence of intact leaves at room temperature. Biochim. Biophys. Acta 1556, 239–246.

Fraser, J.M., Tulk, S.E., Jeans, J.A., Campbell, D.A., Bibby, T.S., Cockshutt, A.M., 2013. Photophysiological and photosynthetic complex changes during iron starvation in *Synechocystis* sp. PCC 6803 and *Synechococcus* elongatus PCC 7942. PLoS One 8, e59861.

Fratamico, A., Tocquin, P., Franck, F., 2016. The chlorophyll *a* fluorescence induction curve in the green microalga *Haematococcus pluvialis*: further insight into the nature of the P–S–M fluctuation and its relationship with the "low-wave" phenomenon at steady-state. Photosynth. Res. 128, 271–285.

Fromme, P., Grotjohann, I., 2011. Structure of cyanobacterial photosystems I and II. In: Peschek, G.A., Obinger, C., Renger, G. (Eds.), Bioenergetic Processes of Cyanobacteria: From Evolutionary Singularity to Ecological Diversity. Springer, Dordrecht, pp. 285–335.

Fromme, P., Jordan, P., Krauss, N., 2001. Structure of photosystem I. Biochim. Biophys. Acta 1507, 5–31.

Fromme, P., Schlodder, E., Jansson, S., 2003. Structure and function of the antenna system in photosystem I. In: Green, B.R., Parson, W.W. (Eds.), Light-Harvesting Antennas in Photosynthesis. Kluwer, Dordrecht, pp. 253–279.

Fujita, Y., Murakami, A., Aizawa, K., Ohki, K., 1994. Short-term and long-term adaptation of the photosynthetic apparatus: homeostatic properties of thylakoids. In: Bryant, D.A., Govindjee (Eds.), The Molecular Biology of Cyanobacteria. Advances in Photosynthesis and Respiration. vol. 1. Kluwer Academic Publishers, Dordrecht, pp. 677–692.

Gantt, E., 1981. Phycobilisomes. Annu. Rev. Plant Physiol. 32, 327–347.

Gao, K., Yu, H., Brown, M.T., 2007. Solar PAR and UV radiation affects the physiology and morphology of the cyanobacterium *Anabaena* sp. PCC 7120. J. Photochem. Photobiol. B 89, 117–124.

Gao, X., Sun, T., Pei, G., Chen, L., Zhang, W., 2016. Cyanobacterial chassis engineering for enhancing production of biofuels and chemicals. Appl. Microbiol. Biotechnol. 100, 3401–3413.

Gasanov, R., Abilov, Z.K., Gazanchyan, R.M., Kurbanova, U.M., Khanna, R., Govindjee, 1979. Excitation energy transfer in photosystems I and II from grana and in photosystem I from stroma lamellae, and identification of emission bands with pigment-protein complexes at 77 K. Z. Pflanzenphysiol. 95, 149–169.

Genty, B., Briantais, J.-M., Baker, N.R., 1989. The relationship between the quantum yield ofphotosynthetic electron transport and quenching of chlorophyll fluorescence. Biochim. Biophys. Acta 990, 87–92.

Ghosh, A.K., Govindjee, 1966. Transfer of the excitation energy in Anacystis nidulans grown to obtain different pigment ratios. Biophys. J. 6, 611–619.

Giera, W., Gibasiewicz, K., Ramesh, V.M., Lin, S., Webber, A.N., 2009. Electron transfer from A_0 to A_1 in photosystem I from *Chlamydomonas reinhardtii* occurs in both the A and B branch with 25-30-ps lifetime. Phys. Chem. Chem. Phys. 11, 186–191.

Glazer, A.N., 1984. Phycobilisome—a macromolecular complex optimized for light energy-transfer. Biochim. Biophys. Acta 768, 29–51.

Glazer, A.N., 1989. Light guides. Directional energy transfer in a photosynthetic antenna. J. Biol. Chem. 264, 1–4.

Glazer, A.N., Gindt, Y., Chan, C.F., Sauer, K., 1994. Selective disruption of energy flow from phycobilisomes to photosystem I. Photosynth. Res. 40, 167–173.

Gobets, B., van Grondelle, R., 2001. Energy transfer and trapping in photosystem I. Biochim. Biophys. Acta 1507, 80–99.

Gobets, B., van Amerongen, H., Monshouwer, R., Kruip, J., Rögner, M., van Grondelle, R., Dekker, J.P., 1994. Polarized site-selected fluorescence spectroscopy of isolated photosystem I particles. Biochim. Biophys. Acta 1188, 75–85.

Goedheer, J.C., 1961. Energy transfer from carotenoids to chlorophyll in blue-green, red and green algae and greening bean leaves. Biochim. Biophys. Acta 172, 252–265.

Golbeck, J.H., 1987. Structure, function and organization of the photosystem I reaction center complex. Biochim. Biophys. Acta 895, 167–204.

Golbeck, J.H. (Ed.), 2006. Photosystem I. The Light-Driven Plastocyanin:Ferredoxin Oxidoreductase. Springer, Dordrecht, pp. 713.

Gorbunov, M.Y., Kuzminov, F.I., Fadeev, V.V., Kim, J.D., Falkowski, P.G., 2011. A kinetic model of non-photochemical quenching in cyanobacteria. Biochim. Biophys. Acta 1807, 1591–1599.

Govindjee, 1963. Observations on P750A from *Anacystis nidulans*. Naturwissenschaften 50, 720–721.

Govindjee, 1995. Sixty-three years since Kautsky: chlorophyll a fluorescence. Aust. J. Plant Physiol. 22, 131–160.

Govindjee, 1999. Carotenoids in photosynthesis: a historical perspective. In: Frank, H.A., Young, A.J., Britton, G., Cogdell, R.J. (Eds.), The Photochemistry of Cyanobacteria. Kluwer Academic Publishers, Dordrecht, pp. 1–19.

Govindjee, 2004. Chlorophyll a fluorescence: a bit of basics and history. In: Papageorgiou, G.C., Govindjee (Eds.), Chlorophyll *a* Fluorescence: A Signature of Photosynthesis. Advances in Photosynthesis and Respiration, vol. 19. Springer, Dordrecht, pp. 1–41.

Govindjee, Papageorgiou, G.C., 1971. Chlorophyll fluorescence and photosynthesis: fluorescence transients. In: Photophysiology. Acad. Press, New York/London, pp. 1–46.

Govindjee, Satoh, K., 1986. Fluorescence properties of chlorophyll b- and chlorophyll c-containing algae. In: Govindjee, Amesz, J., Fork, D.C. (Eds.), Light Emission by Plants and Bacteria. Academic Press, Orlando, pp. 497–537.

Govindjee, Shevela, D., 2011. Adventures with cyanobacteria: a personal perspective. Front. Plant Sci. 2, 28.

Govindjee, Wasielewski, M.R., 1989. Photosystem II: from a femtosecond to a millisecond. In: Briggs, G.E. (Ed.), Photosynthesis. Alan Liss Publishers, New York, pp. 71–103.

Govindjee, Yang, L., 1966. Structure of the red fluorescence band in chloroplasts. J. Gen. Physiol. 49, 763–780.

Govindjee, Pulles, M.P.J., Govindjee, R., van Gorkom, H.J., Duysens, L.N.M., 1976. Inhibition of reoxidation of secondary-electron acceptor of photosystem II by bicarbonate depletion. Biochim. Biophys. Acta 449, 602–605.

Govindjee, Amesz, J., Fork, D.C. (Eds.), 1986. Light Emission by Plants and Bacteria. Academic Press, Orlando, pp. 638.

Govindjee, Kern, J.F., Messinger, J., Whitmarsh, J., 2010. Photosystem II. In: Encyclopedia of Life Sciences (ELS). John Wiley & Sons, Ltd., Chichester.

Govindjee, Shevela, D., Björn, L., 2017. Evolution of the Z-scheme of photosynthesis: a perspective. Photosynth. Res. 133, 5–15.

Groot, M.L., Peterman, E.J., van Kan, P.J., van Stokkum, I.H., Dekker, J.P., van Grondelle, R., 1994. Temperature-dependent triplet and fluorescence quantum yields of the photosystem II reaction center described in a thermodynamic model. Biophys. J. 67, 318–330.

Groot, M.-L., Peterman, E.J.G., van Stokkum, I.H.M., Dekker, J.P., van Grondelle, R., 1995. Triplet and fluorescing states of the CP47 antenna complex of photosystem II studied as a function of temperature. Biophys. J. 68, 281–290.

Groot, M.-L., Frese, R.N., de Weerd, F.L., Bromek, K., Pettersson, Å., Peterman, E.J.G., van Stokkum, I.H.M., van Grondelle, R., Dekker, J.P., 1999. Spectroscopic properties of the CP43 core antenna protein of photosystem II. Biophys. J. 77, 3328–3340.

Guikema, J.A., Sherman, L.A., 1984. Influence of iron deprivation on the membrane composition of *Anacystis nidulans*. Plant Physiol. 74, 90–95.

Guissé, B., Srivastava, A., Strasser, R.J., 1995. The polyphasic rise of the chlorophyll *a* fluorescence (O–K–J–I–P) in heat stressed leaves. Arch. Sci. Genève 48, 147–160.

Gupta, S., Guttman, M., Leverenz, R.L., Zhumadilova, K., Pawlowski, E.G., Petzold, C.J., Lee, K.K., Ralston, C.Y., Kerfeld, C.A., 2015. Local and global structural drivers for the photoactivation of the orange carotenoid protein. Proc. Natl. Acad. Sci. U. S. A. 112, E5567–E5574.

Gurchiek, J.K., Bao, H., Domínguez-Martín, M.A., McGovern, S.E., Marquardt, C.E., Roscioli, J.D., Ghosh, S., Kerfeld, C.A., Beck, W.F., 2018. Fluorescence and excited-state conformational dynamics of the Orange Carotenoid protein. J. Phys. Chem. B 122, 1792–1800.

Guskov, A., Kern, J., Gabdulkhakov, A., Broser, M., Zouni, A., Saenger, W., 2009. Cyanobacterial photosystem II at 2.9-Å resolution and the role of quinones, lipids, channels and chloride. Nature 16, 334–342.

Guskov, A., Gabdulkhakov, A., Broser, M., Glöckner, C., Hellmich, J., Kern, J., Frank, J., Müh, F., Saenger, W., Zouni, A., 2010. Recent progress in the crystallographic studies of photosystem II. ChemPhysChem 11, 1160–1171.

Gwizdala, M., Wilson, A., Kirilovsky, D., 2011. In vitro reconstitution of the cyanobacterial photoprotective mechanism mediated by the orange carotenoid protein in *Synechocystis* PCC 6803. Plant Cell 23, 2631–2643.

Gwizdala, M., Wilson, A., Omairi-Nasser, A., Kirilovsky, D., 2013. Characterization of the *Synechocystis* PCC 6803 fluorescence recovery protein involved in photoprotection. Biochim. Biophys. Acta 1827, 348–354.

Gwizdala, M., Berera, R., Kirilovsky, D., van Grondelle, R., Krüger, T.P.J., 2016. Controlling light harvesting with light. J. Am. Chem. Soc. 138, 11616–11622.

Gwizdala, M., Botha, J.L., Wilson, A., Kirilovsky, D., van Grondelle, R., Krüger, T.P.J., 2018a. Switching an individual phycobilisome off and on. J. Phys. Chem. Lett. 9, 2426–2432.

Gwizdala, M., Krüger, T.P.J., Wahadoszamen, M., Gruber, J.M., van Grondelle, R., 2018b. Phycocyanin: one complex, two states, two functions. J. Phys. Chem. Lett. 9, 1365–1371.

Hall, J., Renger, T., Müh, F., Picorel, R., Krausz, E., 2016. The lowest-energy chlorophyll of photosystem II is adjacent to the peripheral antenna: emitting states of CP47 assigned via circularly polarized luminescence. Biochim. Biophys. Acta 1857, 1580–1593.

Harris, D., Tal, O., Jallet, D., Wilson, A., Kirilovsky, D., Adir, N., 2016. Orange carotenoid protein burrows into the phycobilisome to provide photoprotection. Proc. Natl. Acad. Sci. U. S. A. 113, E1655–E1662.

Harris, D., Bar-Zvi, S., Lahav, A., Goldshmid, I., Adir, N., 2018. The structural basis for the extraordinary energy-transfer capabilities of the phycobilisome. In: Harris, J.R., Boekema, E.J. (Eds.), Membrane Protein Complexes: Structure and Function, Subcellular Biochemistry. vol. 87. Springer Nature, Singapore, pp. 57–82.

Havaux, M., Guedeney, G., He, Q., Grossman, A.R., 2003. Elimination of high-light-inducible polypeptides related to eukaryotic chlorophyll a/b-binding proteins results in aberrant photoacclimation in *Synechocystis* PCC6803. Biochim. Biophys. Acta 1557, 21–33.

Havaux, M., Guedeney, G., Hagemann, M., Yeremenko, N., Matthijs, H.C., Jeanjean, R., 2005. The chlorophyll-binding protein IsiA is inducible by high light and protects the cyanobacterium *Synechocystis* PCC 6803 from photooxidative stress. FEBS Lett. 579, 2289–2293.

Hays, A.M.A., Vasiliev, I.R., Golbeck, J.H., Debus, R.J., 1999. Role of D1-His190 in the proton-coupled oxidation of tyrosine Y_Z in manganese-depleted photosystem II. Biochemistry 38, 11852–11865.

He, Q., Dolganov, N., Björkman, O., Grossman, A.R., 2001. The high light-inducible polypeptides in *Synechocystis* PCC6803: expression and function in high light. J. Biol. Chem. 276, 306–314.

Heathcote, P., Williams-Smith, D.L., Sihra, C.K., Evans, M.C., 1978. The role of the membrane-bound iron–sulphur centres A and B in the photosystem I reaction centre of spinach chloroplasts. Biochim. Biophys. Acta 503, 333–342.

Hendrickson, L., Furbank, R.T., Chow, W.S., 2004. A simple alternative approach to assessing the fate of absorbed light energy using chlorophyll fluorescence. Photosynth. Res. 82, 73–81.

Hippler, M., Reichert, J., Sutter, M., Zak, E., Altschmied, L., Schröer, U., Herrmann, R.G., Haehnel, W., 1996. The plastocyanin binding domain of photosystem I. EMBO J. 15, 6374–6384.

Hodges, M., Cornic, G., Briantais, J.-M., 1989. Chlorophyll fluorescence from spinach leaves: resolution of non-photochemical quenching. Biochim. Biophys. Acta 974, 289–293.

Holland, S.C., Kappell, A.D., Burnap, R.L., 2015. Redox changes accompanying inorganic carbon limitation in *Synechocystis* sp. PCC 6803. Biochim. Biophys. Acta 1847, 355–363.

Holt, T.K., Krogmann, D.W., 1981. A carotenoid-protein from cyanobacteria. Biochim. Biophys. Acta 637, 408–414.

Holt, N.E., Kennis, J.T.M., Fleming, G.R., 2004. Femtosecond fluorescence upconversion studies of light harvesting by β-carotene in oxygenic photosynthetic core proteins. J. Phys. Chem. B 108, 19029–19035.

Holzwarth, A.R., 1996. Data analysis of time-resolved measurements. In: Amesz, J., Hoff, A.J. (Eds.), Biophysical Techniques in Photosynthesis. Kluwer, Dordrecht, pp. 75–92.

Holzwarth, A.R., Müler, M.G., Reus, M., Nowaczyk, M., Sander, J., Rogner, M., 2006a. Kinetics and mechanism of electron transfer ion intact photosystem II and in isolated reaction center: pheophytin is the primary electron acceptor. Proc. Natl. Acad. Sci. U. S. A. 103, 6895–6900.

Holzwarth, A.R., Müler, M.G., Niklas, J., Lubitz, W., 2006b. Ultrafast transient absorption studies on photosystem I reaction centers from *Chlamydomonas reinhardtii*. 2: mutations near the P700 reaction center chlorophylls provide new insight into the nature of the primary electron donor. Biophys. J. 90, 552–565.

Hu, X., Ritz, T., Damjanović, A., Schulten, K., 1997. Pigment organization and transfer of electronic excitation in the photosynthetic unit of purple bacteria. J. Phys. Chem. B 101, 3854–3871.

Hu, J., Jin, L., Wang, X., Cai, W., Liu, Y., Wang, G., 2014. Response of photosynthetic systems to salinity stress in the desert cyanobacterium *Scytonema javanicum*. Adv. Space Res. 53, 30–36.

Huang, C., Yuan, X., Zhao, J., Bryant, D.A., 2003. Kinetic analyses of state transitions of the cyanobacterium *Synechococcus* sp. PCC 7002 and its mutant strains impaired in electron transport. Biochim. Biophys. Acta 1607, 121–130.

Hughes, J.L., Smith, P.J., Pace, R.J., Krausz, E., 2007. Low-energy absorption and luminescence of higher plant photosystem II core samples. J. Lumin. 122–123, 284–287.

Ihalainen, J.A., D'Haene, S., Yeremenko, N., van Roon, H., Arteni, A.A., Boekema, E.J., van Grondelle, R., Matthijs, H.C.P., Dekker, J.P., 2005. Aggregates of the chlorophyll-binding protein IsiA (CP43′) dissipate energy in cyanobacteria. Biochemistry 44, 10846–10853.

Ilík, P., Pavlovič, A., Kouřil, R., Alboresi, A., Morosinotto, T., Allahverdieyeva, Y., Aro, E.-M., Yamamoto, H., Shikanai, T., 2017. Alternative electron transport mediated by flavodiiron proteins is operational in organisms from cyanobacteria up to gymnosperms. New Phytol. 214, 967–972.

Ivanov, A.G., Krol, M., Sveshnikov, D., Selstam, E., Sandström, S., 2006. Iron deficiency in cyanobacteria causes monomerization of photosystem I trimers and reduces the capacity for state transitions and the effective absorption cross section of photosystem I in vivo. Plant Physiol. 141, 1436–1445.

Jallet, D., Gwizdala, M., Kirilovsky, D., 2012. ApcD, ApcF and ApcE are not required for the Orange Carotenoid protein related phycobilisome fluorescence quenching in the cyanobacterium *Synechocystis* PCC 6803. Biochim. Biophys. Acta 1817, 1418–1427.

Joliot, P., 1965. Cinétiques de réactions liées à l'émission d'oxygène photosynthétique. Biochim. Biophys. Acta 102, 116–134. (in French).

Joliot, P., Joliot, A., 1999. In vivo analysis of the electron transfer within photosystem-I: are the two phylloquinones involved? Biochemistry 38, 11130–11136.

Joliot, P., Kok, B., 1975. Oxygen evolution in photosynthesis. In: Govindjee (Eds.), Bioenergetics of Photosynthesis. Academic Press, New York, pp. 388–413.

Joliot, P., Barbieri, G., Chabaud, R., 1969. Un nouveau modèle des centres photochimiques du système II. Photochem. Photobiol. 10, 309–329.

Jordan, P., Fromme, P., Witt, H.T., Klukas, O., Saenger, W., Krauss, N., 2001. Three-dimensional structure of cyanobacterial photosystem I at 2.5 Å resolution. Nature 411, 909–917.

Joshua, S., Mullineaux, C.W., 2004. Phycobilisome diffusion is required for light-state transitions in cyanobacteria. Plant Physiol. 135, 2112–2119.

Joshua, S., Mullineaux, C.W., 2005. The rpaC gene product regulates phycobilisome–photosystem II interaction in cyanobacteria. Biochim. Biophys. Acta 1709, 58–68.

Joshua, S., Bailey, D., Mann, N.H., Mullineaux, C.W., 2005. Involvement of phycobilisome diffusion in energy quenching in cyanobacteria. Plant Physiol. 138, 1577–1585.

Kalaji, H.M., Goltsev, V., Bosa, K., Allakhverdiev, S., Strasser, R.J., Govindjee, 2012. Experimental in vivo measurements of light emission in plants: a perspective dedicated to David Walker. Photosynth. Res. 114, 69–96.

Kalaji, H.M., Schansker, G., Ladle, R.J., et al., 2014. Frequently asked questions about chlorophyll fluorescence: practical issues. Photosynth. Res. 122, 121–158.

Kalaji, H.M., Jajoo, A., Oukarroum, A., Brestic, M., Zivcak, M., Samborska, I.A., Cetner, M.D., Łukasik, I., Goltsev, V., Ladle, R.J., 2016. Chlorophyll a fluorescence as a tool to monitor physiological status of plants under abiotic stress conditions. Acta Physiol. Plant. 38, 102.

Kalaji, H.M., Schansker, G., Brestic, M., et al., 2017. Frequently asked questions about chlorophyll fluorescence, the sequel. Photosynth. Res. 132, 13–66.

Kamyia, N., Shen, J.R., 2003. Crystal structure of oxygen-evolving photosystem II from Thermosynechococcus vulcanis at 3.7-angstrom resolution. Proc. Acad. Sci. USA 100, 98–103.

Kaňa, R., 2013. Mobility of photosynthetic proteins. Photosynth. Res. 116, 465–479.

Kaňa, R., Prášil, O., Komárek, O., Papageorgiou, G.C., Govindjee, 2009. Spectral characteristic of fluorescence induction in a model cyanobacterium, Synechococcus sp. (PCC 7942). Biochim. Biophys. Acta 1787, 1170–1178.

Kaňa, R., Kotabová, E., Komárek, O., Šedivá, B., Papageorgiou, G.C., Govindjee, Prášil, O., 2012. The slow S to M fluorescence rise in cyanobacteria is due to a State 2 to State 1 transition. Biochim. Biophys. Acta 1817, 1237–1247.

Karapetyan, N.V., Holzwarth, A.R., Rögner, M., 1999. The photosystem I trimer of cyanobacteria: molecular organization, excitation dynamics and physiological significance. FEBS Lett. 460, 395–400.

Karapetyan, N.V., Schlodder, E., van Grondelle, R., Dekker, J.P., 2006. The long wavelength chlorophylls in photosystem I. In: Golbeck, J.H., Govindjee, Sharkey, T. (Eds.), The Light-Driven Plastocyanin: Ferredoxin Oxidoreductase. Advances in Photosynthesis and Respiration, vol. 24. Springer, Dordrecht, pp. 177–192.

Karapetyan, N.V., Bolychevtseva, Y.V., Yurina, N.P., Terekhova, I.V., Shubin, V.V., Brecht, M., 2014. Long-wavelength chlorophylls in photosystem I of cyanobacteria: origin, localization, and functions. Biochemistry (Mosc.) 79, 213–220.

Kargul, J., Olmos, J.D.J., Krupnik, T., 2012. Structure and function of photosystem I and its application in biomimetic solar-to-fuel systems. J. Plant Physiol. 169, 1639–1653.

Kautsky, H., Hirsch, A., 1931. Neue Versuche zur Kohlensaureassimilation. Naturwissenschaften 19, 964.

Kawamura, M., Mimuro, M., Fujita, Y., 1979. Quantitative relationship between two reaction centers in the photosynthetic system of blue-green algae. Plant Cell Physiol. 20, 697–705.

Kehoe, D.M., 2010. Chromatic adaptation and the evolution of light color in cyanobacteria. Proc. Natl. Acad. Sci. U. S. A. 107, 9029–9030.

Kerfeld, C.A., Kirilovsky, D., 2013. Structural, mechanistic and genomic insights into OCP-mediated photoprotection. In: Chauvat, F., Cassier-Chauvat, C. (Eds.), Advances in Botanical Research: Genomics in Cyanobacteria. vol. 65. Elsevier, Oxford/Amsterdam, pp. 1–26.

Kerfeld, C.A., Sawaya, M.R., Brahmandam, V., Cascio, D., Ho, K.K., Trevithick-Sutton, C.C., Krogmann, D.W., Yeates, T.O., 2003. The crystal structure of a cyanobacterial water-soluble carotenoid binding protein. Structure 11, 55–65.

Kerfeld, C.A., Melnicki, M.R., Sutter, M., Dominguez-Martin, M.A., 2017. Structure, function and evolution of the cyanobacterial orange carotenoid protein and its homologs. New Phytol. 215, 937–951.

Khanna, N., Lindblad, P., 2015. Cyanobacterial hydrogenases and hydrogen metabolism revisited: recent progress and future prospects. Int. J. Mol. Sci. 16, 10537–10561.

Khanna, R., Govindjee, Wydrzynski, T., 1977. Site of bicarbonate effect in Hill reaction. Evidence from the use of artificial electron acceptors and donors. Biochim. Biophys. Acta 462, 208–214.

Kirilovsky, D., 2015. Modulating energy arriving at photochemical reaction centers: orange carotenoid protein-related photoprotection and state transitions. Photosynth. Res. 126, 3–17.

Kirilovsky, D., Kerfeld, C.A., 2016. Cyanobacterial photoprotection by the orange carotenoid protein. Nat. Plants 2, 16180.

Kirilovsky, D., Kaňa, R., Prášil, O., 2014. Mechanisms modulating energy arriving at reaction centers in cyanobacteria. In: Demmig-Adams, B., Garab, G., Adams, W. III, Govindjee (Eds.), Non-Photochemical Quenching and Energy Dissipation in Plants, Algae and Cyanobacteria. Advances in Photosynthesis and Respiration, vol. 40. Springer, Dordrecht, pp. 471–502.

Kitajima, M., Butler, W.L., 1975. Quenching of chlorophyll fluorescence and primary photochemistry in chloroplasts by dibromothymoquinone. Biochim. Biophys. Acta 376, 105–115.

Kitchener, R.L., Grunden, M.A., 2018. Methods for enhancing cyanobacterial stress tolerance to enable improved production of biofuels and industrially relevant chemicals. Appl. Microbiol. Biotechnol. 102, 1617–1628.

Klimov, V.V., Klevanik, A.V., Shuvalov, V.A., Krasnovsky, A.A., 1977. Reduction of pheophytin in the primary light reaction of photosystem II. FEBS Lett. 82, 183–186.

Koblížek, M., Kaftan, D., Nedbal, L., 2001. On the relationship between the non-photochemical quenching of the chlorophyll fluorescence and the photosystem II light harvesting efficiency. A repetitive flash fluorescence induction study. Photosynth. Res. 68, 141–152.

Kodru, S., Malavath, T., Devadasu, E., Nellaepalli, S., Stirbet, A., Subramanyam, R., Govindjee, 2015. The slow S to M rise of chlorophyll a fluorescence reflects transition from State 2 to State 1 in the green alga *Chlamydomonas reinhardtii*. Photosynth. Res. 125, 219–231.

Kojima, K., Suzuki-Maenaka, T., Kikuchi, T., Nakamoto, H., 2006. Roles of the cyanobacterial isiABC operon in protection from oxidative and heat stresses. Physiol. Plant. 128, 507–519.

Kok, B., 1957. Absorption changes induced by the photochemical reaction of photosynthesis. Nature 179, 583–584.

Kok, B., 1963. Fluorescence studies. In: Kok, B., Jagendorf, A.T. (Eds.), Photosynthetic Mechanisms of Green Plants. Natl. Acad. Sci.-Natl. Res. Council, Washington, DC, pp. 45–55. Publ. 1145.

Kok, B., Forbush, B., McGloin, M., 1970. Cooperation of charges in photosynthetic O_2 evolution. 1. A linear four step mechanism. Photochem. Photobiol. 11, 457–475.

Kolber, Z.S., Prášil, O., Falkowski, P.G., 1998. Measurements of variable chlorophyll fluorescence using fast repetition rate techniques: defining methodology and experimental protocols. Biochim. Biophys. Acta 1367, 88–106.

Komenda, J., Sobotka, R., 2016. Cyanobacterial high-light-inducible proteins—protectors of chlorophyll-protein synthesis and assembly. Biochim. Biophys. Acta 1857, 288–295.

Kondo, K., Ochiai, Y., Katayama, M., Ikeuchi, M., 2007. The membrane associated CpcG2-phycobilisome in *Synechocystis*: a new photosystem I antenna. Plant Physiol. 144, 1200–1210.

Kondo, K., Mullineaux, C.W., Ikeuchi, M., 2009. Distinct roles of CpcG1-phycobilisome and CpcG2-phycobilisome in state transitions in a cyanobacterium *Synechocystis* sp. PCC 6803. Photosynth. Res. 99, 217–225.

Kouřil, R., Zygadlo, A., Arteni, A.A., de Wit, C.D., Dekker, J.P., Jensen, P.E., Scheller, H.V., Boekema, E.J., 2005. Structural characterization of a complex of photosystem I and light-harvesting complex II of *Arabidopsis thaliana*. Biochemistry 44, 10935–10940.

Krause, G.H., Weis, E., 1991. Chlorophyll fluorescence and photosynthesis: the basics. Annu. Rev. Plant Physiol. Plant Mol. Biol. 42, 313–349.

Krausz, E., Hughes, J.L., Smith, P.J., Pace, R.J., Årsköld, S., 2005. Assignment of the low-temperature fluorescence in oxygen evolving photosystem II. Photosynth. Res. 84, 193–199.

Krey, A., Govindjee, 1964. Fluorescence changes in *Porphyridium* exposed to green light of different intensity: a new emission band at 693 nm and its significance to photosynthesis. Proc. Natl. Acad. Sci. U. S. A. 52, 1568–1572.

Kruip, J., Bald, D., Boekema, E., Rögner, M., 1994. Evidence for the existence of trimeric and monomeric photosystem I complexes in thylakoid membranes from cyanobacteria. Photosynth. Res. 40, 279–286.

Kurisu, G., Zhang, H., Smith, J.L., 2003. Structure of the cytochrome b_6f complex of oxygenic photosynthesis: tuning the cavity. Science 302, 1009–1014.

Kusama, Y., Inoue, S., Jimbo, H., Takaichi, S., Sonoike, K., Hihara, Y., Nishiyama, Y., 2015. Zeaxanthin and echinenone protect the repair of photosystem II from inhibition by singlet oxygen in *Synechocystis* sp. PCC 6803. Plant Cell Physiol. 56, 906–916.

Lai, M.C., Lan, E.I., 2015. Advances in metabolic engineering of cyanobacteria for photosynthetic biochemical production. Metabolites 5, 636–658.

Laible, P.D., Zipfel, W., Owens, T.G., 1994. Excited state dynamics in chlorophyll-based antennae: the role of transfer equilibrium. Biophys. J. 66, 844–860.

Lamb, J.J., Røkke, G., Hohmann-Marriott, M.F., 2018. Chlorophyll fluorescence emission spectroscopy of oxygenic organisms at 77 K. Photosynthetica 56, 105–124.

Larkum, A.W.D., Kuhl, M., 2005. Chlorophyll d: the puzzle resolved. Trends Plant. Sci. 10, 355.

Lazár, D., 1999. Chlorophyll *a* fluorescence induction. Biochim. Biophys. Acta 1412, 1–28.

Lazár, D., 2003. Chlorophyll *a* fluorescence rise induced by high light illumination of dark-adapted plant tissue studied by means of a model of photosystem II and considering photosystem II heterogeneity. J. Theor. Biol. 220, 469–503.

Lazár, D., 2006. The polyphasic chlorophyll *a* fluorescence rise measured under high intensity of exciting light. Funct. Plant Biol. 33, 9–30.

Lazár, D., 2009. Modelling of light-induced chlorophyll *a* fluorescence rise (O-J-I-P transient) and changes in 820 nm-transmittance signal of photosynthesis. Photosynthetica 47, 483–498.

Lazár, D., 2013. Simulations show that a small part of variable chlorophyll *a* fluorescence originates in photosystem I and contributes to overall fluorescence rise. J. Theor. Biol. 335, 249–264.

Lazár, D., 2015. Parameters of photosynthetic energy partitioning. J. Plant Physiol. 175, 131–147.

Lazár, D., Schansker, G., 2009. Models of chlorophyll a fluorescence transients. In: Laisk, A., Nedbal, L., Govindjee, Sharkey, T.D. (Eds.), Photosynthesis in Silico: Understanding Complexity from Molecules to Ecosystems. Advances in Photosynthesis and Respiration, vol. 29. Springer, Dordrecht, pp. 85–123.

Lea-Smith, D.J., Bombelli, P., Vasudevan, R., Howe, C.J., 2016. Photosynthetic, respiratory and extracellular electron transport pathways in cyanobacteria. Biochim. Biophys. Acta 1857, 247–255.

Leverenz, R.L., Sutter, M., Wilson, A., Gupta, S., Thurotte, A., Bourcier de Carbon, C., Petzold, C.J., Ralston, C., Perreau, F., Kirilovsky, D., Kerfeld, C.A., 2015. A 12 Å carotenoid translocation in a photoswitch associated with cyanobacterial photoprotection. Science 348, 1463–1466.

Ley, A.C., Butler, W.L., 1980. Energy distribution in the photochemical apparatus of *Porphyridium cruentum* in State I and State II. Biochim. Biophys. Acta 592, 349–363.

Li, Y., van der Est, A., Lucas, M.G., et al., 2006. Directing electron transfer within photosystem I by breaking H-bonds in the cofactor branches. Proc. Natl. Acad. Sci. U. S. A. 103, 2144–2149.

Li, Z., Wakao, S., Fischer, B.B., Niyogi, K.K., 2009. Sensing and responding to excess light. Annu. Rev. Plant Biol. 60, 239–260.

Lia, D., Xiea, J., Zhaoa, J., Xiaa, A., Lib, D., Gon, Y., 2004. Light-induced excitation energy redistribution in *Spirulina platensis* cells: "spillover" or "mobile PBSs"? Biochim. Biophys. Acta 1608, 114–121.

Liu, L.N., 2016. Distribution and dynamics of electron transport complexes in cyanobacterial thylakoid membranes. Biochim. Biophys. Acta 1857, 256–265.

Liu, L.N., Chen, X.L., Zhang, Y.Z., Zhou, B.C., 2005. Characterization, structure and function of linker polypeptides in phycobilisomes of cyanobacteria and red algae: an overview. Biochim. Biophys. Acta 1708, 133–142.

Liu, H., Zhang, H., Niedzwiedzki, D.M., Prado, M., He, G., Gross, M.L., Blankenship, R.E., 2013. Phycobilisomes supply excitations to both photosystems in a megacomplex in cyanobacteria. Science 342, 1104–1107.

Liu, H., Zhang, H., Orf, G.S., Lu, Y., Jiang, J., King, J.D., Wolf, N.R., Gross, M.L., Blankenship, R.E., 2016. Dramatic domain rearrangements of the cyanobacterial Orange Carotenoid protein upon photoactivation. Biochemistry 55, 1003–1009.

Liu, H., Lu, Y., Wolf, B., Saer, R., King, J.D., Blankenship, R.E., 2018. Photoactivation and relaxation studies on the cyanobacterial orange carotenoid protein in the presence of copper ion. Photosynth. Res. 135, 143–147.

Llansola-Portoles, M.J., Sobotka, R., Kish, E., Shukla, M.K., Pascal, A.A., Polívka, T., Robert, B., 2017. Twisting a β-carotene, an adaptive trick from nature for dissipating energy during photoprotection. J. Biol. Chem. 292, 1396–1403.

Loll, B., Kern, J., Saenger, W., Zouni, A., Biesiadka, J., 2005. Towards complete factor arrangement in the 3.0 angstrom resolution structure of photosystem II. Nature 438, 1040–1044.

Lu, C., Vonshak, A., 1999. Characterization of PSII photochemistry in salt-adapted cells of cyanobacterium *Spirulina platensis*. New Phytol. 141, 231–239.

Lu, Y., Liu, H., Saer, R., Li, V.L., Zhang, H., Shi, L., Goodson, C., Gross, M.L., Blankenship, R.E., 2017. A molecular mechanism for nonphotochemical quenching in cyanobacteria. Biochemistry 56, 2812–2823.

Lyu, H., Lazár, D., 2017. Modeling the light-induced electric potential difference (ΔΨ), the pH difference (ΔpH) and the proton motive force across the thylakoid membrane in C3 leaves. J. Theor. Biol. 413, 11–23.

Ma, F., Zhang, X., Zhu, X., Li, T., Zhan, J., Chen, H., He, C., Wang, Q., 2017. Dynamic changes of IsiA-containing complexes during long-term iron deficiency in *Synechocystis* sp. PCC 6803. Mol. Plant. 10, 143–154.

MacGregor-Chatwin, C., Sener, M., Barnett, S.F.H., Hitchcock, A., Barnhart-Dailey, M.C., Maghlaoui, K., Barber, J., Timlin, J.A., Schulten, K., Hunter, C.N., 2017. Lateral segregation of photosystem I in cyanobacterial thylakoids. Plant Cell 29, 1119–1136.

Magdaong, N.C.M., Blankenship, R.E., 2018. Photoprotective, excited-state quenching mechanisms in diverse photosynthetic organisms. J. Biol. Chem. 293, 5018.

Makita, H., Hastings, G., 2015. Directionality of electron transfer in cyanobacterial photosystem I at 298 and 77K. FEBS Lett. 589, 1412–1417.

Makita, H., Hastings, G., 2016. Modeling electron transfer in photosystem I. Biochim. Biophys. Acta 1857, 723–733.

Maksimov, E.G., Klementiev, K.E., Shirshin, E.A., Tsoraev, G.V., Elanskaya, I.V., Paschenko, V.Z., 2015a. Features of temporal behavior of fluorescence recovery in *Synechocystis* sp. PCC6803. Photosynth. Res. 125, 167–178.

Maksimov, E.G., Shirshin, E.A., Sluchanko, N.N., Zlenko, D.V., Parshina, E.Y., Tsoraev, G.V., Klementiev, K.E., Budylin, G.S., Schmitt, F.-J., Friedrich, T., Fadeev, V.V., Paschenko, V.Z., Rubin, A.B., 2015b. The signaling state of orange carotenoid protein. Biophys. J. 109, 595–607.

Maksimov, E.G., Sluchanko, N.N., Slonimskiy, Y.B., Mironov, K.S., Klementiev, K.E., Moldenhauer, M., Friedrich, T., Los, D.A., Paschenko, V.Z., Rubin, A.B., 2017. The unique protein-to-protein carotenoid transfer mechanism. Biophys. J. 113, 402–414.

Malkin, S., Telfer, A., Barber, J., 1986. Quantitative analysis of State 1-State 2 transitions in intact leaves using modulated fluorimetry—evidence for changes in the absorption cross-section of the two photosystems during state transitions. Biochim. Biophys. Acta 848, 48–57.

Mamedov, M., Govindjee, Nadtochenko, V., Semenov, A., 2015. Primary electron transfer processes in photosynthetic reaction centers from oxygenic organisms. Photosynth. Res. 125, 51–63.

Mao, H.B., Li, G.F., Ruan, X., Wu, Q.Y., Gong, Y.D., Zhang, X.F., Zhao, N.M., 2002. The redox state of plastoquinone pool regulates state transitions via cytochrome b_6f complex in *Synechocystis* sp. PCC 6803. FEBS Lett. 519, 82–86.

Mar, T., Govindjee, 1972. Kinetic models of oxygen evolution in photosynthesis. J. Theor. Biol. 36, 427–446.

Martin, J.H., Fitzwater, S.E., 1988. Iron-deficiency limits phytoplankton growth in the Northeast Pacific subarctic. Nature 331, 341–343.

Matthijs, H.C.P., van der Staay, G.W.M., Mur, L.R., 1994. Prochlorophytes: the 'other' cyanobacteria. In: Bryant, D.A. (Ed.), The Molecular Biology of Cyanobacteria. Kluwer Academic Publishers, Dordrecht, pp. 49.

McFadden, G.I., 2001. Primary and secondary endosymbiosis and the origin of plastids. J. Phycol. 37, 951–959.

McGrath, J.M., Long, S.P., 2014. Can the cyanobacterial carbon-concentrating mechanism increase photosynthesis in crop species? A theoretical analysis. Plant Physiol. 164, 2247–2261.

Melkozernov, A.N., Bibby, T.S., Lin, S., Barber, J., Blankenship, R.E., 2003. Time-resolved absorption and emission show that the CP43′ antenna ring of iron-stressed *Synechocystis* sp. PCC6803 is efficiently coupled to the photosystem I reaction center core. Biochemistry 42, 3893–3903.

Milanovsky, G.E., Ptushenko, V.V., Golbeck, J.H., Semenov, A.Y., Cherepanov, D.A., 2014. Molecular dynamics study of the primary charge separation reactions in photosystem I: effect of the replacement of the axial ligants to the electron acceptor A0. Biochim. Biophys. Acta 1837, 1472–1483.

Miller, A.G., Espie, G.S., Canvin, D.T., 1991. The effects of inorganic carbon and oxygen on fluorescence in the cyanobacterium *Synechococcus* UTEX 625. Can. J. Bot. 69, 1151–1160.

Mimuro, M., 2004. Photon capture, exciton migration and trapping and fluorescence emission in cyanobacteria and red algae. In: Papageorgiou, G.C., Govindjee (Eds.), Chlorophyll a Fluorescence: A Signature of Photosynthesis. Advances in Photosynthesis and Respiration, vol. 19. Springer, Dordrecht, pp. 174–195.

Mimuro, M., Lipschultz, C.A., Gantt, E., 1986. Energy flow in the phycobilisomes of *Nostoc* sp. (Mac): two independent terminal pigments. Biochim. Biophys. Acta 852, 126–132.

Mimuro, M., Kobayashi, M., Murakami, A., Tsuchiya, T., Miyashita, H., 2008. Oxygen-evolving cyanobacteria. In: Renger, G. (Ed.), Primary Processes of Photosynthesis, Part 1. RSC Publishing, Cambridge, pp. 261–300.

Mirkovic, T., Ostrumov, E.E., Anna, J.M., van Grondelle, R., Govindjee, Scholes, G.D., 2017. Light absorption and energy transfer in the antenna complexes of photosynthetic organisms. Chem. Rev. 117, 249–293.

Mishra, K.B., Mishra, A., Klem, K., Govindjee, 2016. Plant phenotyping: a perspective. Indian J. Plant Physiol. 21, 514–527.

Mishra, K.B., Mishra, A., Kubásek, J., Urban, O., Heyer, A.G., Govindjee, 2018. Low temperature induced modulation of photosynthesis in non-acclimated and cold acclimated *Arabidopsis thaliana:* chlorophyll *a* fluorescence measurements. Photosynth. Res. . (submitted for publication).

Misumi, M., Katoh, H., Tomo, T., Sonoike, K., 2016. Relationship between photochemical quenching and non-photochemical quenching in six species of cyanobacteria reveals species difference in redox state and species commonality in energy dissipation. Plant Cell Physiol. 57, 1510–1517.

Mitchell, P., 1966. Chemiosmotic coupling in oxidative and photosynthetic phosphorylation. Biol. Rev. 4, 445–502.

Miyashita, H., Hisato, I., Norihide, K., 1996. Chlorophyll d as a major pigment. Nature 383, 402.

Mohanty, P., Govindjee, 1973. Light-induced changes in the fluorescence yield of chlorophyll *a* in *Anacystis nidulans* II. The fast changes and the effect of photosynthetic inhibitors on both the fast and slow fluorescence induction. Plant Cell Physiol. 14, 611–629.

Mohanty, P., Govindjee, 1974. The slow decline and the subsequent rise of chlorophyll fluorescence transients in intact algal cells. Plant Biochem. J. 1, 78–106.

Mohanty, P., Papageorgiou, G., Govindjee, 1971. Fluorescence induction in the red alga *Porphyridium cruentum*. Photochem. Photobiol. 14, 667–682.

Moldenhauer, M., Sluchanko, N.N., Buhrke, D., Zlenko, D.V., Tavraz, N.N., Schmitt, F.J., Hildebrandt, P., Maksimov, E.G., Friedrich, T., 2017. Assembly of photoactive orange carotenoid protein from its domains unravels a carotenoid shuttle mechanism. Photosynth. Res. 133, 327–341.

Montgomery, B.L., 2017. Seeing new light: recent insights into the occurrence and regulation of chromatic acclimation in cyanobacteria. Curr. Opin. Plant Biol. 37, 18–23.

Morton, J., Hall, J., Smith, P., Akita, F., Koua, F.H.M., Shen, J.-R., Krausz, E., 2014. Determination of the PS I content of PS II core preparations using selective emission: a new emission of PS II at 780 nm. Biochim. Biophys. Acta 1837, 167–177.

Müller, P., Li, X., Niyogi, K.K., 2001. Non-photochemical quenching. A response to excess light energy. Plant Physiol. 125, 1558–1566.

Müller, M.G., Slavov, C., Luthra, R., Redding, K.E., Holzwarth, A.R., 2010. Independent initiation of primary electron transfer in the two branches of the photosystem I reaction center. Proc. Natl. Acad. Sci. U. S. A. 107, 4123–4128.

Mullineaux, C.W., 2008. Phycobilisome-reaction centre interaction in cyanobacteria. Photosynth. Res. 95, 175–182.

Mullineaux, C.W., 2014. Co-existence of photosynthetic and respiratory activities in cyanobacterial thylakoid membranes. Biochim. Biophys. Acta 1837, 503–511.

Mullineaux, C., Allen, J.F., 1986. The State 2 transition in the cyanobacterium *Synechococcus* 6301 can be driven by respiratory electron flow into the plastoquinone pool. FEBS Lett. 205, 155–160.

Mullineaux, C.W., Allen, J.F., 1990. State 1-State 2 transitions in the cyanobacterium *Synechococcus* 6301 are controlled by the redox state of electron carriers between photosystems I and II. Photosynth. Res. 23, 297–311.

Mullineaux, C.W., Emlyn-Jones, D., 2005. State transitions: an example of acclimation to low-light stress. J. Exp. Bot. 56, 389–393.

Mullineaux, C.W., Boult, M., Sanders, C.E., Allen, J.F., 1986. Fluorescence induction transients indicate altered absorption cross-section during light-state transitions in the cyanobacterium *Synechococcus* 6301. Biochim. Biophys. Acta 851, 147–150.

Mullineaux, C.W., Tobin, M.J., Jones, G.R., 1997. Mobility of photosynthetic complexes in thylakoid membranes. Nature 390, 421–424.

Munday Jr., J.C., Govindjee, 1969a. Light-induced changes in the fluorescence yield of chlorophyll a in vivo. III. The dip and the peak in the fluorescence transient of *Chlorella pyrenoidosa*. Biophys. J. 9, 1–21.

Munday Jr., J.C., Govindjee, 1969b. Light-induced changes in the fluorescence yield of chlorophyll a in vivo. IV. The effect of preillumination on the fluorescence transient of *Chlorella pyrenoidosa*. Biophys. J. 9, 22–35.

Murata, N., 1969a. Control of excitation transfer in photosynthesis. I. Light-induced change of chlorophyll a fluorescence in *Porphyridium cruentum*. Biochim. Biophys. Acta 172, 242.

Murata, N., 1969b. Control of excitation transfer in photosynthesis. II. Magnesium ion-dependent distribution of excitation energy between two pigment systems in spinach chloroplasts. Biochim. Biophys. Acta 189, 171–181.

Murata, N., 1970. Control of excitation transfer in photosynthesis. IV. Kinetics of chlorophyll a fluorescence in *Porphyra yezoensis*. Biochim. Biophys. Acta 205, 379–389.

Murata, N., Nishiyama, Y., 2018. ATP is a driving force in the repair of photosystem II during photoinhibition. Plant Cell Environ. 41, 285–299.

Murata, N., Nishimura, M., Takamiya, A., 1966. Fluorescence of chlorophyll in photosynthetic systems. III. Emission and action spectra of fluorescence–three emission bands of chlorophyll A and the energy transfer between two pigment systems. Biochim. Biophys. Acta 126, 234–243.

Myers, J., 1971. Enhancement studies in photosynthesis. Annu. Rev. Plant Physiol. 22, 289–312.

Nedbal, L., Trtílek, M., Kaftan, D., 1999. Flash fluorescence induction: a novel method to study regulation of photosystem II. J. Photochem. Photobiol. B: Biol. 48, 154–157.

Nelson, N., Junge, W., 2015. Structure and energy transfer in photosystems of oxygenic photosynthesis. Annu. Rev. Biochem. 84, 659–683.

Nelson, N., Yocum, C.F., 2006. Structure and function of photosystems I and II. Annu. Rev. Plant Biol. 57, 521–565.

Neubauer, C., Schreiber, U., 1987. The polyphasic rice of chlorophyll fluorescence upon onset of strong continuous illumination: I. Saturation characteristics and partial control by the photosystem II acceptor side. Z. Naturforsch. 42c, 1246–1254.

Nevo, R., Charuvi, D., Shimoni, E., Schwarz, R., Kaplan, A., Ohad, I., Reich, Z., 2007. Thylakoid membrane perforations and connectivity enable intracellular traffic in cyanobacteria. EMBO J. 26, 1467–1473.

Ni, L., Acharya, K., Hao, X., Li, S., Li, Y., Li, Y., 2012. Effects of artemisinin on photosystem II performance of *Microcystis aeruginosa* by in vivo chlorophyll fluorescence. Bull. Environ. Contam. Toxicol. 89, 1165–1169.

Niedzwiedzki, D.M., Tronina, T., Liu, H., Staleva, H., Komenda, J., Sobotka, R., Blankenship, R.E., Polívka, T., 2016. Carotenoid-induced non-photochemical quenching in the cyanobacterial chlorophyll synthase-HliC/D complex. Biochim. Biophys. Acta 1857, 1430–1439.

Nilkens, M., Kress, E., Lambrev, P., Miloslavina, Y., Müller, M., Holzwarth, A.R., Jahns, P., 2010. Identification of a slowly inducible zeaxanthin-dependent component of non-photochemical quenching of chlorophyll fluorescence generated under steady-state conditions in Arabidopsis. Biochim. Biophys. Acta 1797, 466–475.

Nobel, P.S., 2009. Photochemistry of photosynthesis. In: Photochemical and Environmental Plant Physiology. fourth ed.. Academic Press (Elsevier), Amsterdam, pp. 228–275.

Novoderezhkin, V.I., Andrizhiyevskaya, E.G., Dekker, J.P., van Grondelle, R., 2005. Pathways and timescales of primary charge separation in the photosystem II reaction center as revealed by a simultaneous fit of time-resolved fluorescence and transient absorption. Biophys. J. 89, 1464–1481.

Novoderezhkin, V.I., Dekker, J.P., van Grondelle, R., 2007. Mixing of exciton and charge-transfer states in photosystem II reaction centers: modeling of Stark spectra with modified Redfield theory. Biophys. J. 93, 1293–1311.

Novoderezhkin, V.I., Romero, E., Dekker, J.P., van Grondelle, R., 2011. Multiple charge-separation pathways in photosystem II: modeling of transient absorption kinetics. ChemPhysChem 12, 681–688.

Nürnberg, D.J., Morton, J., Santabarbara, S., Telfer, A., Joliot, P., Antonaru, L.A., Ruban, A.V., Cardona, T., Krausz, E., Boussac, A., Fantuzzi, A., Rutherford, A.W., 2018. Photochemistry beyond the red limit in chlorophyll f–containing photosystems. Science 360, 1210–1213.

Ogawa, T., Sonoike, K., 2015. Dissection of respiration and photosynthesis in the cyanobacterium *Synechocystis* sp. PCC6803 by the analysis of chlorophyll fluorescence. J. Photochem. Photobiol. B 144, 61–67.

Ogawa, T., Sonoike, K., 2016. Effects of bleaching by nitrogen deficiency on the quantum yield of photosystem II in *Synechocystis* sp. PCC 6803 revealed by chlorophyll fluorescence measurement. Plant Cell Physiol. 57, 558–567.

Ogawa, T., Harada, T., Ozaki, H., Sonoike, K., 2013. Disruption of the ndhF1 gene affects chlorophyll fluorescence through state transition in the cyanobacterium *Synechocystis* sp. PCC 6803, resulting in apparent high efficiency of photosynthesis. Plant Cell Physiol. 54, 1164–1171.

Ogawa, T., Misumi, M., Sonoike, K., 2017. Estimation of photosynthesis in cyanobacteria by pulse-amplitude modulation chlorophyll fluorescence: problems and solutions. Photosynth. Res. 133, 63–73.

Okayama, S., Butler, W.L., 1972. The influence of cytochrome b_{559} on the fluorescence yield of chloroplasts at low temperature. Biochim. Biophys. Acta 267, 523–552.

Ong, L.J., Glazer, A.N., 1991. Phycoerythrins of marine unicellular cyanobacteria. I. Bilin types and locations and energy transfer pathways in *Synechococcus* sp. phycoerythrins. J. Biol. Chem. 266, 9515–9527.

Öquist, G., 1971. Changes in pigment composition and photosynthesis induced by iron-deficiency in blue-green-alga *Anacystis nidulans*. Physiol. Plant. 25, 188–191.

Orf, G.S., Saer, R.G., Niedzwiedzki, D.M., Zhang, H., McIntosh, C.L., Schultz, J.W., Mirica, L.M., Blankenship, R.E., 2016. Evidence for a cysteine-mediated mechanism of excitation energy regulation in a photosynthetic antenna complex. Proc. Natl. Acad. Sci. U. S. A. 113, E4486–E4493.

Osmond, B., Chow, W.S., Wyber, R., Zavafer, A., Keller, B., Pogson, B.J., Robinson, S.A., 2017. Relative functional and optical absorption cross-sections of PSII and other photosynthetic parameters monitored *in situ*, at a distance with a time resolution of a few seconds, using a prototype light induced fluorescence transient (LIFT) device. Funct. Plant Biol. 44, 985–1006.

Oukarroum, A., Schansker, G., Strasser, R.J., 2009. Drought stress effects on photosystem I content and photosystem II thermotolerance analyzed using Chl *a* fluorescence kinetics in barley varieties differing in their drought tolerance. Physiol. Plant. 137, 188–199.

Oxborough, K., Baker, N.R., 1997. Resolving chlorophyll *a* fluorescence images of photosynthetic efficiency into photochemical and non-photochemical components—calculation of qP and Fv'/Fm' without measuring Fo'. Photosynth. Res. 54, 135–142.

Pålsson, L.-O., Dekker, J.P., Schlodder, E., Monshouwer, R., van Grondelle, R., 1996. Polarized site-selective fluorescence spectroscopy of the long-wavelength emitting chlorophylls in isolated photosystem I particles of *Synechococcus elongatus*. Photosynth. Res. 48, 239–246.

Pålsson, L.-O., Flemming, C., Gobets, B., van Grondelle, R., Dekker, J.P., Schlodder, E., 1998. Energy transfer and charge separation in photosystem I: P700 oxidation upon selective excitation of the longwavelength antenna chlorophylls of *Synechococcus elongatus*. Biophys. J. 74, 2611–2622.

Papáček, S., Jablonský, J., Matonoha, C., Kaňa, R., Kindermann, S., 2015. FRAP & FLIP: two sides of the same coin? In: Ortuño, F., Rojas, I. (Eds.), Bioinformatics and Biomedical Engineering. IWBBIO 2015. Lecture Notes in Computer Science. vol. 9044. Springer, Cham, pp. 444–455.

Papageorgiou, G.C., 1975. Chlorophyll fluorescence: an intrinsic probe of photosynthesis. In: Govindjee (Eds.), Bioenergetics of Photosynthesis. Academic Press, New York, pp. 319–372.

Papageorgiou, G.C., 1977. Photosynthetic activity of diimidoester-modified cells, permeaplasts, and cell-free membrane fragments of the blue-green alga *Anacystis nidulans*. Biochim. Biophys. Acta 461, 379–391.

Papageorgiou, G.C., 1996. The photosynthesis of cyanobacteria (blue bacteria) from the perspective of signal analysis of chlorophyll *a* fluorescence. J. Sci. Ind. Res. 155, 596–617.

Papageorgiou, G.C., Alygizaki-Zorba, A., 1997. A sensitive method for the estimation of the cytoplasmic osmolality of cyanobacterial cells using chlorophyll a fluorescence. Biochim. Biophys. Acta 1335, 1–4.

Papageorgiou, G.C., Govindjee, 1967. Changes in intensity and spectral distribution of fluorescence. Effect of light treatment on normal and DCMU-poisoned Anacystis nidulans. Biophys. J. 7, 375–389.

Papageorgiou, G.C., Govindjee, 1968a. Light-induced changes in the fluorescence yield of chlorophyll *a* in vivo. I. *Anacystis nidulans*. Biophys. J. 8, 1299–1315.

Papageorgiou, G.C., Govindjee, 1968b. Light induced changes in the fluorescence yield of chlorophyll *a* in vivo. II. *Chlorella pyrenoidosa*. Biophys. J. 8, 1316–1328.

Papageorgiou, G.C., Govindjee (Eds.), 2004. Chlorophyll *a* Fluorescence: A Signature of Photosynthesis. Advances in Photosynthesis and Respiration, vol. 19. Springer, Dordrecht, pp. 818.

Papageorgiou, G.C., Govindjee, 2011. Photosystem II fluorescence: slow changes–scaling from the past. J. Photochem. Photobiol. B 104, 258–270.

Papageorgiou, G.C., Govindjee, 2014. The non-photochemical quenching of the electronically excited state of chlorophyll *a* in plants: definitions, timelines, viewpoints, open questions. In: Demmig-Adams, B., Garab, G., Adams, W.W. III, Govindjee, Sharkey, T.D. (Eds.), Nonphotochemical Quenching and Energy Dissipation in Plants, Algae and Cyanobacteria. Advances in Photosynthesis and Respiration, vol. 40. Springer, Dordrecht, pp. 1–44.

Papageorgiou, G.C., Alygizaki-Zorba, A., Ladas, N., Murata, N., 1998. A method to probe the cytoplasmic osmolality and water and solute fluxes across the cell membrane of cyanobacteria with chlorophyll *a* fluorescence: experiments with *Synechococcus* sp. PCC 7942. Physiol. Plant. 102, 215–224.

Papageorgiou, G.C., Govindjee, Govindjee, R., Mimuro, M., Stamatakis, K., Alygizaki-Zorba, A., Murata, N., 1999. Light-induced and osmotically-induced changes in chlorophyll *a* fluorescence in two *Synechocystis* sp. PCC 6803 strains that differ in membrane lipid unsaturation. Photosynth. Res. 59, 125–136.

Papageorgiou, G.C., Tsimilli-Michael, M., Stamatakis, K., 2007. The fast and slow kinetics of chlorophyll a fluorescence induction in plants, algae and cyanobacteria: a viewpoint. Photosynth. Res. 94, 275–290.

Pawlowicz, N.P., Groot, M.L., van Stokkum, I.H.M., Breton, J., van Grondelle, R., 2007. Charge separation and electron transfer in the photosystem II core complex studied by femtosecond midinfrared spectroscopy. Biophys. J. 93, 2732–2742.

Peers, G., Truong, T.B., Ostendorf, E., Busch, A., Elrad, D., Grossman, A.R., Hippler, M., Niyogi, K.K., 2009. An ancient light-harvesting protein is critical for the regulation of algal photosynthesis. Nature 462, 518–521.

Pfündel, E.E., Klughammer, C., Mister, A., Cerovic, Z.G., 2013. Deriving fluorometer-specific values of relative PSI fluorescence intensity from quenching of F_0 fluorescence in leaves of *Arabidopsis thaliana* and *Zea mays*. Photosynth. Res. 114, 189–206.

Prokhorenko, V.I., Holzwarth, A.R., 2000. Primary process and structure of the photosystem II reaction center: a photon echo study. J. Phys. Chem. B 104, 11563–11578.

Pushkar, Y., Yano, J., Sauer, K., Boussac, A., Yachandra, V.K., 2008. Structural changes in the $_{Mn4Ca}$ cluster and the mechanism of photosynthetic water splitting. Proc. Natl. Acad. Sci. U. S. A. 105, 1879–1884.

Quick, W.P., Stitt, M., 1989. An examination of factors contributing to non-photochemical quenching of chlorophyll fluorescence in barley leaves. Biochim. Biophys. Acta 977, 287–296.

Rabinowitch, E., Govindjee, 1969. Photosynthesis. John Wiley and Sons Inc., New York, p. 273.

Rakhimberdieva, M.G., Bolychevtseva, Y.V., Elanskaya, I.V., Karapetyan, N.V., 2007. Protein-protein interactions in carotenoid triggered quenching of phycobilisome fluorescence in *Synechocystis* sp. PCC 6803. FEBS Lett. 581, 2429–2433.

Raszewski, G., Diner, B.A., Schlodder, E., Renger, T., 2008. Spectroscopic properties of reaction center pigments in photosystem II core complexes: revision of the multimer model. Biophys. J. 95, 105–119.

Reimers, J.R., Biczysko, M., Bruce, D., Coker, D.F., Frankcombe, T.J., Hashimoto, H., et al., 2016. Challenges facing an understanding of the nature of low-energy excited states in photosynthesis. Biochim. Biophys. Acta 1857, 1627–1640.

Reinot, T., Chen, J., Kell, A., Jassas, M., Robben, K.C., Zazubovich, V., Jankowiak, R., 2016. On the conflicting estimations of pigment site energies in photosynthetic complexes: a case study of the CP47 complex. Anal. Chem. Insights 11, 35–48.

Renger, T., Schlodder, E., 2010. Primary photophysical processes in photosystem II: bridging the gap between crystal structure and optical spectra. Chem. Phys. Chem. 11, 1141–1153.

Reppert, M., Acharya, K., Neupane, B., Jankowiak, R., 2010. Lowest electronic states of the CP47 antenna protein complex of photosystem II: simulation of optical spectra and revised structural assignments. J. Phys. Chem. B 114, 11884–11898.

Retegan, M., Neese, F., Panatazis, D.A., Lubitz, W., 2014. Electronic structure of the oxygen-evolving complex in photosystem II prior to O-O bond formation. Science 345, 804–808.

Ried, A., Reinhardt, B., 1980. Distribution of excitation energy between photosystem I and photosystem II in red algae. III. Quantum requirements of the induction of a State 2-State 1 transition. Biochim. Biophys. Acta 592, 76–86.

Rijgersberg, C.P., Amesz, J., 1980. Fluorescence and energy transfer in phycobiliprotein-containing algae at low temperature. Biochim. Biophys. Acta 593, 261–271.

Robinson, H.H., Crofts, A.R., 1983. Kinetics of the changes in oxidation-reduction reactions of the photosystem II quinone acceptor complex, and the pathway for deactivation. FEBS Lett. 153, 221–226.

Rochaix, J.-D., 2014. Regulation and dynamics of the light-harvesting system. Annu. Rev. Plant Biol. 65, 287–309.

Romero, E., Mozzo, M., van Stokkum, I.H.M., Dekker, J.P., van Grondelle, R., Croce, R., 2008. The origin of the low-energy form of photosystem I light-harvesting complex Lhca4: mixing of the lowest exciton with a charge-transfer state. Biophys. J. 96, 35–37.

Romero, E., van Stokkum, I.H.M., Novoderezhkin, V.I., Dekker, J.P., van Grondelle, R., 2010. Two different charge separation pathways in photosystem II. Biochemistry 49, 4300–4307.

Rose, S., Minagawa, J., Seufferheld, M., Padden, S., Svensson, B., Kolling, D.R.J., Crofts, A.R., Govindjee, 2008. D1-arginine257 mutants (R257E, K, and Q) of *Chlamydomonas reinhardtii* have a lowered Q_B redox potential: analysis of thermoluminescence and fluorescence measurements. Photosynth. Res. 98, 449–468.

Rousseau, F., Setif, P., Lagoutte, B., 1993. Evidence for the involvement of Psi-E subunit in the reduction of ferredoxin by photosystem-I. EMBO J. 12, 1755–1765.

Rutherford, A.W., Govindjee, Inoue, Y., 1984. Charge accumulation and photochemistry in leaves studied by thermoluminescence and delayed light. Proc. Natl. Acad. Sci. U. S. A. 81, 1107–1111.

Savikhin, S., Xu, W., Martinsson, P., Chitnis, P.R., Struve, W.S., 2001. Kinetics of charge separation and $A_0^- \rightarrow A_1$ electron transfer in photosystem reaction centers. Biochemistry 40, 9282–9290.

Schansker, G., Tóth, S.Z., Strasser, R.J., 2005. Methylviologen and dibromothymoquinone treatments of pea leaves reveal the role of photosystem I in the Chl *a* fluorescence rise OJIP. Biochim. Biophys. Acta 1706, 250–261.

Schansker, G., Tóth, S.Z., Holzwarth, A.R., Garab, G., 2014. Chlorophyll *a* fluorescence: beyond the limits of the Q_A model. Photosynth. Res. 120, 43–58.

Schatz, G.H., Brock, H., Holzwarth, A.R., 1987. Picosecond kinetics of fluorescence and absorbance changes in photosystem II particles excited at low photon density. Proc. Natl. Acad. Sci. U. S. A. 84, 8414–8418.

Schatz, G.H., Brock, H., Holzwarth, A.R., 1988. A kinetic and energetic model for the primary processes in photosystem II. Biophys. J. 54, 397–405.

Schlodder, E., Cetin, M., Byrdin, M., Terekhova, I.N., Karapetyan, N.V., 2005. $P700^+$- and $^3P700$-induced quenching of the fluorescence at 760 nm in trimeric photosystem I complexes from the cyanobacterium *Arthrospira platensis*. Biochim. Biophys. Acta 1706, 53–67.

Schlodder, E., Hussels, M., Cetin, M., Karapetyan, N.V., Brecht, M., 2011. Fluorescence of the various red antenna states in photosystem I complexes from cyanobacteria is affected differently by the redox state of P700. Biochim. Biophys. Acta 1807, 1423–1431.

Schluchter, W.M., Shen, G.H., Zhao, J.D., Bryant, D.A., 1996. Characterization of psaI and psaL mutants of *Synechococcus* sp strain PCC 7002: a new model for state transitions in cyanobacteria. Photochem. Photobiol. 64, 53–66.

Schreiber, U., 1986. Detection of rapid induction kinetics with a new type of high-frequency modulated chlorophyll fluorometer. Photosynth. Res. 9, 261–272.

Schreiber, U., 2004. Pulse-amplitude-modulation (PAM) fluorometry and saturation pulse method: an overview. In: Papageorgiou, G.C., Govindjee (Eds.), Chlorophyll a Fluorescence: a Signature of Photosynthesis. Advances in Photosynthesis and Respiration, vol. 19. Springer, Dordrecht, pp. 279–319.

Schreiber, U., Neubauer, C., 1987. The polyphasic rice of chlorophyll fluorescence upon onset of strong continuous illumination: II. Partial control by the photosystem II donor side and possible ways of interpretation. Z. Naturforsch. 42c, 1255–1264.

Schreiber, U., Neubauer, C., 1990. O_2-dependent electron flow, membrane energization and the mechanism of non-photochemical quenching of chlorophyll fluorescence. Photosynth. Res. 25, 279–293.

Schreiber, U., Schliwa, U., Bilger, W., 1986. Continuous recording of photochemical and non-photochemical chlorophyll fluorescence quenching with a new type of modulation fluorometer. Photosynth. Res. 10, 51–62.

Schreiber, U., Endo, T., Mi, H., Asada, K., 1995. Quenching analysis of chlorophyll fluorescence by the saturation pulse method: particular aspects relating to the study of eukaryotic algae and cyanobacteria. Plant Cell Physiol. 36, 873–882.

Schuurmans, R.M., van Alphen, P., Schuurmans, J.M., Matthijs, H.C.P., Hellingwerf, K.J., 2015. Comparison of the photosynthetic yield of cyanobacteria and green algae: different methods give different answers. PLoS One 10, e0139061.

Schwabe, T.M.E., Boekema, E.J., Berry, S., Chitnis, P.R., Pistorius, E., Kruip, J., 2001. Dynamics of photosystem I: Ca^{2+}-based oligomerization and response to iron deficiency by induction of a new antenna built by IsiA. In: Osmond, C.B. (Ed.), Proceedings of the 12th International Congress on Photosynthesis. CSIRO Publishing, Brisbane. S6:003.

Schweitzer, R.H., Brudvig, G.W., 1997. Fluorescence quenching by chlorophyll cations in photosystem II. Biochemistry 36, 11351–11359.

Schweitzer, R.H., Melkozernov, A.N., Blankenship, R.E., Brudvig, G.W., 1998. Time-resolved fluorescence measurements of photosystem II: the effect of quenching by oxidized chlorophyll Z. J. Phys. Chem. B 102, 8320–8326.

Şener, M.K., Park, S., Lu, D., Damjanovic, A., Ritz, T., Fromme, P., Schulten, K., 2004. Excitation migration in trimeric cyanobacterial photosystem I. J. Chem. Phys. 120, 11183–11195.

Shao, J., Yu, G., Wu, Z., Peng, X., Li, R., 2010. Responses of *Synechocystis* sp. PCC 6803 (cyanobacterium) photosystem II to pyrene stress. J. Environ. Sci. (China) 22, 1091–1095.

Shapiguzov, A., Ingelsson, B., Samol, I., Andres, C., Kessler, F., Rochaix, J.-D., Vener, A.V., Goldschmidt-Clermont, M., 2010. The PPH1 phosphatase is specifically involved in LHCII dephosphorylation and state transitions in Arabidopsis. Proc. Natl. Acad. Sci. U. S. A. 107, 4782–4787.

Shelaev, I.V., Gostev, F.E., Nadtochenko, V.A., Shkuropatov, A.Y., Zabelin, A.A., Mamedov, M.D., Semenov, A.Y., Sarkisov, O.M., Shuvalov, V.A., 2008. Primary light-energy conversion in tetrameric chlorophyll structure of photosystem II and bacterial reaction centers: II. Fempto- and picosecond charge separation in PSII D1/D2/Cyt b559 complex. Photosynth. Res. 98, 95–103.

Shelaev, I.V., Gostev, F.E., Mamedov, M.D., Sarkisov, O.M., Nadtochenko, V.A., Shuvalov, V.A., Semenoc, A.Y., 2010. Femtosecond primary charge separation in *Synechocystis* sp. PCC 6803 photosystem I. Biochim. Biophys. Acta 1797, 1410–1420.

Shelaev, I.V., Gostev, F.E., Vishnev, M.I., et al., 2011. Alternative electron donors P680 and ChlD1 in photosystem II reaction centers. Photochem. Photobiol. 104, 44–50.

Shen, J.R., 2015. The structure of photosystem II and the mechanism of water oxidation in photosynthesis. Annu. Rev. Plant Biol. 66, 23–48.

Shen, G., Boussiba, S., Vermaas, W.F., 1993. *Synechocystis* sp PCC 6803 strains lacking photosystem I and phycobilisome function. Plant Cell 5, 1853–1863.

Sherman, D.M., Troyan, T.A., Sherman, L.A., 1994. Localization of membrane-proteins in the cyanobacterium *Synechococcus* sp Pcc7942—radial asymmetry in the photosynthetic complexes. Plant Physiol. 106, 251–262.

Shevela, D., Eaton-Rye, J.J., Shen, J.R., Govindjee, 2012. Photosystem II and the unique role of bicarbonate: a historical perspective. Biochim. Biophys. Acta 1817, 1134–1151.

Shevela, D., Pishchalinikov, R.Y., Eichacker, L.A., Govindjee, 2013. Oxygenic photosynthesis in cyanobacteria. In: Srivastava, A.K., Rai, A.N., Neilan, B.A. (Eds.), Stress Biology of Cyanobacteria. Molecular Mechanisms to Cellular Responses. CRC Press, Boca Raton, pp. 3–40.

Shih, P.M., Matzke, N.J., 2013. Primary endosymbiosis events date to the later Proterozoic with cross-calibrated phylogenetic dating of duplicated ATPase proteins. Proc. Natl. Acad. Sci. U. S. A. 110, 12355–12360.

Shikanai, T., Yamamoto, H., 2017. Contribution of cyclic and pseudo-cyclic electron transport to the formation of proton motive force in chloroplasts. Mol. Plant 10, 20–29.

Shinkarev, V.P., Govindjee, 1993. Insight into the relationship of chlorophyll a fluorescence yield to the concentration of its natural quenchers in oxygenic photosynthesis. Proc. Natl. Acad. Sci. U. S. A. 90, 7466–7469.

Shinkarev, V.P., Xu, C., Govindjee, Wraight, C.A., 1997. Kinetics of the oxygen evolution step in plants determined from flash-induced chlorophyll *a* fluorescence. Photosynth. Res. 51, 43–49.

Shirshin, E.A., Nikonova, E.E., Kuzminov, F.I., Sluchanko, N.N., Elanskaya, I.V., Gorbunov, M.Y., Fadeev, V.V., Friedrich, T., Maksimov, E.G., 2017. Biophysical modeling of in vitro and in vivo processes underlying regulated photoprotective mechanism in cyanobacteria. Photosynth. Res. 133, 261–271.

Shubin, V.V., Murthy, S.D.S., Karapetyan, N.V., Mohanty, P., 1991. Origin of the 77 K variable fluorescence at 758 nm in the cyanobacterium *Spirulina platensis*. Biochim. Biophys. Acta 1060, 28–36.

Shubin, V.V., Tsuprun, V.L., Bezsmertnaya, I.N., Karapetyan, N.V., 1993. Trimeric forms of the photosystem I reaction center complex pre-exist in the membranes of the cyanobacterium *Spirulina platensis*. FEBS Lett. 334, 79–82.

Siefermann-Harms, D., 1987. The light-harvesting and protective functions of carotenoids in photosynthetic membranes. Physiol. Plant. 69, 561–568.

Siegbabahn, P.E.M., 2011. Recent theoretical studies of water oxidation in photosystem II. J. Photochem. Photobiol. B: Biol. 104, 94–99.

Silverstein, T., Cheng, L., Allen, J.F., 1993. Chloroplast thylakoid protein phosphatase reactions are redox-independent and kinetically heterogeneous. FEBS Lett. 334, 101–105.

Singh, A.K., Sherman, L.A., 2007. Reflections on the function of IsiA, a cyanobacterial stress-inducible, Chl-binding protein. Photosynth. Res. 93, 17–25.

Six, C., Thomas, J.C., Garczarek, L., Ostrowski, M., Dufresne, A., Blot, N., Scanlan, D.J., Partensky, F., 2007. Diversity and evolution of phycobilisomes in marine *Synechococcus* sp.: a comparative genomics study. Genome Biol. 8, R259.

Sluchanko, N.N., Slonimskiy, Y.B., Moldenhauer, M., Friedrich, T., Maksimov, E.G., 2017. Deletion of the short N-terminal extension in OCP reveals the main site for FRP binding. FEBS Lett. 591, 1667–1676.

Snyder, U.K., Biggins, J., 1987. Excitation energy redistribution in the cryptomonad alga *Cryptomonas ovata*. Biochim. Biophys. Acta 892, 48–55.

Soitamo, A., Havurinne, V., Tyystjärvi, E., 2017. Photoinhibition in marine picocyanobacteria. Physiol. Plant. 161, 97–108.

Sonani, R.R., Gardiner, A., Rastogi, R.P., Cogdell, R., Robert, B., Madamwar, D., 2018. Site, trigger, quenching mechanism and recovery of non-photochemical quenching in cyanobacteria: recent updates. Photosynth. Res. 137, 171–180.

Sonoike, K., Hihara, Y., Ikeuchi, M., 2001. Physiological significance of the regulation of photosystem stoichiometry upon high light acclimation of *Synechocystis* sp. PCC 6803. Plant Cell Physiol. 42, 379–384.

Srivastava, A.K., Rai, A.N., Neilan, B.A. (Eds.), 2013. Stress Biology of Cyanobacteria. Molecular Mechanisms to Cellular Responses. CRC Press, Boca Raton, pp. 375.

Staleva, H., Komenda, J., Shukla, M.K., Šlouf, V., Kaňa, R., Polivka, T., Sobotka, R., 2015. Mechanism of photoprotection in the cyanobacterial ancestor of plant antenna proteins. Nat. Chem. Biol. 11, 287–291.

Stamatakis, K., Papageorgiou, G.C., 1999. Phycobilisome-to-photosystem I excitation transfer is enhanced in water-depleted cells and depressed in water replete cells of cyanobacterium *Synechococcus* sp. PCC7942. In: Argyroudi-Akoyunoglou, J.H., Senger, H. (Eds.), The Chloroplast: From Molecular Biology to Biotechnology. Kluwer Academic Publishers, Dordrecht, pp. 47–54.

Stamatakis, K., Papageorgiou, G.C., 2001. The osmolality of the cell suspension regulates phycobilisome-to-photosystem I excitation transfers in cyanobacteria. Biochim. Biophys. Acta 1506, 172–181.

Stamatakis, K., Ladas, N.P., Papageorgiou, G.C., 2005. Facilitated water transport in cyanobacterium *Synechococcus* sp. PCC 7942 studied by phycobilisome-sensitized chlorophyll a fluorescence. Photosynth. Res. 84, 181–185.

Stamatakis, K., Tsimilli-Michael, M., Papageorgiou, G.C., 2007. Fluorescence induction in the phycobilisome-containing cyanobacterium *Synechococcus* sp PCC 7942: analysis of the slow fluorescent transient. Biochim. Biophys. Acta 1767, 766–772.

Stamatakis, K., Tsimilli-Michael, M., Papageorgiou, G.C., 2014. On the question of the light-harvesting role of β-carotene in photosystem II and photosystem I core complexes. Plant Physiol. Biochem. 81, 121–127.

Steinbach, G., Schubert, F., Kaňa, R., 2015. Cryo-imaging of photosystems and phycobilisomes in *Anabaena* sp. PCC 7120 cells. J. Photochem. Photobiol. B 152, 395–399.

Stemler, A., 1982. The functional role of bicarbonate in photosynthetic light reaction II. In: Govindjee (Eds.), Photosynthesis: Development, Carbon Metabolism, and Plant Productivity. Academic Press, New York, pp. 513–539.

Stirbet, A., 2013. Excitonic connectivity between photosystem II units: what is it, and how to measure it? Photosynth. Res. 116, 189–214.

Stirbet, A., Govindjee, 2011. On the relation between the Kautsky effect (chlorophyll *a* fluorescence induction) and photosystem II: basics and applications of the OJIP fluorescence transient. J. Photochem. Photobiol. B Biol. 104, 236–257.

Stirbet, A., Govindjee, 2012. Chlorophyll a fluorescence induction: a personal perspective of the thermal phase, the J-I-P rise. Photosynth. Res. 113, 15–61.

Stirbet, A., Govindjee, 2016. The slow phase of chlorophyll a fluorescence induction in silico: origin of the S-M fluorescence rise. Photosynth. Res. 130, 193–213.

Stirbet, A., Govindjee, Strasser, B.J., Strasser, R.J., 1998. Chlorophyll a fluorescence induction in higher plants: modeling and numerical simulation. J. Theor. Biol. 193, 131–151.

Stirbet, A.D., Rosenau, P., Ströder, A.C., Strasser, R.J., 2001. Parameter optimisation of fast chlorophyll fluorescence induction model. Math. Comput. Simul. 56, 443–450.

Stirbet, A., Riznichenko, G.Y., Rubin, A.B., Govindjee, 2014. Modeling chlorophyll *a* fluorescence transient: relation to photosynthesis. Biochemistry (Mosc.) 79, 291–323.

Stirbet, A., Lazár, D., Kromdijk, J., Govindjee, 2018. Chlorophyll *a* fluorescence induction: can just a one-second measurement be used to quantify abiotic stress responses? Photosynthetica 56, 86–104.

Stoitchkova, K., Zsiros, O., Jávorfi, T., Páli, T., Andreeva, A., Gombos, Z., Garab, G., 2007. Heat- and light-induced reorganizations in the phycobilisome antenna of *Synechocystis* sp. PCC 6803. Thermo-optic effect. Biochim. Biophys. Acta 1767, 750–756.

Strasser, B.J., 1997. Donor side capacity of photosystem II probed by chlorophyll *a* fluorescence transients. Photosynth. Res. 52, 147–155.

Strasser, R.J., Govindjee, 1991. The F_0 and the O-J-I-P fluorescence rise in higher plants and algae. In: Argyroudi-Akoyunoglou, J.H. (Ed.), Regulation of Chloroplast Biogenesis. Plenum Press, New York, pp. 423–426.

Strasser, B.J., Strasser, R.J., 1995. Measuring fast fluorescence transients to address environmental questions: the JIP test. In: Mathis, P. (Ed.), Photosynthesis: From Light to Biosphere. vol. 5. Kluwer Academic, Dordrecht, pp. 977–980.

Strasser, R.J., Srivastava, A., Govindjee, 1995. Polyphasic chlorophyll a fluorescence transient in plants and cyanobacteria. Photochem. Photobiol. 61, 32–42.

Strasser, R.J., Tsimilli-Michael, M., Srivastava, A., 2004. Analysis of the chlorophyll fluorescence transient. In: Papageorgiou, G.C., Govindjee (Eds.), Chlorophyll *a* Fluorescence: A Signature of Photosynthesis. Advances in Photosynthesis and Respiration, vol. 19. Springer, Dordrecht, pp. 321–362.

Sudhir, P.R., Pogoryelov, D., Kovacs, L., Garab, G., Murthy, S.D., 2005. The effects of salt stress on photosynthetic electron transport and thylakoid membrane proteins in the cyanobacterium *Spirulina platensis*. J. Biochem. Mol. Biol. 38, 481–485.

Suggett, D.J., Prášil, O., Borowitzka, M.A. (Eds.), 2010. Chlorophyll A Fluorescence in Aquatic Sciences. Methods and Applications. Springer, Dordrecht, pp. 332.

Sun, J., Hao, S., Radle, M., Xu, W., Shelaev, I., Nadtochenko, V., Shuvalov, V., Semenov, A., Gordone, H., van der Est, A., Golbeck, J.H., 2014. Evidence that histidine forms a coordination bond to the A_{0A} and A_{0B} chlorophylls and asecond H-bond to the A_{1A} and A_{1B} phylloquinones in $M688H_{PsaA}$ and $M668H_{PsaB}$ variants of *Synechocystis* sp. PCC 6803. Biochim. Biophys. Acta 1837, 1362–1375.

Sutter, M., Wilson, A., Leverenz, R.L., Lopez-Igual, R., Thurotte, A., Salmeen, A.E., Kirilovsky, D., Kerfeld, C.A., 2013. Crystal structure of the FRP and identification of the active site for modulation of OCP-mediated photoprotection in cyanobacteria. Proc. Natl. Acad. Sci. U. S. A. 110, 10022–10027.

Tamary, E., Kiss, V., Nevo, R., Adam, Z., Bernát, G., Rexroth, S., Rögner, M., Reich, Z., 2012. Structural and functional alterations of cyanobacterial phycobilisomes induced by high-light stress. Biochim. Biophys. Acta 1817, 319–327.

Tang, K., Ding, W.L., Höppner, A., Zhao, C., Zhang, L., Hontani, Y., Kennis, J.T., Gärtner, W., Scheer, H., Zhou, M., Zhao, K.H., 2015. The terminal phycobilisome emitter, L_{CM}: a light-harvesting pigment with a phytochrome chromophore. Proc. Natl. Acad. Sci. U. S. A. 112, 15880–15885.

Tetenkin, V.I., Gulyaev, B.A., Seibert, M., Rubin, A.B., 1989. Spectral properties of stabilized D1/D2/cytochrome b559 photosystem II reaction center complex. FEBS Lett. 250, 459–463.

Thornton, L.E., Ohkawa, H., Roose, J.L., Kashino, Y., Keren, N., Pakrasi, H.B., 2004. Homologs of plant PsbP and PsbQ proteins are necessary for regulation of photosystem II activity in the cyanobacterium *Synechocystis* 6803W. Plant Cell 16, 2164–2175.

Thurotte, A., Lopez-Igual, R., Wilson, A., Comolet, L., Bourcier de Carbon, C., Xiao, F., Kirilovsky, D., 2015. Regulation of Orange Carotenoid protein activity in cyanobacterial photoprotection. Plant Physiol. 169, 737–747.

Thurotte, A., de Carbon, C.B., Wilson, A., Talbot, L., Cot, S., López-Igual, R., Kirilovsky, D., 2017. The cyanobacterial fluorescence recovery protein has two distinct activities: orange carotenoid protein amino acids involved in FRP interaction. Biochim. Biophys. Acta. 1858, 308–317.

Tian, L., Farooq, S., van Amerongen, H., 2013. Probing the picosecond kinetics of the photosystem II core complex in vivo. Phys. Chem. Chem. Phys. 15, 3146–3154.

Tikhonov, A.N., 2013. pH-dependent regulation of electron transport and ATP synthesis in chloroplasts. Photosynth. Res. 116, 511–534.

Tomek, P., Lazár, D., Ilík, P., Naus, J., 2001. On the intermediate steps between the O and P steps in chlorophyll *a* fluorescence rise measured at different intensities of exciting light. Aust. J. Plant Physiol. 28, 1151–1160.

Tóth, S.Z., Schansker, G., Strasser, R.J., 2007. A non-invasive assay of the plastoquinone pool redox state based on the OJIP-transient. Photosynth. Res. 93, 193–203.

Trissl, H.-W., Gao, Y., Wulf, K., 1993. Theoretical fluorescence induction curves derived from coupled differential equations describing the primary photochemistry of photosystem II by an exciton-radical pair equilibrium. Biophys. J. 64, 974–988.

Tsimilli-Michael, M., Strasser, R.J., 2008. In vivo assessment of plants' vitality: applications in detecting and evaluating the impact of mycorrhization on host plants. In: Varma, A. (Ed.), Mycorrhiza: State of the Art, Genetics and Molecular Biology, Eco-Function, Biotechnology, Eco-Physiology, Structure and Systematics. third ed. Springer, Dordrecht, pp. 679–703.

Tsimilli-Michael, M., Stamatakis, K., Papageorgiou, G.C., 2009. Dark-to-light transition in *Synechococcus* sp. PCC 7942 cells studied by fluorescence kinetics assesses plastoquinone redox poise in the dark and photosystem II fluorescence component and dynamics during State 2 to State 1 transition. Photosynth. Res. 99, 243–255.

Ueda, T., Nomoto, N., Koga, M., Ogasa, H., Ogawa, Y., Matsumoto, M., Stampoulis, P., Sode, K., Terasawa, H., Shimada, I., 2012. Structural basis of efficient electron transport between photosynthetic membrane proteins and plastocyanin in spinach revealed using nuclear magnetic resonance. Plant Cell 24, 4173–4186.

Ueno, Y., Aikawa, S., Niwa, K., Abe, T., Murakami, A., Kondo, A., Akimoto, S., 2017. Variety in excitation energy transfer processes from phycobilisomes to photosystems I and II. Photosynth. Res. 133, 235–243.

Umena, Y., Kawakami, K., Shen, J.R., Kamiya, N., 2011. Crystal structure of oxygen-evolving photosystem II at 1.9 Å resolution. Nature 473, 55–60.
Vajravel, S., Kis, M., Klodawska, K., Laczko-Dobos, H., Malec, P., Kovács, L., Gombos, Z., Toth, T.N., 2017. Zeaxanthin and echinenone modify the structure of photosystem I trimer in *Synechocystis* sp. PCC 6803. Biochim. Biophys. Acta 1858, 510–518.
Valkunas, L.L., Geacintov, N.E., France, L., Breton, J., 1991. The dependence of the shapes of fluorescence inductions curves in chloroplasts on the duration of illumination pulses. Biophys. J. 59, 397–408.
van Amerongen, H., Croce, R., 2013. Light harvesting in photosystem II. Photosynth. Res. 116, 251–263.
van de Meene, A.M., Hohmann-Mariott, M.F., Vermaas, W.F., Roberson, R.W., 2006. The three-dimensional structure of the cyanobacterium *Synechocystis* sp. PCC6803. Arch. Microbiol. 184, 259–270.
van der Lee, J., Bald, D., Kwa, S.L.S., van Grondelle, R., Rögner, M., Dekker, J.P., 1993. Steady-state polarized-light spectroscopy of isolated photosystem-I complexes. Photosynth. Res. 35, 311–321.
van der Weij-de Wit, C.D., Dekker, J.P., van Grondelle, R., van Stokkum, I.H.M., 2011. Charge separation is virtually irreversible in photosystem II core complexes with oxidized primary quinone acceptor. J. Phys. Chem. A 115, 3947–3956.
van der Woude, A.D., Gallego, R.P., Vreugdenhil, A., Veetil, V.P., Chroumpi, T., Hellingwerf, K.J., 2016. Genetic engineering of *Synechocystis* PCC6803 for the photoautotrophic production of the sweetener erythritol. Microb. Cell Fact. 15, 60.
van Stokkum, I.H.M., Larsen, D.S., van Grondelle, R., 2004. Global and target analysis of time-resolved spectra. Biochim. Biophys. Acta 1657, 82–104.
van Stokkum, I.H.M., van Oort, B., van Mourik, F., Gobets, B., Van Amerongen, H., 2008. (Sub)Picosecond spectral evolution of fluorescence studied with a synchroscan streak-camera system and target analysis. In: Aartsma, T.J., Matysik, J. (Eds.), Biophysical Techniques in Photosynthesis. Springer, Dordrecht, pp. 223–240.
van Stokkum, I.H.M., Gwizdala, M., Tian, L., Snellenburg, J.J., van Grondelle, R., van Amerongen, H., Berera, R., 2018. A functional compartmental model of the *Synechocystis* PCC 6803 phycobilisome. Photosynth. Res. 135, 87–102.
Vass, I., Govindjee, 1996. Thermoluminescence from the photosynthetic apparatus. Photosynth. Res. 48, 117–126.
Veetil, V.P., Angermayr, S.A., Hellingwerf, K.J., 2017. Ethylene production with engineered *Synechocystis* sp PCC 6803 strains. Microb. Cell Fact. 16, 34.
Velthuys, B.R., 1981. Electron-dependent competition between plastoquinone and inhibitors for binding to photosystem II. FEBS Lett. 126, 277–281.
Velthuys, B.R., Amesz, J., 1974. Charge accumulation at the reducing side of system 1 of photosynthesis. Biochim. Biophys. Acta 325, 138–148.
Vener, A.V., van Kan, P.J., Rich, P.R., Ohad, I., Andersson, B., 1997. Plastoquinol at the quinol oxidation site of reduced cytochrome *bf* mediates signal transduction between light and protein phosphorylation: thylakoid protein kinase deactivation by a single-turnover flash. Proc. Natl. Acad. Sci. U. S. A. 94, 1585–1590.
Vermaas, W.F.J., 2001. Photosynthesis and respiration in cyanobacteria. In: Encyclopedia of Life Sciences. John Wiley & Sons, London, pp. 1–7.
Vermaas, W.F.J., 2007. Targeted genetic modification of cyanobacteria: new biotechnological applications. In: Richmond, A. (Ed.), Handbook of Microalgal Culture. Blackwell Science, Oxford, pp. 457–470.
Vermaas, W.F.J., van Rensen, J.J., Govindjee, 1982. The interaction between bicarbonate and the herbicide ioxynil in the thylakoid membrane and the effects of amino acid modification on bicarbonate action. Biochim. Biophys. Acta 681, 242–247.
Vermaas, W.F.J., Timlin, J.A., Jones, H.D.T., Sinclair, M.B., Nieman, L.T., Hamad, S.W., Melgaard, D.K., Haaland, D.M., 2008. In vivo hyperspectral confocal fluorescence imaging to determine pigment localization and distribution in cyanobacterial cells. Proc. Natl. Acad. Sci. U. S. A. 105, 4050–4055.
Vernotte, C., Astier, C., Olive, J., 1990. State-1-State-2 adaptation in the cyanobacteria *Synechocystis*-PCC-6714 wild-type and *Synechocystis*-PCC-6803 wild-type and phycocyanin-less mutant. Photosynth. Res. 26, 203–212.
Vinnemeier, J., Kunert, A., Hagemann, M., 1998. Transcriptional analysis of the isiAB operon in salt-stressed cells of the cyanobacterium *Synechocystis* sp. PCC 6803. FEMS Microbiol. Lett. 169, 323–330.
Vogt, L., Vinyard, D.J., Khan, S., Brudvig, G.W., 2015. Oxygen evolving complex of photosystem II: an analysis of second-shel residues and hydrogen-bonding networks. Curr. Opin. Chem. Biol. 25C, 152–158.
Wang, S., Pan, X., 2012. Effects of Sb(V) on growth and chlorophyll fluorescence of *Microcystis aeruginosa* (FACHB-905). Curr. Microbiol. 65, 733–741.
Wang, R.T., Stevens, C.L.R., Myers, J., 1977. Action spectra for photoreactions I and II of photosynthesis in the blue-green alga *Anacystis nidulans*. Photochem. Photobiol. 25, 103–108.
Wang, Y., Mao, L., Hu, X., 2004. Insight into the structural role of carotenoids in the photosystem I: a quantum chemical analysis. Biophys. J. 86, 3097–3111.
Wang, Q., Hall, C.L., Al-Adami, M.Z., He, Q., 2010. IsiA is required for the formation of photosystem I supercomplexes and for efficient state transition in *Synechocystis* PCC 6803. PLoS One 5, e10432.
Wang, S., Zhang, D., Pan, X., 2012. Effects of arsenic on growth and photosystem II (PSII) activity of *Microcystis aeruginosa*. Ecotoxicol. Environ. Saf. 84, 104–111.
Wang, J., Liu, Q., Feng, J., Lv, J., Xie, S., 2016. Photosynthesis inhibition of pyrogallol against the bloom-forming cyanobacterium *Microcystis aeruginosa* TY001. Pol. J. Environ. Stud. 25, 2601–2608.
Wasielewski, M.R., Fenton, J.M., Govindjee, 1987. The rate of formation of $P700^+ A_0^-$ photosystem I particles from spinach as measured by picosecond transient absorption spectroscopy. Photosynth. Res. 12, 181–190.
Wasielewski, M.R., Johnson, D.G., Seibert, M., Govindjee, 1989. Determination of the primary charge separation rate in isolated photosystem II reaction centers with 500-fs time resolution. Proc. Natl. Acad. Sci. U. S. A. 86, 524–528.
Watanabe, M., Ikeuchi, M., 2013. Phycobilisome: architecture of a light harvesting supercomplex. Photosynth. Res. 116, 265–276.
Watanabe, M., Semchonok, D., Webber-Birungi, M., Shigeki, E., Kondo, K., Narikawa, R., Ohmori, M., Boekema, E., Ikeuchi, M., 2014. Attachment of phycobilisomes in an antenna photosystem I super-complex of cyanobacteria. Proc. Natl. Acad. Sci. U. S. A. 111, 2512–2517.

Wei, X., Su, X., Cao, P., Liu, X., Chang, W., Li, M., Zhang, X., Liu, Z., 2016. Structure of spinach photosystem II–LHCII supercomplex at 3.2 Å resolution. Nature 534, 69–74.

Wientjes, E., Croce, R., 2012. PMS: photosystem I electron donor or fluorescence quencher. Photosynth. Res. 111, 185–191.

Wientjes, E., van Amerongen, H., Croce, R., 2013. LHCII is an antenna of both photosystems after long-term acclimation. Biochim. Biophys. Acta 1827, 420–426.

Wilson, A., Ajlani, G., Verbavatz, J.-M., Vass, I., Kerfeld, C.A., Kirilovsky, D., 2006. A soluble carotenoid protein involved in phycobilisome-related energy dissipation in cyanobacteria. Plant Cell 18, 992–1007.

Wilson, A., Boulay, C., Wilde, A., Kerfeld, C.A., Kirilovsky, D., 2007. Light-induced energy dissipation in iron-starved cyanobacteria: roles of OCP and IsiA proteins. Plant Cell 19, 656–672.

Wilson, A., Punginelli, C., Gall, A., Bonetti, C., Alexandre, M., Routaboul, J.M., Kerfeld, C.A., van Grondelle, R., Robert, B., Kennis, J.T., Kirilovsky, D., 2008. A photoactive carotenoid protein acting as light intensity sensor. Proc. Natl. Acad. Sci. U. S. A. 105, 12075–12080.

Wittmershaus, B.P., Wolf, V.M., Vermaas, W.F.J., 1992. Temperature dependence and polarization of fluorescence from photosystem I in the Cyanobacterium *Synechocystis* sp. PCC 6803. Photosynth. Res. 31, 75–87.

Wollman, F.A., Delepelaire, P., 1984. Correlation between changes in light energy distribution and changes in thylakoid membrane polypeptide phosphorylation in *Chlamydomonas reinhardtii*. J. Cell. Biol. 98, 1–7.

Wraight, C.A., 1981. Oxidation-reduction physical chemistry of the acceptor quinone complex in bacterial photosynthetic reaction centers: evidence for a new model of herbicide activity. Isr. J. Chem. 21, 348–354.

Wraight, C.A., Crofts, A.R., 1970. Energy-dependent quenching of chlorophyll a fluorescence in isolated chloroplasts. Eur. J. Biochem. 17, 319–327.

Wydrzynski, T., Satoh, K. (Eds.), 2005. Photosystem II: The Light-Driven Water-Plastoquinone Oxidoreductase. Advances in Photosynthesis and Respiration, vol. 22. Springer, Dordrecht, pp. 756.

Yamanaka, G., Lundellg, D.J., Glazer, A.N., 1982. Molecular architecture of a light-harvesting antenna—isolation and characterization of phycobilisome subassembly particles. J. Biol. Chem. 257, 4077–4086.

Yamazaki, I., Mimuro, M., Murao, T., Yamazaki, T., Yoshihara, K., Fujita, Y., 1984. Excitation energy transfer in the light harvesting antenna system of the red alga *Porphyridium cruentum* and the blue green alga *Anacystis nidulans*: analysis of time-resolved fluorescence spectra. Photochem. Photobiol. 39, 233–240.

Yang, S.Z., Su, Z.Q., Li, H., Feng, J.J., Xie, J., Xia, A.D., Gong, Y.D., Zhao, J.Q., 2007. Demonstration of phycobilisome mobility by the time and space-correlated fluorescence imaging of a cyanobacterial cell. Biochim. Biophys. Acta 1767, 15–21.

Young, I.D., Ibrahim, M., Chatterjee, R., Gul, S., Fuller, F., Koroidov, S., et al., 2016. Structure of photosystem II and substrate binding at room temperature. Nature 540, 453–457.

Yousef, N., Pistorius, E.K., Michel, K.P., 2003. Comparative analysis of idiA and isiA transcription under iron starvation and oxidative stress in *Synechococcus elongatus* PCC 7942 wild-type and selected mutants. Arch. Microbiol. 180, 471–483.

Zehr, J.P., 2011. Nitrogen fixation by marine cyanobacteria. Trends Microbiol. 19, 162–173.

Zhang, S., Scheller, H.V., 2004. Light-harvesting complex II binds to several small subunits of photosystem I. J. Biol. Chem. 279, 3180–3187.

Zhang, T., Gong, H., Wen, X., Lu, C., 2010. Salt stress induces a decrease in excitation energy transfer from phycobilisomes to photosystem II but an increase to photosystem I in the cyanobacterium *Spirulina platensis*. J. Plant. Physiol. 167, 951–958.

Zhang, X., Ma, F., Zhu, X., Zhu, J., Rong, J., Zhan, J., Chen, H., He, C., Wanga, W., 2017. The acceptor side of photosystem II is the initial target of nitrite stress in *Synechocystis* sp. Strain PCC 6803. Appl. Environ. Microbiol. 83, e02952-16.

Zhou, J., Zhang, H., Zhang, Y., Li, Y., Ma, Y., 2012. Designing and creating a modularized synthetic pathway in cyanobacterium *Synechocystis* enables production of acetone from carbon dioxide. Metab. Eng. 14, 394–400.

Zhu, X.G., Govindjee, Baker, N.R., deSturler, E., Ort, D.R., Long, S.P., 2005. Chlorophyll a fluorescence induction kinetics in leaves predicted from a model describing each discrete step of excitation energy and electron transfer associated with photosystem II. Planta 223, 114–133.

Zito, F., Finazzi, G., Delosme, R., Nitschke, W., Picot, D., Wollman, F.A., 1999. The Qo site of cytochrome b_6f complexes controls the activation of the LHCII kinase. EMBO J. 18, 2961–2969.

Zlenko, D.V., Krasilnikov, P.M., Stadnichuk, I.N., 2016. Structural modeling of the phycobilisome core and its association with the photosystems. Photosynth. Res. 130, 347–356.

Zouni, A., Witt, H.T., Kern, J., Fromme, P., Krauss, N., Saenger, W., Orth, P., 2001. Crystal structure of photosystem II from *Synechococcus elongatus* at 3.8 Å resolution. Nature 409, 739–743.

FURTHER READING

Flores, E., Herrero, A. (Eds.), 2014. The Cell Biology of Cyanobacteria. Caister Academic Press, Poole, UK, ISBN: 978-1-908230-38-6, pp. 308.

Los, D.A. (Ed.), 201 chemistry of the acceptor quinone complex in bacterial photosynthetic reaction 7. Cyanobacteria: Omics and Manipulation. Caister Academic Press, Poole, UK, ISBN: 978-1-910190-55-5, pp. 256.

Los, D.A., 2018. Cyanobacteria: Signalling and Regulation Systems. Caister Academic Press, Poole, UK, ISBN: 978-1-910190-87-6, pp. 318.